UNIVERSITA' VITA-SALUTE SAN RAFFAELE

CORSO DI DOTTORATO DI RICERCA INTERNAZIONALE IN MEDICINA MOLECOLARE

CURRICULUM IN

Neuroscience and Experimental Neurology

Intrinsic cellular cues influencing astrocyte-to-neuron conversion.

DoS: Dr. Vania Broccoli
Second Supervisor: Dr. Ernest Arenas

Tesi di DOTTORATO di RICERCA di Laura Pintado

matr. 015587
Ciclo di dottorato: XXXV
SSD: BIO11

Anno Accademico 2021/2022

RELEASE OF PHD THESIS

Il/la sottoscritto/a / *I, the undersigned* *Laura Pintado Almeida*

Matricola / *registration number* *015587*
nat_ a/ born *in* *Las Palmas de Gran Canaria*

il/*on* *15.05.1994*

autore della tesi di Dottorato di ricerca dal titolo / *author of the PhD Thesis titled*

Intrinsic cellular cues influencing astrocyte-to-neuron conversion

□AUTORIZZA la Consultazione della tesi / AUTHORIZE *the public release of the thesis*

x NON AUTORIZZA la Consultazione della tesi per ..12.....mesi /

DO NOT AUTHORIZE *the public release of the thesis for* ...12 .....*months*

a partire dalla data di conseguimento del titolo e precisamente / *from the PhD thesis date, specifically*

Dal / *from* ...../...../..... Al / *to* ...../...../.....

Poiché /*because*:

X l'intera ricerca o parti di essa sono potenzialmente soggette a brevettabilità/ *The whole project or parts of it may be the subject of a patent application.*

□ ci sono parti di tesi che sono già state sottoposte a un editore o sono in attesa di pubblicazione/ *Parts of the thesis have been or are being submitted to a publisher or are in the press.*

□ la tesi è finanziata da enti esterni che vantano dei diritti su di esse e sulla loro pubblicazione/ *the thesis project is financed by external bodies that have rights over it and its publication.*

E' fatto divieto di riprodurre, in tutto o in parte, quanto in essa contenuto / *reproduction of the thesis in whole or in part is forbidden*

Data /Date11.01.2023 Firma/Signature

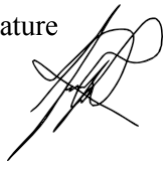

DECLARATION

This thesis has been:
- composed by myself and has not been used in any previous application for a degree. Throughout the text, I use both 'I' and 'We' interchangeably.
- has been written according to the editing guidelines approved by the University.

Permission to use images and other material covered by copyright has been sought and obtained. For the following image/s (1.5, 1.6), it was not possible to obtain permission and is/are therefore included in the thesis under the "fair use" exception (Italian legislative Decree no. 68/2003).

1. ***Electrophysiological analysis****:*

   Electrophysiological analysis (Results, chapter 5.1, figure 5.1 d), which were performed by Dr. Simone Brusco, Stem Cell and Neurogenesis Unit, Division of Neuroscience, San Raffaele Scientific Institute, Milan, Italy.

2. ***SAMMY-seq experiments***

   All protocols for SAMMY-seq were performed together with Chiara Lanzuolo as a collaboration (Methods 5.7.2). Institute of Biomedical Technologies (ITB)-CNR. Chromatin and Nuclear architecture Laboratory at Istituto Nazionale di Genetica Molecolare "Romeo ed Enrica Invernizzi".

3. ***FACS acquisition and analysis: FACS analysis.***

   FACS were performed in collaboration with Dr. Sharon Muggeo and Dr. Mattia Zaghi,. Stem Cell and Neurogenesis Unit, Division of Neuroscience, San Raffaele Scientific Institute, Milan, Italy.

4. ***Statistical analysis for genomic experiments***

   All genomic data processing was performed by Dr. Mattia Zaghi as a collaborator of the project (Methods 5.8). Stem Cell and Neurogenesis Unit, Division of Neuroscience, San Raffaele Scientific Institute, Milan, Italy.

Figures in INTRODUCTION chapter are "fairly used" for educational purpose only, based on "Decreto legislativo del 9.3.03, n68-art. 70 - «Attuazione della direttiva 2001/29/CE sull'armonizzazione di taluni aspetti del diritto d'autore e dei diritti connessi nella società ` dell'informazione». All sources of information are acknowledged by means of reference.

ABSTRACT

For a tissue to regenerate, the cells living within it must be able to replace damaged or lost cells. Although some organs in the human body have this ability, injuries to the central nervous system often result in permanent functional damage. Therefore, direct glial reprogramming may offer significant potential for studying disease-modifying strategies. While there have been many substantial scientific findings in the field, in vivo results have been currently challenged, with reports showing limited-to-no neuronal conversion. As a result, several aspects must be considered when applying this strategy. We reason that the cell environment and maturity state influence these discrepancies. Accordingly, we mainly investigate the latter aspect to identify intrinsic factors possibly hindering astrocyte conversion.

We tested the efficiency of reprogramming in different in vitro models in which we induced a maturation state in astrocytes by expressing the factors Rorb and Fezf2. Furthermore, by directly isolating and purifying astrocytes from the adult mouse. Already in vitro, we observed a drastic decrease in neuron yield compared to reprogrammed postnatal astrocytes. Interestingly, during astrocyte maturation, we identified a significant enrichment signal of the heterochromatin marks H3K9me3 and H3K27me3 accompanied by a loss of chromatin accessibility at many target sites of the proneuronal factor Ascl1, known to drive neurogenesis during development and widely used in cell conversion studies. Consequently, we hypothesized that in vivo, chromatin changes occur during maturation to protect cell identity, which might hinder transcriptional factors neuronal induction that is otherwise not observed during postnatal stages.

Our current analyses add to the understanding of how the maturation state might impact the cell propensity to overgo reprogramming. We suggest that when targeting astrocytes for fate conversion, it should be contemplated that their functional maturity, at least in the cortex, can already influence their potential to be reprogrammed.

Table of contents

Acronyms and Abbreviations

Ascl1/Mash1 - Achaete-Scute Family BHLH Transcription Factor

AAV - Adeno-associated virus

ATAC-seq- Assay for Transposase Accessible Chromatin sequencing

bHLH - basic-helix-loop-helix

BMP - Bone Morphogenic Protein

BPTF - Bromodomain-proximal PHD finger

ChIP-seq - Chromatin immunoprecipitation sequencing

CTCF - CCCTC-binding factor

CUT&Tag- Cleavage Under Targets and Tagmentation

Cre - *cis*-regulatory elements

CNS - Central Nervous System

3D - Three-dimensional

dCAS9 - dead CRISPR-associated protein 9

Dans - Dopaminergic neurons

DCX - Doublecortin

DEGs - Differentially Expressed Genes

DMRs - Differentially Methylated regions

Dnmt3a - DNA methyltransferase 3a

GCL - Granular cell layer

GO - Gene Ontology

HATs - Histone Acetyl Transferase

HDACs - Histone Deacetylases

Hi-C - High Throughput in situ Chromatin Conformation Capture

IF - Immunofluorescence

iPSC - Induced pluripotent cells

iN/iNC - Induced neurons/ Induced neuronal cells

KATs - Lysine Acetyl Transferase

KMTs - Lysine Methyl Transferase

LADs - Lamina-associated domains

meDIP-seq - methylated-DNA immunoprecipitation sequencing

MEFs - Mouse embryonic fibroblasts

MyoD1-2 - Myoblast determination protein 1 and 2

Myt1l - Myelin Transcription Factor 1 Like

Neurog2/Ngn2 - Neurogenin 2

NPCs - Neural Precursors Cells

Nf-kβ - Nuclear factor kappa-light-chain-enhancer of activated B cells

PcG - Polycomb proteins

PGL - Periglomerular like interneurons

PD - Parkinson's disease

PRC1 - Polycomb repressive complex 1

PRC2 - Polycomb repressive complex 2

PSCs - Pluripotent Stem Cells

Ptbp1 - Polypyrimidine tract binding protein 1

ROS - Reactive oxidative species

RTqPCR – Real Time quantitative polymerase chain reaction.

SCNT - Somatic cell nuclear transfer

Sox9 - SRY-Box Transcription Factor 9

SM - Small molecules

SVZ - Sub-Ventricular Zone

SGZ - Subgranular zone

TSSs - Transcription start sites

TFs - Transcriptional factors

TADs - Topological associated domains

List of Figures

Introduction

Results

Methods

1. Introduction

The human body comprises 37.2 trillion cells, forming all your tissues and organs. This is possible as various complex molecular processes take place during development, helping cells to specialize into different types, going from neurons to blood cells (Fasching *et al*, 2021). In particular, stem cells are pluripotent and uncommitted cells that differentiate, giving rise to various tissue-specific cell types, through a set of complex transcriptional and epigenetic networks (Bernstein *et al*, 2007). Hereof, for the determination of cell identity, different cues are available guiding cell fate. Specifically, the way cells communicate is crucial for such a process, and they do so by releasing a variety of molecules acting as external cues. By doing this, there is a timely coordination in their division and differentiation taking place under different cellular environments. In this regard, the Bone Morphogenic Protein (BMP), Wnt, and Nodal pathways are known to induce specific lineage of cells (Hogan, 1996; Yamaguchi, 2001; Schier, 2003; Murry & Keller, 2008; Armingol *et al*, 2022). Additionally, besides these former cues, the internal aspects of the cell also contribute to this journey. For instance, they have a specific set of genes whose expression guides their behavior and indicates where they belong. This set of properties enables cells to develop unique features and particular functions (Perrimon *et al*, 2012; Aravantinou-Fatorou & Thomaidou, 2020). Therefore, a variety of cell functions take place during development, including acting as inducers or responders within wide signaling networks, as the ones along with many other well-known molecular cascades, such as the Hippo, JAK/STAT, or Nf-kβ pathways. As a starting step, some cells need to be directed toward a determined fate, therefore they need to have the competence to do both, detect and receive signals induced by neighboring cells, known as inducers. Consequently, a fully committed cell may then serve as a guide for incoming cells (Jr & Waddington, 1943; Perrimon *et al*, 2012). Essentially, different signaling pathways are responsible not just for developmental switches but also for other important biological processes such as apoptosis, migration, and proliferation (Perrimon et al., 2012; Wilcockson et al., 2017).

Certainly, many milestones have been achieved in understanding the process of forming fully mature differentiated cells in multicellular organisms (Paksa & Rajagopal, 2017). In 1940, few years after DNA was recognized as the molecular basis of heredity, Conrad Hal Waddington proposed his classic view of cell fate hierarchy, according to which lineage commitment and differentiation was a unidirectional and irreversible process (Bhattacharya *et al*, 2011). His famous diagram illustrated this differentiation concept of lineage specification in an 'epigenetic landscape' as a means of describing the developmental restriction upon cell differentiation (*Figure 1.1)* (Rajagopal & Stanger, 2016; Paksa & Rajagopal, 2017). Interestingly, 19 years before the breakthrough work by Yamanaka came out, the transcription factor myoblast determination (MyoD) was already known to transdifferentiate fibroblasts into acquiring muscle-specific properties as early as 1987 by Davis and colleagues (Davis *et al*, 1987). Certainly, the notion of cell plasticity has been substantiated in several experiments carried out during the past 40 years. Accordingly, the ability of a cell to transform into another cell type is recognized not only by gene perturbation experiments, but also know to occur spontaneously (Zhou & Melton, 2018; Leaman *et al*, 2022) . Indeed, it is possible for cellular identities established during development to change during the lifespan of an organism (Rajagopal & Stanger, 2016). A particularly interesting example are the differentiated cells from the liver, the hepatocyte and the cholangiocyte, as they can regenerate itself when damaged. This is especially interesting, considering the mentioned fact that some cells have the intrinsic capacity to switch their fate when they need to. Indeed, previous studies have reported how upon an insult these two cell types can transdifferentiate into the lineage of the other (Raven *et al*, 2017; Schaub *et al*, 2018; Leaman *et al*, 2022). This is not limited to the liver, and other organs like the pancreas have shown de-differentiation and properties (Zhou & Melton, 2018). However, despite that nowadays the concept of cell state is seen as a dynamic process, not all fully differentiated cells inherit this endogenous cellular plasticity and upon damage or injury, they fail to regenerative (Zamboni *et al*, 2020).

1.1 The brains regenerative capacity

There is a limited capacity for spontaneous regeneration of the central nervous system (CNS), comprising the brain, spinal cord, and retina (Tam *et al*, 2014). Therefore, with few regenerative strategies available, patients with CNS injuries or diseases have few treatment options (Llorens-Bobadilla *et al*, 2020; Arvidsson *et al*, 2002; Zamboni *et al*, 2020).

Neurodegeneration is an umbrella term subsuming a heterogeneous family of neurodegenerative diseases commonly characterized by the pathological hallmark of abnormally aggregated protein in the brain. This phenomenon results in the progressive deterioration of the CNS impairing its neuronal circuits and its proper function (Seeley *et al*, 2009; Arendt *et al*, 2016; Kempuraj *et al*, 2016). The fact that neurodegeneration involves a progressive loss of neurons in the brain, highlights the potential of cell replacement and regenerative therapy, transplantation, and gene therapy among others therapeutic possibilities (Qian *et al*, 2020).

1.2 Direct reprogramming

Potential disease-modifying strategies for neurodegenerative diseases are being developed, with the last decades focusing on the restoration of the underlying diseased network, as with cell therapies. In line with this, studies to induce fate-switch of neural and non-neural cells in a transcription factor based-manner have been increasingly performed over the last decade (Cieślar-Pobuda *et al*, 2017; Janowska *et al*, 2019). This technology employs somatic cells for the generation of induced pluripotent stem cells (iPSCs) and induced neuronal cells (iNCs). To apply this in human research, disease- and patient-specific cell lines have been derived from patients diagnosed with neurodegenerative disease (Park *et al*, 2008; Soldner *et al*, 2011). The conversion of a somatic cell type into another, while bypassing a pluripotent state, represents not only a rapid way by which researchers must

generate the needed cells in the laboratory compared to induced pluripotent stem cell reprogramming (Kelaini *et al*, 2014; Wang *et al*, 2021a), but also a way in which tumorigenesis is potentially avoided (Fang *et al*, 2018; Cieślar-Pobuda *et al*, 2017) However, is worth mentioning that direct cell reprogramming, albeit avoiding a pluripotent state, an intermediate transcriptional state is induced until the desired phenotype is reached (Treutlein *et al*, 2016).

In the past century, a paradigm shift has been experienced within the field of cell conversion. Currently, basic notions of cell differentiation are well established ever since the unidirectional process model by Waddington in 1957 for reprogramming was challenged (Waddington, 1957; Waddington, 2012). To recapitulate, Waddington's landscape model firstly proposed how only cells belonging from the same germ layer can only differentiate from one type into another in a unidirectional manner. However, as aforementioned, nowadays this view has been reassessed with a huge body of evidence supporting the opposite, this new theory has been labelled as the cook island model (Gascón *et al*, 2017; Kelaini *et al*, 2014). What this model state is how cells from various lineages have the capacity to undergo trans-differentiation in vivo into cells belonging from other lineages, even from different germ layers, contrasting Waddington's model (Masserdotti *et al*, 2016; Gascón *et al*, 2017). Accordingly, throughout the last years, different research groups have presented studies on the molecular mechanisms driving cell conversion using a diversity of cells, like fibroblasts, mouse embryonic stem cells (Berninger *et al*, 2007; Heinrich *et al*, 2010; Caiazzo *et al*, 2011; Liu *et al*, 2013; Rivetti Di Val Cervo *et al*, 2017; Colasante *et al*, 2019) and even peripheral blood mononuclear cells (Tanabe *et al*, 2018) providing more insights into the mechanisms safeguarding cell identity (Brumbaugh *et al*, 2019).

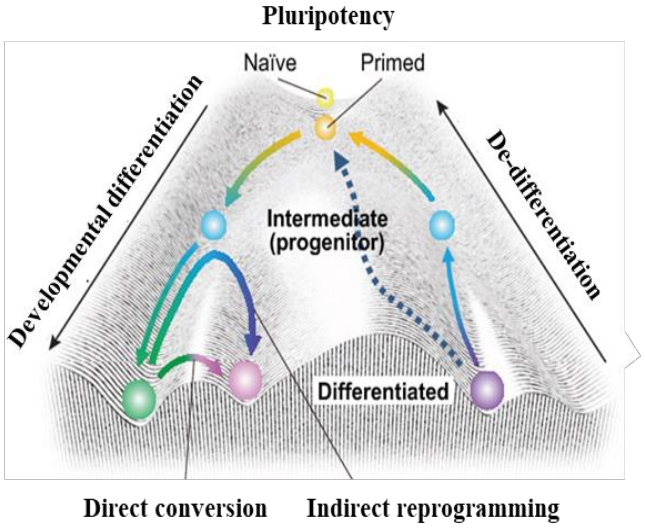

Figure 1.1 Conrad Waddington model of cellular manipulation a. *Epigenetic landscape model proposed by Conrad Waddington with the current approaches to manipulate cell identity. Taken from (Takahashi & Yamanaka, 2015)*

1.2.1 Potential applications with direct reprogramming

In order to understand and develop potential treatments for human disease, researchers are investing specifically, in the improvement of direct cell reprogramming methods. Reprogramming totally differentiated cells across lineages has uncovered how cells hold tremendous plasticity to reverse their fate commitment, arising new possibilities for generating powerful disease models and in regenerative medicine (Barker *et al*, 2018). Moreover, one favoring aspect of direct reprogramming as a promising approach for disease modelling relies on studies showing how patient-specific cell lines, retain age-associated cellular and epigenetics marks of the starter cell (Takeda et al., 2018). Accordingly, it has been reported how neurons induced from human fibroblasts by transcription factors retained donor-age-dependent transcriptomic signatures including their age-associated defects. On the contrary, cellular parameters such as the telomere length, mitochondrial function, DNA damage response and global heterochromatin were reset after iPSC induction (Mertens *et al*, 2015). Therefore, direct reprogramming

seems an adequate technique for the study of a variety of diseases, such as neurodegeneration like PD (Addis *et al*, 2011; Park *et al*, 2008; Soldner *et al*, 2011; Gascón *et al*, 2017; Rivetti Di Val Cervo *et al*, 2017) and its applicability goes through a wide range of possibilities from cell transplantation to regenerative medicine (Fan *et al*, 2020; Fang *et al*, 2018; Barker *et al*, 2018). However, the field of cellular reprogramming still harbors important hurdles that need to be overcome before it can be clinically translatable. Besides the efficiency rate tends to be low, it is known how in vitro reprogrammed cells remain immature, another aspect that hinders cell conversion is the specific epigenetic mark designed to each cell during embryogenesis, potentially acting as a barrier for a full identity conversion (Masserdotti *et al*, 2015). Herein, it is of high interest to unravel the underlying molecular mechanisms behind the changes in cell identity during direct lineage reprogramming in both, healthy and pathological conditions (Ring *et al*, 2012; Gascón *et al*, 2017).

1.2.2 Cell conversion with proneuronal factors expression

Reprogramming somatic cells with defined factors, which converts them from one lineage into another, has fundamentally altered our perception of cell identity and fate. This is normally accomplished through the ectopic expression of different molecules like transcriptional factors (TFs), alone or in conjunction with small molecules or other proteins with facilitating properties to alter cell identity (Wang *et al*, 2021a)

A wide variety of bioactive compounds have been identified to play a helpful role in boosting the enforced neurogenesis driving differentiation and, furthermore, prompting targeted cell maturation (Huangfu *et al*, 2008; Yamanaka, 2009; Federation *et al*, 2014; Ma *et al*, 2019; Janowska *et al*, 2019). Small compounds (SM) with a low molecular weight (900 Da) are known to act as potent modulators of glial activity, with epigenetic and transcriptional regulatory properties. A long list of small molecules has been tested and found to exert effective conversion

abilities. These compounds are becoming one of the preferred choices in research as they have differential effects depending on the cell type being used. A wide easily available selection of compounds exists, with diverse effectiveness in cell permeability and the possibility to develop sequential administration strategies (*Figure 1.2)* (Qin *et al*, 2017; Zhou & Sun, 2019; Basu & Tiwari, 2021).

Compound	Pathway	Effect	References
Forskolin	cAMP pathway	Activation	Liu et al., 2013, 2015; Li et al., 2015
Dorsomorphin	TGFβ, BMP	Inhibition	Liu et al., 2013, 2015
Noggin	BMP	Inhibition	Ladewig et al., 2012
LDN193189	TGFβ, BMP	Inhibition	Hu et al., 2015
RepSox	TGFβ	Inhibition	Hu et al., 2015
SB431542	SMAD	Inhibition	Zhang et al., 2015
Y27632	ROCK	Inhibition	Hu et al., 2015
Thiazovivin	ROCK	Inhibition	Zhang et al., 2015
SAG	Shh pathway	Activation	Zhang et al., 2015
Purmorphamine	Shh pathway	Activation	Zhang et al., 2015
DAPT	Notch signalling	Inhibition	Zhang et al., 2015
CHIR99021	GSK-3	Inhibition	Zhang et al., 2015
TTNPB	Retinoic acid	Activation	Zhang et al., 2015
Valproic acid	Chromatin modification	HDAC inhibition	Hu et al., 2015
ISX9	Ca^{2+} signalling	Activation	Li et al., 2015
I-BET151	BET family proteins	Inhibition	Li et al., 2015

Figure 1.2. List of small molecules and pathways action widely used to directly induce neuronal reprogramming. *Image taken from (Masserdoti et al, 2016).*

Additionally, and a wider approach used for converting cells, to modulate the transcription rate of genes involved in cell differentiation, DNA-binding proteins like transcriptional factors are also selected. These molecules specifically bind to regulatory sequences of the DNA known as distal *cis*-regulatory elements (Cre), or enhancer. Frequently, these elements affect which genes are turned on or off in the genome and are positioned thousands of base pairs from the transcription

start sites (TSSs) of their regulated genes (Hafner & Boettiger, 2022). Thereby these factors have a plethora of cellular functions by controlling gene transcription, protein synthesis, and ultimately cellular homeostasis (Adcock & Caramori, 2009). A characteristic feature of TFs is that some are ubiquitous, that is, common to several cell types, and some are cell-specific determining the phenotypic profile of a cell (Adcock & Caramori, 2009). The expression of the latter molecules has been previously shown to efficiently reprogram cell lineage conversion, both in vitro (Vierbuchen *et al*, 2010; Caiazzo *et al*, 2011; Masserdotti *et al*, 2015) and in vivo (Qian *et al*, 2012; Li & Chen, 2016; Liu *et al*, 2013; Colasante *et al*, 2019; Rivetti Di Val Cervo *et al*, 2017).

In normal development, cellular specification is highly regulated also by the collective actions of TFs, controlling cell-specific gene networks. For instance, Oct4, Klf4 and Sox2 are three important pluripotency factors known to influence the epigenome beyond their initial binding points (Mayran *et al*, 2018). Indeed, a number of transcription factors have been shown to be capable of converting one type of cell into another, (*Figure 1.3*) after the discovery that one single factor was able to fully convert mouse embryonic fibroblasts (MEFs) into myoblasts just by the forced expression of MyoD2 (Davis *et al*, 1987). Accordingly, the lineage-specific pro-neural factor such as Achaete-Scute Family bHLH Transcription Factor (Ascl1/Mash) is also known for its involvement in cell fate decisions and to be sufficient to convert cells from one lineage into another, making it a reliable master regulator. Indeed, Ascl1 is a well characterized factor shown to generate neurons from cells pertaining to unrelated lineages, (Pang *et al*, 2011; Chanda *et al*, 2014; Vierbuchen *et al*, 2010) even from peripheral blood cells (Tanabe *et al*, 2018). It is considered to be a key gene during development, usually being activated upstream in specialization pathways (Kelaini *et al*, 2014). In a later section, we will go into greater detail about this protein and its molecular effects during cell conversion.

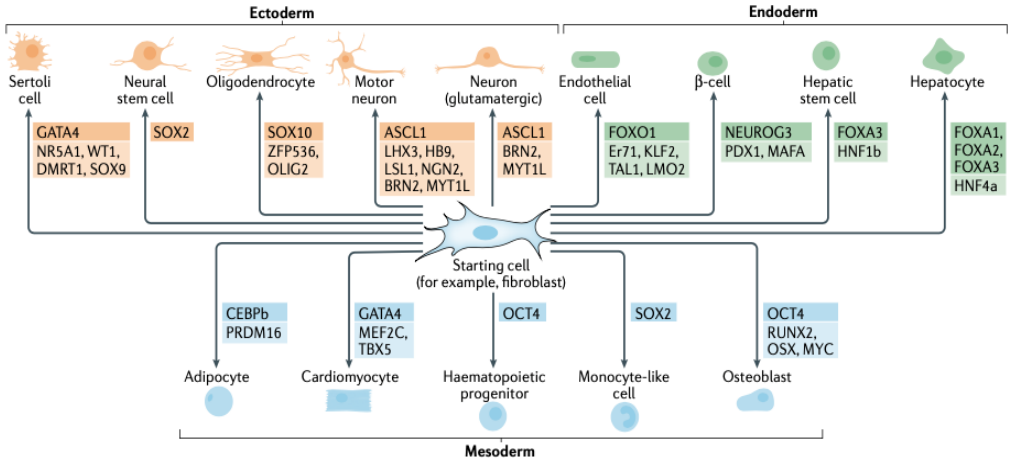

Figure. 1.3 Trans-germ layer lineage conversion. *Scheme taken from (Wang et al, 2021a).*

All in all, transcription factor-based reprogramming has been used for testing the effect of cell fate determinants that are known to be active during development. With gain-of-function experiments, it can be demonstrated how specific genes are necessary and sufficient to control certain processes of cell specification and differentiation. However, one potential limitation in this regard is that different factors can play a role in the establishment of lineage boundaries (Hersbach *et al*, 2022). However, this can be overcome by questioning and identifying key factors in the process and employing them accordingly to the efficacy strength they exert during cell fate implementation (Yamanaka, 2009; Gascón *et al*, 2017).

In conclusion, the conversion process has thus, been thoroughly studied, resulting in extensive information on how both bioactive compounds, TFs and SM alone or in combination, can affect the generation of neural progenitors, glia cells and neurons, both in vitro and in vivo (Blanchard *et al*, 2015; Torper *et al*, 2015; Pereira *et al*, 2017; Steiner *et al*, 2018; Li *et al*, 2019; Yamanaka, 2009; Ring *et al*, 2012; Liu *et al*, 2013). Furthermore, the differentiation of subtype-specific neurons by different combinations of transcriptional factors have demonstrated to successfully work in the conversion into functional induced neurons (iNs) (Yang *et al*, 2019; Pang *et al*, 2011; Colasante *et al*, 2019; Li *et al*, 2019). Interestingly,

reprogramming studies have shown promising results when aiming to apply the current knowledge to pathology, such as obtaining induced dopaminergic neurons from fibroblasts derived from PD patients (Caiazzo et al., 2011), or testing how brain injury can alter glial cell state to ease the identity switch in vivo, towards a neuronal fate (Zamboni *et al*, 2020).

Although there have been many studies in the field, from in vitro, to in vivo employing different CNS areas and under pathological paradigms, some discrepancies have been reported, with positive and negative results of glial conversion towards neurons (Wu *et al*, 2020; Chen *et al*, 2020; Puls *et al*, 2020; Chen, 2021; Xiang *et al*, 2021; Wang *et al*, 2021a). In fact, current impactful studies are reporting contradictory results regarding the efficiency of reprogramming even when applying previous approaches to overcome conversion barriers (Leib *et al*, 2022; Wang *et al*, 2021b).

1.3 Challenging the field

Indeed, since reprogramming can work fairly good in vitro, nevertheless, in vivo discrepancies appear, and results are met with skepticism (Leaman *et al*, 2022). Generally, it can be speculated, that among many variables identified, in vitro settings, not only is missing the whole environment cells are in but also how this one changes upon an insult (Grande *et al*, 2013). It has been reported that the local microenvironments including injury conditions have significant influence on the efficacy of reprogramming and subsequent survival of newly generated neurons in the mature murine brain.

Nevertheless, in vitro studies are still useful for elucidating many hurdles still encountered during trans differentiation that can then be applied to improve in vivo application. For instance, in vitro experiments using postnatal cortical astrocytes lead to the identification of a metabolic barrier that later proved useful in the injured mouse cerebral cortex by demonstrating the high conversion efficiency obtained by

protecting neurons from death and reactive oxidative species (ROS) during direct reprogramming of glia and many other types of cells (Gascón *et al*, 2016). This highlights how microenvironments are key players in the conversion process, as just by improving the environment to protect neurons from further damage promoted yield of induced neurons, ultimately aiming to promote circuit reformation and function (Barker *et al*, 2018; Gascón *et al*, 2016).

In this regard, it has been suggested that reprogrammed reactive astrocytes with stem cell characteristics can become neurons more easily and efficiently than quiescent astrocytes (Palmer *et al*, 1999; Grande *et al*, 2013). However, when trying to tackle this, new results reported how adeno-associated viruses (AAVs) had significant 'leakage' to nearby neurons when expressing *Neurod1* (Wang *et al*, 2021b) and since, other groups have confirmed limited glia conversion in cortex and striatum (Leib *et al*, 2022). Additionally, in PD mouse models, in the last few years new articles claim no astrocyte conversion in the substantia nigra and striatum, being devoid of astrocyte-originating dopaminergic neurons (Dans) when downregulating the repressor for reprogramming polypyrimidine tract binding protein 1 *(Ptbp1*) (Hoang *et al*, 2021; Chen *et al*, 2022; Wang *et al*, 2021b; Xiang *et al*, 2021; Qian *et al*, 2020). On top of that, they concluded that conversion was not observed regardless of the physiological or pathological conditions related to Parkinson's disease. It is extremely important to note that previous research has indicated the opposite, providing results on how astrocytes can become dopaminergic neurons when *Ptbp1* is repressed (Qian *et al*, 2020). This is of importance as based on this latter positive finding with this strategy, gene therapy has been proposed as a new repair strategy for patients with neurological disorders, such as Parkinson's disease, by inhibiting *Ptbp1*.

Additionally, when manipulating cell identity, inherent characteristics of the cells have been reported to determine their identity (Russo *et al*, 2021). Indeed, in neurons, mitochondrial function is particularly important, but the degree to which this organelle adapts to the induced fate is uncertain. Therefore, Russo and colleagues by monitoring fate transition during reprogramming revealed a delayed

and partial adaptation of mitochondrial function to the neuronal identity. By engineering the transcriptome of mitochondrial proteins through a deactivated or "dead" Cas9 (dCas9) they observed an improved reprogramming, thus demonstrating a broader role of mitochondrial proteins during fate conversion indicating that mitochondrial proteins act as enablers and drivers in this process (Russo *et al*, 2021).

Apparently, there is still a great deal of uncertainty regarding fate erasure and mechanisms for resolving cell identity conflicts. Seemingly, it is currently possible to convert any cell type into any other cell using a variety of different reprogramming paradigms. However, despite this variety and studies investigating the underlying molecular mechanisms of cell fate switch (Aydin *et al*, 2019; Yagi *et al*, 2021; Hersbach *et al*, 2022), besides the mentioned potential limitations, basic question remains open. Indeed, recent studies, tackles this by looking at the binding properties of pioneer factors in the genome during reprogramming and also how different cocktails of factors may also compete with each other or reach synergy in their conversion program (Lee *et al*, 2020; Aydin *et al*, 2019; Hersbach *et al*, 2022).

Ultimately, there has been much skepticism about the interpretation of the results from in vivo reprogramming due to their ambiguity. Certainly, after the meticulous study that genetically restricting AAVs transgene expression to glia might not be as specific as it appeared to be (Xiang *et al*, 2021; Leaman *et al*, 2022) increased the skepticism. Not only does this have implications for the extensive literature in this field, but it also raises questions about gene transfer tools for mediating conversion. Therefore, prior to aiming toward clinical application in pathological conditions, new and different approaches must be considered to really understand how conversion happens in a healthy adult brain, by understanding not only the nature of the different cells to target for conversion but also the one we aim to achieve (Barker et al., 2018) and in which manner.

Considering these results, it is necessary to consider new variables that affect conversion efficiency, and moreover, consider them holistically to ensure a proper transdifferentiation. This raises several obvious questions, such as the potential

effect the environment has on a cell as well as the influence that the development state may have in reprogramming, especially in vivo. Thus, along with local (healthy and disease) environment influences, a necessary next step would be to investigate how the developmental stage of the starting cell can affect the outcome of neuronal reprogramming (Gascón *et al*, 2017).

1.4 Factors influencing the In vivo vs In vitro discrepancies

1.4.1 The role of the original cell: Astrocytes.

In reprogramming the outcome of the cellular conversion depends heavily on the starting cell type, as it must be taken into consideration many factors such as the genetic or metabolic profile of both, the starting and the target cell. Therefore, considering that astrocytes are cells already within the CNS and that the bigger picture is also to restore an impaired network within the brain, they seem to be the perfect cells to target for this purpose. Besides, as each cell type of origin has a distinct chromatin structure and cellular environment, it can facilitate or hinder the reprogramming process (Gao et al., 2017; Aydin & Mazzoni et al. 2019). Indeed, during lineage conversion, it is believed that the epigenetic landscape of the starting cell is erased, and the cellular identity is reconfigured, often through a state similar to that of stem cells (Treutlein *et al*, 2016). Nevertheless, it is acknowledge that cells possess an epigenetic memory, which cannot be completely erased by direct lineage programming (Hörmanseder, 2021; Leaman *et al*, 2022). Indeed, reprogrammed somatic cells are known to retain memory of origin, such as DNA methylation signatures of its somatic tissue of origin, allowing the cell to differentiate toward lineages related to the donor cell and even also affecting the molecular network activated by transcriptional proteins to induce neuronal fate (Kim *et al*, 2010; Tian *et al*, 2011; Tobin & Kim, 2012). Indeed, this accounts for a current limitation in the field as complete reset of the epigenetic landscape is not reached (Basu & Tiwari, 2021).

Therefore, cells that are developmentally related to the target cell may result in a more feasible fate conversion as related gene regulatory networks, and chromatin landscapes contributes with the efficient upregulation of the genes associated with the new terminal fate (Wang *et al*, 2018; Leaman *et al*, 2022). Considering that astrocytes share a common progenitor with neurons, these cells are expected to be efficiently reprogrammed into neurons by the forced expression of TFs (Herrero-Navarro *et al*, 2021; Heinrich *et al*, 2010). Nevertheless, previous work done in reprogramming in vitro has shown how to successfully differentiate either human or mice fibroblasts into functional neurons (Liu et al., 2012; Liu et al., 2013; Masserdotti et al., 2015; Brulet et al., 2017; Tanabe et al., 2018 & Yang et al., 2019; Li et al; 2019; Aravantinou-Fatorou & Thomaidou, 2020). However, in spite of these studies on transdifferentiation, it is still unclear whether this knowledge can be applied to brain repair upon injury or neurodegeneration as many barriers are still encountered, even when cells are ontogenetically close (Smith *et al*, 2017)(Zhang et al., 2016; Guo et al., 2014). This lack of clarity is due to the overlooked fundamental molecular processes taking place, which are not yet understood nor fully known. Cell fate conversion, for example, entails a conflict of identity as a reprogramming transcription factor challenges the existing cell identity to induce a different (and even conflicting) program depending on the transcription factor and cell used. This was recently provided (Hersbach *et al*, 2022) in a new study in which multiple cell fate conversions were simultaneously analyzed through the development of a new single-cell based technique: Collide-seq, to tackle basic principles concerning fate erasure and the mechanisms to resolve cell identity conflicts.

By using combinatorial and traceable reprogramming factors these scientists reached interesting conclusions regarding the base of the conversion process. In their in vitro model, from the same dish (hence, controlling for culture conditions) of fibroblast they (i) did not find a common mechanism through which fibroblast-specific gene expression loss is initiated; (ii) that higher or lower levels of the factors used does not contribute to major changes, (iii) and that probably when using different factors together, a competition is triggered between cofactors.

Among all conditions they saw these effect to be heightened when combining Ascl1 and MyoD1. Which is interesting considering how these two are mainly known to induce their relative programs based on their DNA-binding affinities.

These results suggest that contrary to what it was expected, the relevant factors endogenously expressed in the initial cell, rather than the molecular capabilities of the fate determinant factors, may limit their reprogramming potential. Moreover, even when conversion is achieved, appropriate maturation of the final cell sometimes is not reached. Probably the failure in the maturation process is due to the potentially epigenetic conflicts between the original and yield cell (Kim *et al*, 2021; Leaman *et al*, 2022). There is no doubt that this is a drawback, as the gain of functional properties is essential for proper integration and interaction with the local tissue where reprogrammed cells are grafted. Therefore, proper understanding of different factors, such as the epigenetic landscape of cells, even of those closely ontogenetically is fundamental to overcome barriers during conversion (Leaman *et al*, 2022).

The work by Heins and colleagues in 2002, with the ectopic expression of the factor Pax6, was the first to successfully convert postnatal glial cells into neurons (Heins *et al*, 2002). From there, plenty of literature is found targeting postnatal astrocytes from the mouse to understand the conversion mechanisms towards obtaining neurons. A variety of factors combinations have been employed and characterized to further understand the final fate acquired. Thus, Ascl1, Neurogenin2, Dlx2, NeuroD1/D4 and Pax6 alone were reported to differentiate astrocytes into neurons in vitro (Heins *et al*, 2002; Berninger *et al*, 2007; Masserdotti *et al*, 2015).

1.4.2 Health brain status during conversion

An interesting point is that it has been reported that particularly reactive astroglia, or glial cells under injury conditions, are considered to be in a cellular

state facilitating reprogramming as after activation. However, the reprogramming capacity was different depending on the brain region (Grande *et al*, 2013). This is believed to be caused because they acquire stem cell potential, and becoming highly proliferative (Buffo *et al*, 2008; Sirko *et al*, 2013; Heinrich *et al*, 2014). However, contradictory results have been reported in this matter suggesting that a minor and selective population of these activated astrocytes has the potential to be reprogrammed (Bardehle *et al*, 2013; Heinrich *et al*, 2014) Indeed, the neuronal induction after an invasive injury or insult like a stroke has proven to be complicated, especially depending on the brain region (Buffo *et al*, 2005). Nevertheless, some studies have shown that this lassive environment seems a prerequisite to facilitate the action of some transcriptional factors, such as Ascl1 or NeuroD1 (Guo *et al*, 2014; Heinrich *et al*, 2014). More interestingly, it has been suggested that the reprogramming capacity due to factors co-expression enhanced the reprogramming outcome (Heinrich *et al*, 2014).

In conclusion, many studies have attempted to reprogram under pathologic conditions, with varying and even contradicting results (Leaman *et al*, 2022). Alternatively, it is plausible that in the adult brain, some regions such as the neocortex and striatum and some resident cells intrinsically retain precursor properties enabling them to be reprogrammed. However, it has even been proposed that for this capacity to be unlocked, strong stimuli like an insult is required (Grande *et al*, 2013).

1.4.3 Developing an identity from the same source

Considering neurons and astrocytes share a common progenitor, one important aspect to consider is the transcriptional program enabling astrocyte identity formation as in the end, these are two distinct cells with their own identity (Herrero-Navarro *et al*, 2021). Therefore, despite coming from a common progenitor cell, transcriptional programs must harbor the differences these cells will display later in development.

Many transcriptional factors have been identified as triggers and regulators of astrocyte differentiation and latter maturation. Interestingly, among these studies there is compelling evidence for a relevant role of the family factors *Nfi*. More interestingly, *Nfia* has been observed to be important not only for the onset of astrogliosis but also throughout the whole maturation process of astrocytes (Lattke *et al*, 2021). Indeed, it has been reported how this factor does so by regulating suppressive and inducting gene expression modules of neuronal and astrocyte fate (Tiwari *et al*, 2018; Lattke *et al*, 2021). Another transcriptional factor involved in defining the astroglia cell fate is SRY-Box Transcription Factor 9 (*Sox9)* (Caiazzo *et al*, 2015) as it was shown to be sufficient in the conversion of embryonic and postnatal mouse fibroblasts into astrocytes. Although few markers are currently used to identify astrocytes, including glial fibrillary acidic protein (*Gfap*) and glutamate transporter 1 *(Glt1*), however, it is also known how *Sox9* is highly enriched in astrocytes (Sun *et al*, 2017; Klum *et al*, 2018; Neyrinck *et al*, 2021). Moreover, this factor shows to specifically label astrocytes outside neurogenic regions, in the subventricular zone (SVZ) and the subgranular zone (SGZ). Moreover, the expression of *Sox9* at mRNA and protein level does not diminish with age or the functional stage cells are found, remaining nuclear also in fully mature astrocytes (Sun *et al*, 2017). The importance that *Sox9* and *Nfi* factors have in astrogliosis has been supported by substantial studies showing how they physically associate in a protein complex and collaborate to control fate induction and glial-specific genes choice in early development (Lattke *et al*, 2021). Overall, many studies have added to the discovery of many markers to properly characterize astrocytes, highlighting the need to not just rely on *Gfap* as its expression has seen to vary greatly depending on the brain region and maturation state of astrocytes with a correlation that is not always proportional, being also expressed on progenitor cells (Escartin *et al*, 2021).

1.4.4 Astrocyte brain region specificity

Single-cell sequencing experiments in adult tissues distinguished astrocyte heterogeneity showing how distinctive transcriptomic profiles predicts the morphological and functional specialization of individual astrocyte subtypes. Moreover, it appears that these complex molecular fingerprints between subtypes are large enough to indicate distinct specializations in the known functions of astrocytes (Batiuk *et al*, 2020). Overall, and together with previous reports (Lattke *et al*, 2021), it is now acknowledged the differentiations process in astrocyte during maturation, inter- and intraregional heterogeneity within the CNS and more intriguingly, a distinct cortical layering and hippocampal compartmentalization of astrocyte subtypes further displaying distinctive morphologies and physiologies (Batiuk *et al*, 2020).

Hereof, the environment, as brain region, can impact chromatin organization and composition within a cell. Hence, chromatin modification in genes targeted by neurogenic TFs driving conversion can differ between these astroglia cells from different regions of the nervous system. As noted in some studies (Chouchane *et al*, 2017; Pollak *et al*, 2013) astrocytes isolated from the cerebellum or neocortex can be converted to produce iNs with some of the hallmarks of neurons from these areas, regardless of TFs ectopic expression**.** Accordingly, it has also been reported how the same factor can trigger specific neuronal gene programs in astrocytes based on their origin within the brain (Herrero-Navarro et al., 2021). Moreover, the specification of neuronal fates can be modulated by microRNAs or long non-coding RNAs expressed in different astroglia cells from different regions (Flynn & Chang, 2014; Jönsson *et al*, 2015). Moreover, it has been reported how *Ascl1* lineage-reprogrammed cortical and cerebellar astroglia generated granular cell layer (GCL) and periglomerular (PGL)-like interneurons at different ratios (Chouchane *et al*, 2017).

To summarize, when converting a cell, not only the type of cell matters, but the environment and brain region where the cell resides can also influence its fate. Even

from the same cell type, different TFs activate distinct gene networks in different CNS regions (Chouchane *et al*, 2017).

1.4.5 The maturation trajectory of astrocytes during brain development

Over the past century, the diversity of astrocytes function has emerged. Nevertheless, there is a gap in the progress done in understanding their early differentiation compared to how astrocytes become functionally (Yang *et al*, 2013). Indeed, within the CNS, astrocytes undergo a dramatic maturation process affecting not only morphology but in the acquisition of important functions. Immature astrocytes play an important role in the vascularization system of the brain vascularization, blood-brain barrier (BBB) establishment, and synaptic formation and elimination. Along with maturation these cells acquire new and fine functions adapted and required for the homeostasis of the mature brain. In this sense, neurons are supported metabolically and trophically by them, hence influencing neuronal activity; the already established BBB is further regulated and modulated, along with the local cerebral blood flow (Tabata, 2015; Lattke *et al*, 2021).

Despite these known roles, the precise mechanisms orchestrating astrocyte maturation and development to form functional neurovascular circuits and carry out these diverse functions remains relatively unknown. Moreover, in vitro-differentiated astrocytes are thought to remain immature. Therefore, possibly the mechanisms identified so far are still unclear as in vitro cells seem to lack the complete maturation profile as those of astrocytes in vivo. A study published this year by Lattke and colleagues., analyzed the molecular mechanisms operating in astrocyte maturation by performing an extensive study looking at the transcriptional and chromatin changes in both, in vivo and in vitro (Lattke *et al*, 2021). The authors concluded that a set of specific transcriptional factors have a pivotal role in inducing different sets of mature genes in cells, which are generally found to be downregulated in-vitro. According to the study, gene ontology analysis showed that these were related to biological functions controlling the establishment of different

astrocyte properties, which mature astrocytes need to function. These set of transcriptional factors identified pertain to the family of ROR (Rorβ), homeobox (Dbx2 and Lhx2) and Fezf2 family. In essence, these data provide a powerful ground to induce maturation of astrocytes In vitro by the ectopic expression of the aforementioned factors prior to reprogramming. This information is valuable considering it can impact the way studies regarding cell reprogramming, using astrocytes, have been taking place. A deeper understanding about astrocytic identity could be gamechanger for the improvements in transdifferentiation towards neurons, especially when applying it for adult subjects.

Wrapping all in, since unlike any other tissue in the organism neurons upon damage or degeneration in the CNS are unable to regenerate, directed glial differentiation aimed towards the restoration of nervous tissue holds great potential for many medical purposes (Smith *et al*, 2017; Janowska *et al*, 2019). All in all, despite we still encounter many challenges contributing to the current lack of understanding of the molecular basis of the reprogramming process, over the past decade the scientific community have provided amazing strides in the advance of this technology (Wang et al., 2021).

Based on the considerations, it is not inaccurate to propose how a cell's environment, epigenetic signatures and its maturation state may influence cell conversion outcome, contributing to the existing discrepancy between the results found in vivo and in vitro.

1.5 Epigenetics

During brain development, different gene expression programs guide the development of different cell types and thereby, the specification of brain regions in an interdependent manner to endow these areas with functional activities. Indeed, specific trajectories in cell identity are determined by the finely tuned co-regulation of specific set of transcripts in a particular and unique spatiotemporal window

(Herrero-Navarro *et al*, 2021). In the mammalian brain, this occurs most dramatically during the "neurogenic switch", thus in the transition from the neurogenic towards the glycogenic competence in progenitor cells (Rowitch & Kriegstein, 2010; Ming & Song, 2011).

This process is regulated by several epigenetic signatures *(Figure 1.4*), including the non-coding genome which harbors all the regulatory sequences involved in gene regulation (Statello *et al*, 2021). Additionally, contrary to permanent changes in the DNA sequence, which happens by genetic alterations as mutations, epigenetic modifications are instead reversible modifications occurring in the DNA and chromatin that regulates gene expression (Rodríguez-Paredes & Esteller, 2011; Lardenoije *et al*, 2015).The epigenetic machinery exerts multiple mechanisms of control, including covalent modifications of DNA, like methylation and demethylation, chromatin remodeling such as acetylation/methylation or phosphorylation and, as mentioned, the posttranscriptional alterations affecting the regulation of non-coding RNA.

This complete set of epigenetics elements across the entire genome form, what is known as the epigenome (Berdasco & Esteller, 2019), and any abnormality can result in the inappropriate activation/inhibition of genes, influencing the tight control of the gene expression programs that governs, among others functions, the proper balance between the stabilization and plasticity of cell differentiation and identity (Mohn & Schübeler, 2009; Asmar *et al*, 2015; Cosenza & Pozzi, 2018). The plethora of molecular processes behind the control of transcriptional programs are specified by synchronized mechanisms comprising transcriptional factors, 3D chromatin organization and the reinforcement action of epigenetics (Becker et al., 2016; Peric-Hupkes et al., 2010).

Accordingly, cell-fate decisions are determined by the complex interplay between the different epigenetic regulatory layers like DNA methylation, chromatin accessibility, histone modifications and the newly study field of 3D chromatin organization.

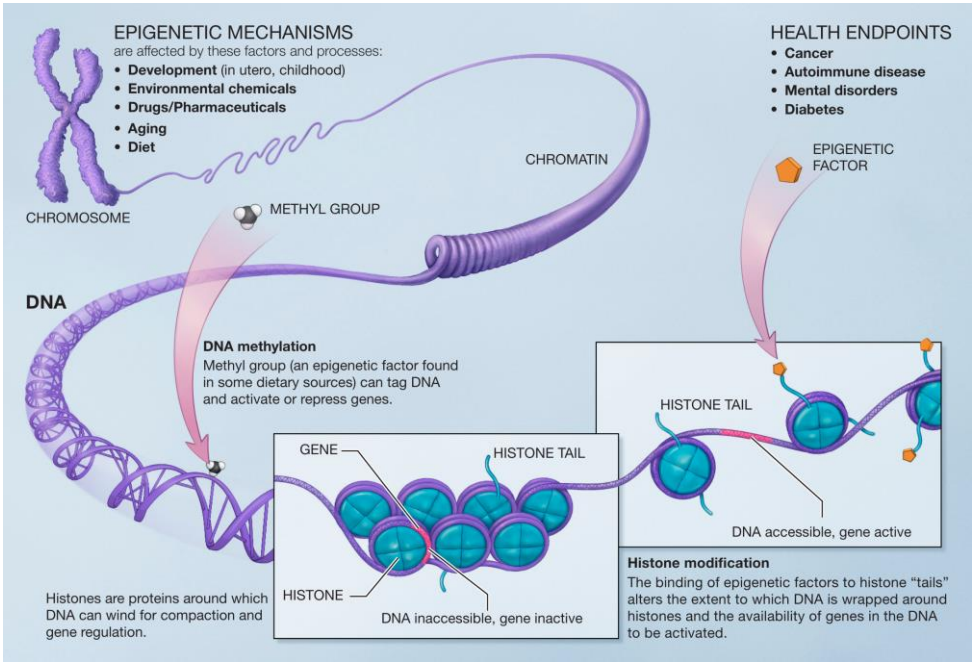

Figure 1.4. Illustration of the different epigenetic mechanisms. *Taken from the NIH via Epigenomics - Epigenetic Mechanisms (nih.gov).*

1.5.1 DNA methylation

De novo DNA methylation is crucial for embryonic brain development, occurring in a tissue-specific manner along the CpG sequence of the mammalian genome and associated with transcriptionally silent and active DNA (Aboelnour & Bonev, 2021). Together with histone proteins, DNA undergo reversible covalent modifications to establish genome contacts in cis regions. Indeed, DNA methylation can alter genome folding through the modulation of the protein-DNA binding properties. Thus, analyzing chromatin marks and DNA methylation patterns in the genome allows one to annotate and predict functions of genome regions .(Aboelnour & Bonev, 2022, 2021).

During cardiac, neuronal, and pancreatic reprogramming it has been reported that DNA methylation changes occur globally(Khurana *et al*, 2021). When converting mice fibroblasts by forcing the expression of neuron-inducing factors, cells presented a reorganized pattern of genomic methylation resembling those of mature cortical neurons. Interestingly, the ectopic expression of *Ascl1* shows to

generate De novo methylation at promoters of lineage specific genes through the upregulation of DNA methyltransferase Dnmt3a (Luo *et al*, 2019). Indeed, a significant reduction of conversion efficiency was observed when Dnmt3a was downregulated (Luo *et al*, 2019). This effect has also been observed in other cell types like acinar and cardiac cells (Fujita *et al*, 2019). In 2021, Zocher et al reported new insight of de novo methylation's role during mice adult hippocampal neurogenesis as a critical regulatory layer in mature neuron maturation and functional integration in the hippocampus (Zocher *et al*, 2021). The researchers demonstrate that hippocampal function depends on proper establishment of neuronal methylomes during adult neurogenesis. Overall, the coordination of reprogramming factors is crucial to reconfiguring the DNA methylation landscape globally to facilitate cell fate conversions.

1.5.2 Chromatin remodelling

DNA and histone methylation is a defining feature of mammalian cellular identity and essential for normal development (Hyland *et al*, 2005; Ziller *et al*, 2013). When eukaryotic cells are not diving, the principal component of the cell nucleus is the chromatin, which is the result of the complex formed by DNA and the positively charged histones. This interaction makes it possible for the DNA to fold into a compacted microscopic space, known as nucleosomes (Annunziato, 2012; Dey *et al*, 2021) .This latter component forms the basic structural unit of chromatin, and it consists of eight histone proteins and approximately 147 base pairs of DNA (Bradbury, 1989; Bendandi *et al*, 2020). It is in the diversity of the histone code states, which allows for the fine tuning in gene expression and regulation (Annunziato, 2012; Lardenoije *et al*, 2015).

Eukaryotic genome is packaged in the form of chromatin , which exists in two conformational states influenced by histone disposition and its given code due to the modification at its N-terminal tails (Huisinga *et al*, 2006). Hence, euchromatin, refers to a decondensed form and open structure enabling transcriptional activation,

whereas a condensed chromatin or heterochromatin, is characterized by a gene-poor compacted structure, blocking transcription (Sebestyén *et al*, 2020; Huisinga *et al*, 2006).

Overall, the structure of chromatin within the nucleus of a cell is critical for regulating gene expression. In this way, heterochromatin regions are highly compacted and therefore, shows a distinct nuclear compartmentalization (Sebestyén *et al*, 2020). This versatile chromatin conformation orchestrates in a switch-like mode diverse genetic programs by the different modification affecting DNA and histones. Accordingly, histone acetylation is the most well-defined epigenetic mechanism known to modify the *ε*-amino group of a protein's amino acid chain (Yang & Seto, 2007; Podobinska *et al*, 2017). Acetylation of the side chains of lysine's neutralizes the charge on histones and therefore, increases chromatin accessibility enabling transcriptional activation as it diminishes their ability to bind to the negatively charged DNA molecule (Glozak & Seto, 2007). Equally important, histone and DNA methylation plays a variety of important roles during mammalian development (Greenberg & Bourc'his, 2019). This is a simple biochemical process which involves transferring one or more methyl groups to the 5^{th} position on the cytosines pyrimidine ring, to form 5-methylcytosine in the DNA and at all basic residues, especially lysine's at histone tails (Jones, 2012; Moore *et al*, 2013; Lardenoije *et al*, 2015). In Vertebrates, and in the case of DNA modifications the establishment and maintenance of methylation is achieved by the help of a conserved family of DNA methyltransferases (DNMTs) in a dynamic or stable fashion (Greer & Shi, 2012). In general, methylation is frequently regarded a 'silencing' epigenetic mark found mostly in heterochromatin (Jones, 2012; Lardenoije *et al*, 2015). Overall, these former modifications are mediated by key proteins acting as epigenetic tools capable of adding, removing or recognizing specific markers in the chromatin. Therefore, depending on their function enzymes are known as erasers, writers and readers (Biswas & Rao, 2018). For instance, on methylation events, and as for lysine alterations occurring at histones, they are known as histone lysine methyltransferase (HKMTs) for histone writers, and histone lysine demethylases (HKDMs) for demethylation processes or erasers

(Lardenoije *et al*, 2015). Importantly, in order to understand where these alterations are, there are histone code readers containing evolutionarily conserved domains, such as the Bromodomain-proximal PHD finger (BPTF), that constitute cellular proteins with the ability to recognize and bind to specialized domains at different chromatin modifications to exert their effects (Mellor, 2006). All in all, a plethora of molecular effectors like methyltransferases and demethylases have been identified to orchestrate the addition and removal of methyl groups from different lysine residues on histones (Greer & Shi, 2012).

Among the different modifications identified, tail methylation mostly occurs at lysins and arginine residues of H3 and H4. Interestingly, the complex interplay these modification holds are distinctive (Asmar *et al*, 2015). Therefore, depending on the histone protein affected, the amino acid being modified or even the number of adenyl or methyl groups added, DNA access can be regulated having different effects on the genetic expression pattern (Ziller *et al*, 2013). Thus, methylation of histone 3 lysine 36 (H3K36me) and try-methylation of lysine 4 (H3K4me3) are associated with gene expression, instead the addition of three methyl groups at histone 3 and 4 at specific lysine groups, H3K27me3, H3K9me3, H4K20me3, respectively are linked to gene repression (Bannister & Kouzarides, 2011; Lardenoije *et al*, 2015). Nevertheless, heterochromatin regions have been usually associated with methylation of H3, more specifically with the better understood H3K27me3 and H3K9me3 marks, referred as heterochromatin-associated histone marks (Becker *et al*, 2016) (Becker et al., 2016).

There is considerable evidence that histone methylation plays a crucial role in nearly all biological processes ranging from DNA repair and cell cycle, transcription identity and development (Greer & Shi, 2012).Despite the fact nucleosome positioning and DNA methylation govern gene pattern expression, how they work together to maintain cell identity is yet unclear (Luo *et al*, 2017). For the establishment and maintenance of a cell differentiated state, besides the activation of the specific transcriptional programs, one integral feature for cells` identity is likewise, the proper silencing of genes of alternative lineages (Becker *et al*, 2017).

Therefore, for any given cell within an organism, the transcriptional landscape defines cell identity and its biological functions (Ye & Sarkar, 2018; Casamassimi & Ciccodicola, 2019). Despite the knowledge heretofore obtained to study gene activation in identity formation, lesser information is available regarding the epigenetic mechanisms behind cell type-inappropriate genes silencing.

Overall, understanding gene repression is an important concern not only for the sake of cell fate control understanding, but for the proper development of models used in cell reprograming approaches.

1.5.3 Epigenetic role in Cell identity and reprogramming

Recapitulating from some notions previously introduced, different cellular features such as cell identity and physiological role are established during development by an orchestrated and complex interplay between the individual master transcriptional factors and the local epigenetic environment which ensures a specific genomic state (Baumann *et al*, 2019; Smith *et al*, 2016). As mentioned, mechanisms controlling these transcription programs are DNA methylation and posttranslational modifications of histones. These may enable for the establishment of an epigenetic footprint ensuring cell identity. Actually, heterochromatin is further divided between "*constitutive*" forming tightly packed genomic areas, which are found at centromeres and telomeres, and present in genes across developmental lineages; and then there is "*facultative*" heterochromatin for locus- or cell type-specific heterochromatin with a dynamic compaction and silencing during development (Nicetto & Zaret, 2019; Methot *et al*, 2021; Padeken *et al*, 2022).

The various proteins involved in the remodeling and modification at the chromatin level play a relevant role in cell reprogramming (Mertens *et al*, 2015). In line with this, several studies have seen how the chromatin domains rich in the constitutive heterochromatin marker H3K9me3 could impede direct

reprogramming (Peric-Hupkes *et al*, 2010; Becker *et al*, 2017). This is explained by the fact that during development it's important for cell identity determination that some regions of the chromatin are more compacted and therefore more transcriptionally repressed to ensure lineage commitment and aberrant engagement in alternative fates.

1.5.4 H3K9me3 as a barrier for cell conversion

Transcriptional factors and epigenetic mechanisms work together to regulate gene expression to establish and maintain cell identity. As a key epigenetic mechanism, heterochromatin formation contributes to genome stability and gene silencing according to cell type. Despite traditionally being associated with noncoding gene regions of the genome, the histone mark H3K9me3 has as a key function in preventing TFs from activating genes that are inappropriate for the lineage in which cells belong (Becker *et al*, 2016; Wang *et al*, 2018). Indeed, H3K9me3-mediated heterochromatin regulates lineage commitment and cell identity in terminally differentiated cells (Nicetto *et al*, 2019; Becker *et al*, 2016; Nicetto & Zaret, 2019; Becker *et al*, 2017). A new understanding of how to modulate cell fate provides further insight into H3K9me3's ability to influence cell identity and goes beyond the idea that H3K9me3 is primarily a mark of constitutive heterochromatin.

In this regard, it has been demonstrated that H3K9me3 domains prevent terminally differentiated cells from converting into different types of cells. Therefore, different strategies for modulating this mark have been applied. Consequently, depletion of Histone methyltransferases (HMTases) has been associated with an increase in Oct4 and Sox2 binding in fibroblasts (Soufi *et al*, 2012); downregulation of H3K9me3-related proteins enhances fibroblast-to-hepatocyte reprogramming (Becker *et al*, 2017); and by suppressing H3K9me3 heterochromatin, iPSC cell reprogramming (Soufi *et al*, 2012) and somatic cell nuclear transfer (SCNT) is improved, while H3K27me3-marked genes are only

marginally activated (Matoba *et al*, 2014; Liu *et al*, 2018; Becker *et al*, 2017), and some can still be bind by TFs and RNA polymerase (Breiling *et al*, 2001).

Nevertheless, limitations are still encountered despite how promising these techniques are in terms of In vivo functionality. When directly reprograming, the converted cell still exhibits a differential gene expression profile in comparison to those of the target cell type (Becker *et al*, 2016). In light of these studies, repressive mechanisms in cell fate conversion should receive the same attention that activators mechanisms have had.

1.6 The 3D Genome Organization as an Epigenetic Determinant

Nuclear organization of the folded genome conforms the three-dimensional (3D) architecture of the chromatin. Several layers have been characterized during the years, from the most simple ones such as chromosomal territories up to interaction between two specific genomic loci as little as 1kb (Pelham-Webb *et al*, 2020). Chromatin structure influence several cellular processes such as cell differentiation and identity (Boettiger *et al*, 2016). This 3D spatial positioning is a robust, yet flexible architecture (Bonev & Cavalli, 2016), that ensures resistance to perturbation during development but contemporaneously allowing the genetic material to be expressed and replicated properly (Rowley & Corces, 2018).

First and foremost, our ability to detect different structural component inside the nucleus relies on our technological resolutions (*Figure 1.5)*. Different technologies have been developed being pivotal to gain insight into genome folding (Kempfer & Pombo, 2020; Bonev & Cavalli, 2016). Specifically, two main techniques have pushed further our knowledge. Microscopy based technologies such as STORM (Rust *et al*, 2006) and PALM (Betzig *et al*, 2006), ligation-based technologies and ligation-free technologies (Rao *et al*, 2014). Even though each can carry their own limitations, the common theme remains their ability to discriminate contacts inside the nucleus, depending on the resolution they can reach. At this stage, the approach that can reach the highest resolution is the ligation-based Hi-C methods (Bonev *et al*, 2017; Rao *et al*, 2014).

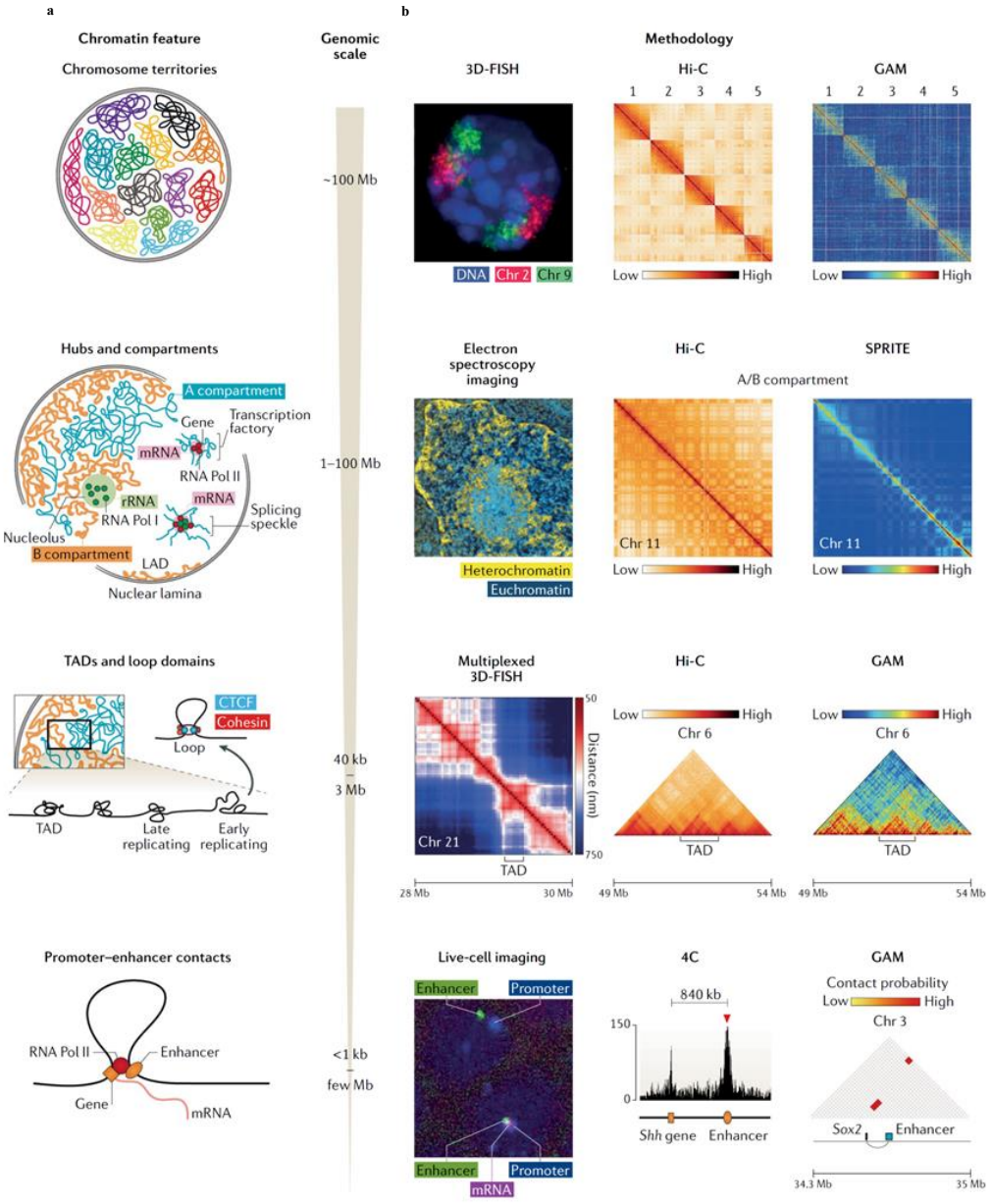

Figure 1.5. Genomic layers and methodologies*. **a**. Different structural chromatin features.* ***b****. Methodologies available to study the different layers of chromatin organization and gene regulation. Taken from (Kempfer & Pombo, 2020).*

At the lowest resolution, up to 1mb, it is possible to divide the genome into different compartments (Lieberman-Aiden *et al*, 2009; Rao *et al*, 2014). Which are widely known as A and B compartments. As we already pointed out, chromatin exist in two versions, depending on its degree of compaction: euchromatin and heterochromatin. Further segregation of these two chromatin types give rise into

these subnuclear A-B compartments. At a higher resolution (<100kb), it is possible to distinguish specific regions characterized by a high self-interaction frequency respect to neighboring domains (Dixon *et al*, 2012). These regions, termed for the first time by Dixon and colleagues, as contact domains or topological domains (TADs), are delimited by well-defined confinements called boundaries as they seem to represent abrupt transitions between these regions in the genome (*Figure 1.6*). More interestingly, these confined regions, in many cases, contain divergent CCCTC-binding factor (CTCF) sites (Kempfer & Pombo, 2020). These anchors generally define another substructure in the chromatin called chromatin loops (Rao *et al*, 2014). Indeed, at a resolution scale of 10-5kb, these loops are thought to be responsible of long-range chromatin contacts, generally bringing into close spatial proximity enhancers with its target promoter, to regulate transcription (Bonev & Cavalli, 2016). Nevertheless, other non CTCF mediated loops types are being described, such as gene loops and polycomb-mediated loops (O'Sullivan *et al*, 2004; Bonev & Cavalli, 2016).

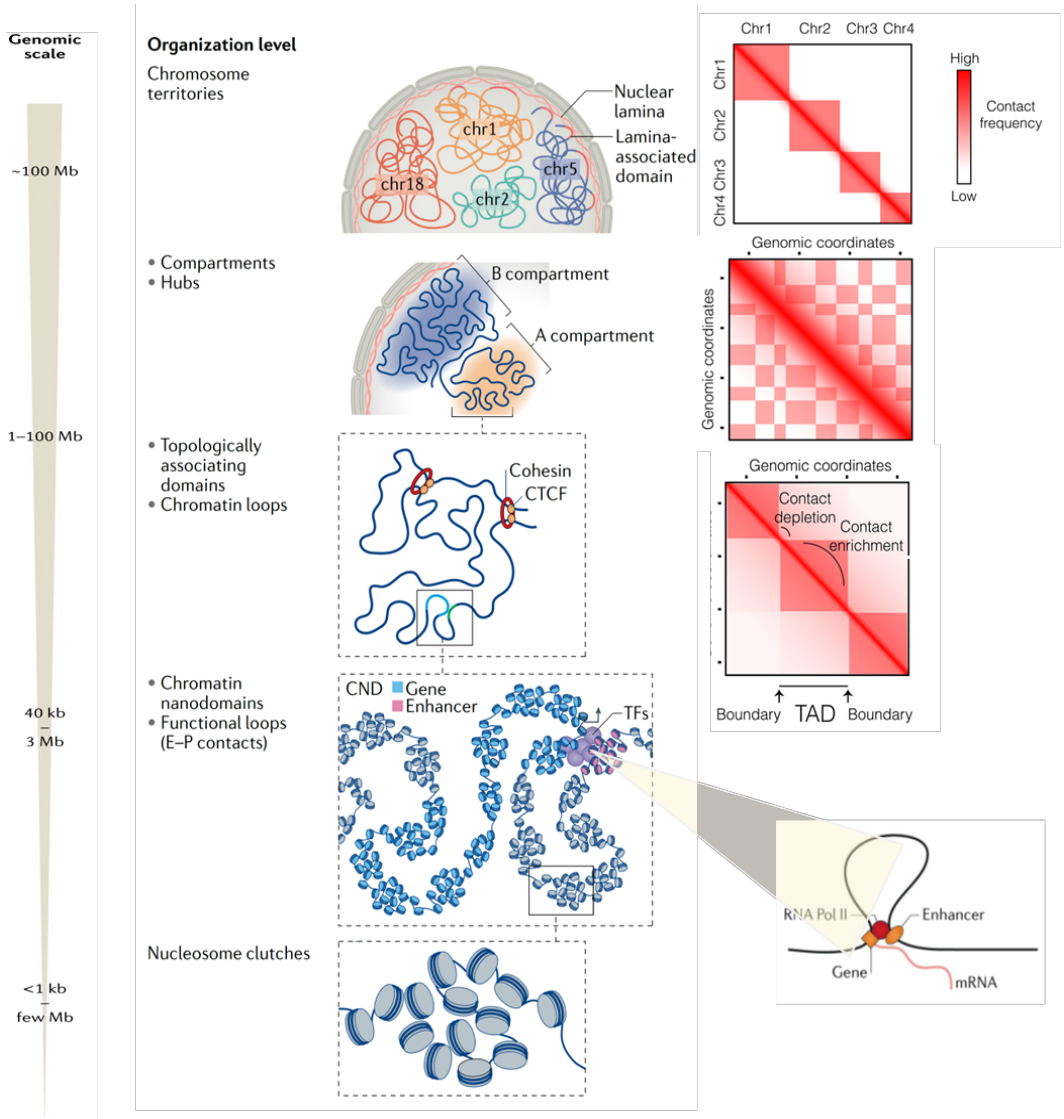

Figure 1.6. Chromatin organization*. The different levels of chromatin organization, with its corresponding genomic scale. Images illustrating each level and how these are presented in genomic analysis. Adapted from (Kempfer & Pombo, 2020; Jerkovic & Cavalli, 2021; Szabo et al., 2019).*

Additionally, these structural elements, together with cohesin have been also described as mediators of lamina-associated domains (LADs) (van Schaik *et al*, 2022) within the nuclear lamina, as another fundamental constituent of chromatin organization (Turgay *et al*, 2017; Rowley & Corces, 2018). These are formed by the interactions between the chromatin and the nuclear envelope via by the intermediate filament proteins A and B-type lamins (*Figure 1.7*) (Turgay *et al*,

2017). Interestingly, during cell differentiation processes, the spatial and temporal regulation of gene expression is linked to LAD association or detachment from the nuclear lamina (van Schaik *et al*, 2020). Indeed, there is a correlation between these LADs, heterochromatin and transcriptional repression (Leemans *et al*, 2019) due to the enrichment of H3K9me2 and H3K9me3 histone modifications at LADs (Kind *et al*, 2013). Additionally, another heterochromatin mark, H3K27me3, is also present at LADs borders (Kind & van Steensel, 2010). Moreover, the association of LADs and a repressive environment has been described by several studies showing how Lamin A functionally interacts with polycomb-group proteins (PcG) (Cesarini *et al*, 2015; Marullo *et al*, 2016; Salvarani *et al*, 2019), which maintains highly condensed DNA genomic regions due to its unique packaging properties (Boettiger *et al*, 2016). Essentially, these form multimeric complexes known as Polycomb Repressive Complex 1 and 2 (PRC1 and PRC2) (Sebestyén *et al*, 2020).

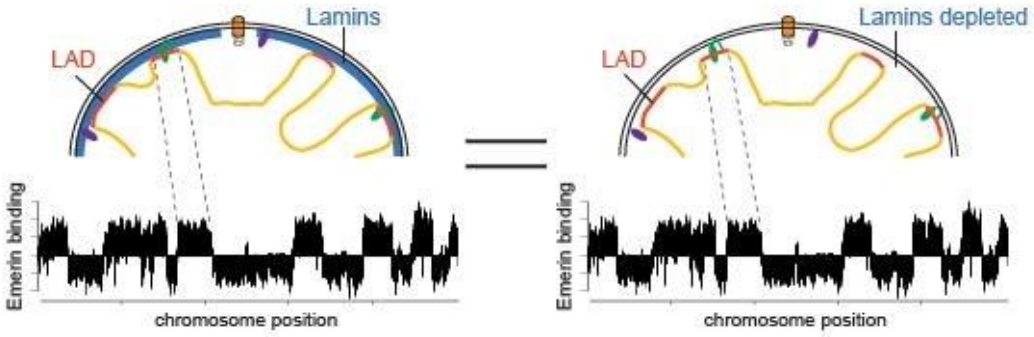

Figure 1.7. Lamina-associated domains in the nucleus*. Adapted* from *(Amendola & van Steensel, 2015).*

The biological importance of the nuclear lamina and its arrangement preservation was underlined by the presence of pathological mutations in lamin A protein in Hutchinson–Gilford Progeria Syndrome (HGPS) in humans (Ullrich & Gordon, 2015). Recently, it has been shown that early alterations in the nuclear lamina does not directly affect the normal distribution of H3K9me3 which is normally observed at later passages in HGPS fibroblasts. Instead, it was found a link with polycomb (PcG) associates loci, altering H3K27me3 distribution.

Therefore, despite there was no apparent changes in overall H3k9me3 distribution, it was those associated to LADs showing a rearrangement toward the center of the nucleus and not at the periphery(Masserdotti *et al*, 2015).

These interesting results were obtained thank to the development of a newly designed technology called Sequential Analysis of Macro-Molecules accessibilitY (SAMMY-seq), for genome-wide characterization of lamina-associated heterochromatic regions. It does so by exploiting the biochemical properties associated with chromatin compaction, and thus its distribution across nuclear compartments as opposed to Hi-C technique, which relies in pair-wise contact interaction without considering the topology of the chromatin (Sebestyén *et al*, 2020).

Overall, chromatin folding is composed in a multi-scale manner where regulatory information resides at each of its levels. Clearly, the 3D genome folding cannot be seen merely as a structural disposition, but essential for relevant biological functions like cell differentiation and for its spatiotemporal regulation of gene expression. Indeed, alterations at any level can lead to genetic alterations and the development of different pathologies (Zheng & Xie, 2019).

In conclusion, by applying chromatin-state mapping studies, inherited cellular states can de deeply analyzed. In the bigger picture, this technology holds great potential to unveil unknown genome function, encompassing the mechanisms of chromatin structure and its interrelationship with transcription, and its contribution to different pathologies (Baker, 2011).

1.7 Ascl1 in neurogenesis and as a pioneer reprogramming factor.

Neuronal circuits are formed by diverse types of neuronal cells in the nervous system. The combinatorial activity of transcription factors generates the array of cellular complexity within the brain. (Aydin *et al*, 2019). In this regard, mammalian neurogenesis is controlled by neurogenic fate determinants pertaining to the evolutionarily conserved basic-helix-loop-helix (bHLH) family, such as

Ascl1/Mash1, which are both, necessary and sufficient for the generation of newborn neurons (Raposo *et al*, 2015; Park *et al*, 2017). These factors ensure the proper balance by which the types of neuronal and glial cells are generated at a specific place and time during development for the formation of functional neural circuits. They regulate many genes and regulatory regions that are involved in cellular processes like proliferation, maturation and cell specification (Castro *et al*, 2011; Dennis *et al*, 2019; Woods *et al*, 2022). More particularly, these factors have been used to reprogram neural cells based on their differentiation properties. Together with Ascl1, another important factor playing a key role in promoting neurogenesis is Neurogenin 1 and 2 (Ngn1/2), by supporting cell cycle exit and neuronal differentiation in a variety of progenitor cells (Bertrand *et al*, 2002; Castro *et al*, 2011; Raposo *et al*, 2015). In fact, these factors enable neuronal identity to be specified, and are considered main regulators of neural determination. Despite the known role of these factors in determining subtype neuronal identity, it has been shown in numerous losses and gain of function studies, that Nng2 and Ascl1 drives the acquisition of a pan-neuronal phenotype and neuronal subtype specification in an independent fashion (Aydin *et al*, 2019). This way, Ascl1 generally promotes the formation of GABAergic inhibitory interneuron differentiation, especially in the ventral telencephalon progenitor cells (Wonders & Anderson, 2006; Wong & Rapaport, 2009), while inhibiting astrocyte identity (Woods *et al*, 2022). Instead, Ngn2 promotes the generation of glutamatergic neurons in the dorsal telencephalon in progenitor cells (Chouchane & Costa, 2019). Nevertheless, despite *Ascl1*-expressing progenitors are well recognized for their contribution to the generation of GABAergic interneurons in the neocortex, it cannot simply be seen as a GABAergic factor (Chouchane *et al*, 2017; Chouchane & Costa, 2019). With the application of many cell-lineage determination experiments it has been demonstrated how this transcription factor promotes diverse neuronal subtypes tall over the central nervous system in a region wise manner (Kim *et al*, 2008; Ali *et al*, 2014; Parras *et al*, 2002). Hence, in the retina, it has shown to promote a glutamatergic fate, whereas in the locus coeruleus and in the basal ganglia it generates noradrenergic neurons and cholinergic neurons (Kim *et al*, 2008;

Chouchane *et al*, 2017). This phenomenon could be partially explained due to post-transcriptional modifications such as its phosphorylation, which influences its ability to activate target genes, causing alternative neuronal phenotypes to be acquired by regulating Ascl1 binding and activation of direct target genes involved in neurogenesis (Li *et al*, 2014; Castro *et al*, 2011; Ali *et al*, 2014; Chouchane & Costa, 2019; Raposo *et al*, 2015). Moreover, alterations in the expression levels of this factors, which oscillates in progenitor cells, could also add for the different effects it has when directing neuronal identity. In this matter, interestingly, Ascl1 oscillatory pattern, promotes the activation of genetic networks important for both proliferation and differentiation of progenitors from the ventral telencephalon; In contrast, sustained expression of Ascl1 activates the genes responsible for cell cycle exit and neuronal differentiation (Jacob *et al*, 2013; Imayoshi & Kageyama, 2014). Indeed, all these factors influencing Ascl1-induced expression of target genes may explain how it modulates alternative neuronal phenotypes (Castro *et al*, 2011; Li *et al*, 2014; Parras *et al*, 2002; Ali *et al*, 2014).

Essentially, Ascl1 is a key transcriptional regulator known to act as an on-target factor since it has the ability to bind to relevant genome sites independently of the chromatin status, therefore, regardless if they are at open or closed chromatin regions in the starting cells (Morris, 2016; Rao *et al*, 2021; Imayoshi & Kageyama, 2014; Aydin *et al*, 2019). Thus, bequeathing this factor with the capability to bind directly to nucleosomes, restructuring the chromatin accessibility, and therefore facilitating the access of other transcription factors to their proper target sites. As a result, factors like Ascl1 can access silenced regions of the genome, shifting the transcriptional profile of the cell altering their fates, shown to occur as early as 12 hours post induction (Larson *et al*, 2021; Rao *et al*, 2021). Additionally, new regulatory roles of TFs are being disclosed, acting as regulators of dynamic chromatin looping and DNA methylation (Noack *et al*, 2022). Consistently, besides changing accessibility in chromatin and its association with cell-type specific chromatin looping, demethylation of DNA has been disclosed. So far, only Ngn2 overexpression has been described to lead to demethylation at its DNA binding

regions and strengthening, ultimately affecting chromatin looping between regulatory regions (Noack *et al*, 2022).

1.7.1 Ascl1 in reprogramming

The role of Ascl1 as a pan neuronal factor and not as a unique GABAergic determinant has been clarified previously. The same has been demonstrated in reprogramming studies of postnatal neocortical astrocytes in which converted neurons that are transplanted into specific brain regions eventually acquire a specific identity with mixed phenotypes between GABA and glutamatergic cells (Chouchane *et al*, 2017). Transplantation of Ascl1-reprogrammed neocortical astrocytes in postnatal cerebral cortex produces only a small number of interneurons, with GABAergic interneurons-like morphology. However, when transplantation occurred in the SVZ, a large fraction of neocortical astrocytes differentiated into Olfactory bulb interneurons (Chouchane *et al*, 2017). This is indicative of how likely environmental signals influence the instruction of different neuronal phenotypes (Chouchane & Costa, 2019).

It is therefore important to note that many studies report how Ascl1 alone is not sufficient to establish a definite neuronal phenotype in vivo (Torper *et al*, 2013; Heinrich *et al*, 2010). Instead, for in vivo cell conversion the combination of Ascl1 with other factors activating gene networks associated with the same neurotransmitter identity, could help for a higher efficiency in transdifferentiating cells (Heinrich *et al*, 2010; Masserdotti *et al*, 2015; Chouchane & Costa, 2019). Interestingly, new research is shedding some new light in the molecular mechanisms of this factor, demonstrating how not only promotes neuronal phenotypes but also alternatives one, such as cardiogenic and myogenic fates ((h)Wang *et a*l, 2022). It is the proper combination of additional factors that enables the right fate to follow.

Overall, as a result of the binding to, and action on cis-regulatory DNA regions of pro-neural factors, these proteins are primarily responsible for the regulation and modulating of the gene expression and the cells transcriptome (de Martin *et al*,

2021). Each TF-DNA interaction is unique, so understanding its determinants needs to take into account multiple mechanisms through which a TF interacts to a specific DNA sequence (Inukai *et al*, 2017). The binding pattern of a given factor can be highly determined by the shape and motif preferences of a given sequence within the DNA (de Martin *et al*, 2021); in addition to phosphorylation as a post-translational modification, dimerization partners and cofactors can also facilitate in a direct or indirect way the binding and molecular cascade activation a particular TFs may have (Hansen *et al*, 2022; Inukai *et al*, 2017). Another aspect that impacts the way a factor attaches to the chromatin is the epigenetic modifications at putative target regions (Mayran & Drouin, 2018; Inukai *et al*, 2017). These modifications include marks influencing chromatin compaction or as explained, variable methylation patterns throughout the DNA. Thus, even though some transcription factors are unaffected by DNA methylation and others are specific for methylation status, large-scale genome-wide mapping indicates that DNA methylation is significantly low at TF-bound genes (Héberlé & Bardet, 2019; Noack *et al*, 2022).

Certainly, many factors can affect TFs binding specificity, including the co-binding and/or competitive binding of additional factors, chromatin environment, and DNA shape.

Therefore, we must understand how different factors engage with chromatin and ultimately affect the activities of other downstream factors during differentiation. This will enable us to better understand neuronal reprogramming and the subtypes that can be obtained (Aydin *et al*, 2019). Interestingly, both *Ascl1* and *Ngn2* bind divergently to preferred E-boxes owing to DNA sequence specificities of their bHLH domains (Masserdotti *et al*, 2015; Aydin *et al*, 2019). Additionally, the sequence context of many TFs preferred motifs can modulate DNA-binding sensitivity, showing how some genes may require co-factor cooccurrence to be properly activated upon binding (Hansen *et al*, 2022). Thus, different regulatory environments are created, affecting downstream factors' binding patterns and regulation activity to establish neuron-specific expression profiles. There are, however, barriers affecting binding and efficient reprogramming from these factors

(Soares *et al*, 2022). For instance, it has been reported how some environmental factors such as prolonged or short culture condition can alter the capacity of astrocytes to be converted by *Ngn2* infection (Masserdotti *et al*, 2016, 2015). In this study they saw how the reprogramming process can be altered by simply adjusting the time a cell is in culture, which determines how accessible a transcriptional factor is to its binding sites. As a result, the permissive condition for conversion is altered. When looking at a possible mechanism mediating this resistance, they observed how the repressor complex REST blocks direct targets of *Ngn2*. However, when the expression of downstream targets was forced, this effect was overcome, suggesting a hierarchical model mediating reprogramming by which downstream factors are still accessible. Interestingly, they also proved how over time, at specific loci, chromatin remodeling occurred, leading to an enrichment in heterochromatin marks, rendering astrocytes resistant for reprogramming. Further supporting the idea that changes in the chromatin state might take place at target loci relevant for TFs action contributing to a refractory state in cells.

Other variables modulating factors binding can be found at the post-transcriptional level. It has already been mentioned that phosphorylation affects the pro-neural activity of bHLH proteins. Indeed, different in vitro cellular models have demonstrated that *Ascl1* and *Ngn2* are directly phosphorylated by proline-directed serine threonine kinases, such as GSK3 and ERK1/2; going from HEK293 cells (Li *et al*, 2014), to neuroblastoma cells (Woods *et al*, 2022) and glioblastoma lines (Azzarelli *et al*, 2022). Indeed, it has been reported how at low levels of activation of this kinase, Ascl1 activates neuronal differentiation genes, and how this is correlated with reduced Ascl1 phosphorylation; whereas at high levels of ERK, Ascl1 favors glial gene activation (Li *et al*, 2014; Dennis *et al*, 2019). More specifically, Ascl1 become phosphorilated on six serine-proline (SP) sites: S62, S88, S185, S189, S202, and S218 (Ghazale *et al*, 2022). Indeed, the activity of Ascl1 and how interacts with putative partners becomes altered through the phosphorylation of some residues outside its bHLH domain (Ali *et al*, 2014; Aydin *et al*, 2019; Ghazale *et al*, 2022).

Besides the effects that post-translational modification has on Ascl1 and following the argument on the influence of the environment, recently, researchers have reported genome-wide effects of over-expressed Ascl1 activity in neuroblastoma cells when expressed in a permissive neurogenic environment (Woods *et al*, 2022). By creating a mutant form of this factor, altering its phosphorylation sites, they managed to over-express a mutated Ascl1 with enhanced activity. What they observed is that existing binding sites are boosted, and new, lower affinity binding sites are created. It appears that these changes in Ascl1 binding pattern led to a significant shift in neuroblastoma cells' transcriptome from one, favoring proliferative growth, toward one that promotes neuronal differentiation. More recently, this approach of tackling phosphorylation status of this factor was aimed to test whether it promotes a more efficient neuronal reprogramming of cortical postnatal (Galante *et al*, 2022) and mature astrocytes in the living brain of mice (Ghazale *et al*, 2022), providing nevertheless, opposite results of these in vivo experiments.

Overall, these studies add up in our understanding of the molecular effects of this factor and its over-expression due to post-translational modification that can alter its strength and binding profile activity. This ultimately impacts the efficiency by which we can obtain not only functional neurons, but also heterogeneous and pure populations of reprogrammed cells both in vitro and in vivo.

Taking together all the previous sections, it has been reported how some epigenetic marks, such as H3K9me3 or H3K20me3, can act as a barrier for reprogramming and the pioneering action of some factors (Mayran *et al*, 2018; Becker *et al*, 2016; Nicetto & Zaret, 2019). Moreover, the general distribution of these in the genome can also change during cell differentiation and maturation. Importantly, Ascl1 can, however potentially access to closed chromatin, but depending on the context can create de novo binding sites and even promote alternative fates. Therefore, in general the identification of potential barriers that prevent pioneer factors from functioning and the complex interactions with cofactors will be crucial for understanding the way chromatin organization and

gene expression is regulated differently at different stages of development (Mayran *et al*, 2018; Hansen *et al*, 2022). Further, it will be fascinating to determine if maturation differences in the cell can already alter the strategy of pioneer factor-mediated chromatin accessibility and its downstream cascade in a cell-type-dependent mechanism.

Certainly, in the establishment of cell identity, numerous complex layers of epigenetic organization exist, controlling transcriptional access to DNA (Leaman *et al*, 2022). Particularly interesting, it has been recently evidenced that a subset of TFs can act as '*molecular bridges'* (Noack *et al*, 2022) as they are associated with local dynamic chromatin looping at its binding sites in vivo, inducing chromatin accessibility and DNA methylation. This ultimately grant these factors the potential to rewire the regulatory 3D genome (Noack et al., 2022). As a whole, there is a complex regulatory system in place to safeguard the various mechanisms involved in gene repression for regulating cell identity. Nonetheless, processes associated with active enhancers and active transcription act in synergy for this purpose (Brumbaugh *et al*, 2019).

2 Main aim of this project

Throughout this thesis work, it was intended to explore the molecular mechanisms behind cell identity and direct cell reprogramming in astrocytes. This study sought to identify new cell-type-specific challenges encountered in reprogramming, especially among adult glial cells in vivo. This work has been carried out to improve both our understanding of the mechanisms orchestrating cell identity induction and those that may hinder it. It is particularly the latter aspect we deem to be an essential knowledge with significant applications, to which we might humbly contribute to better manipulate cell fate conversion.

In general, we set several but related research objectives. Consequently, we performed direct reprogramming of astrocytes into induced neurons (iN), under normal conditions by the ectopic expression of *Ascl1* in culture to promote both, neuronal induction and maturation. Considering how the maturational state heavily impacts cell transcriptional profile and function, we decided to study different ways in which maturation could affect cellular conversion. Thereafter, we performed glia reprogramming in purified cortical astrocytes from the adult mice. During the fate-switch conversion, in every model studied, we could score a general delay in neuronal induction, morphological differences and ability to downregulate astrocytic identity with a greater effect seen in mature cells derived from the brain as compared to postnatal astrocytes. To understand the mechanisms behind these reported differences in adult cells in vitro, deep knowledge of the starting cells is required. However, considering the lack of proper characterization of astrocytes upon maturation, we first studied their chromatin environment during brain development. CUT&Tag allows, in a fast and efficient way, to profile a diversity of histone modifications and factors binding to the chromatin. Our goal is to elucidate, at the transcriptome and chromatin levels, how intrinsic signals contribute to cell identity at different maturation stages in astrocytes and its potential effect in direct reprogramming.

3 Results

3.1 In vitro conversion of postnatal cortical astrocytes efficiently give rise to functional neurons.

While astrocyte heterogeneity has been documented at the morphological, functional and, more recently, at the single-cell level, little is known about their cellular specification and maturation process. A recently published study (Lattke *et al*, 2021) describes how astrocytes undergo significant transcriptional and chromatin changes from postnatal to mature stages, and that in vitro models fail to mimic the in vivo astrocytic phenotype. Thus, the mechanisms identified so far hardly account for astrocyte maturity in vivo. Hence, a major limitation is still encountered in the many studies aiming to reveal the molecular changes driving neuronal conversion. These studies are performed mainly in vitro and on cells which are not completely representative of those present in the adult brain. Therefore, understanding the full conversion process is still restricted, and the gap between in vitro and in vivo remains.

In vitro models, however, are perfect for controlling potential cofounding variables in the experimental setting. Hence, to better analyze whether the maturation state in astrocytes can have an effect on the conversion outcome, we aimed to convert isolated young and adult cortical astrocytes in vitro. We first optimized a basal reprogramming protocol (NDR) using postnatal cells for neuronal conversion (*Fig. 3*). We followed the experimental conditions elsewhere explained (Heinrich *et al*., 2011) and after 21 days the yield neurons were characterized based on the expression of different neuronal markers through immunostaining, RTqPCR and its electrophysiological properties.

Cortical astroglia cultures were prepared from postnatal mice at day 2-3 (Supplementary *Figure S1a*), after a week, cells were passaged and transduced with a Tet-On inducible lentiviral vector encoding *Ascl1* and V5 (rtTA-*Ascl1*.V5) *(Fig.*

3.1a). For the control conditions cells were not infected with the vector encoding for the rtTa. Over 60% of astrocytes were positive for V5, showing high efficiency in the infection rate (*Fig. 3.1 b).* In agreement with previous studies, after 4 days, the vast majority of *Ascl1*-transduced postnatal astrocytes had differentiated into βIII tubulin-positive cells. By 2–3 weeks post-transduction, astroglia-derived neurons exhibited MAP2 immunoreactivity, which is indicative of neuron maturation and dendritic formation. Consistent with the previously described influence that Ascl1 has in promoting a GABAergic identity (*Introduction section 1.7*) during development in the cortex, cells revealed that they predominantly acquired a GABAergic neuronal identity. On the opposite, cells in the non rtTa condition, were negative for both, the microglia (IBA1) and neuronal markers (TUJ1 and MAP2), showing no presence of neurons or contaminating microglia. In the vast majority of transduced cells, drastic morphological changes associated with the expression βIII tubulin were observed only upon the addition of rtTa *(Fig. 3.1 c).* This confirms the ability of the factor to activate the neurogenic differentiation program in an inducible manner.

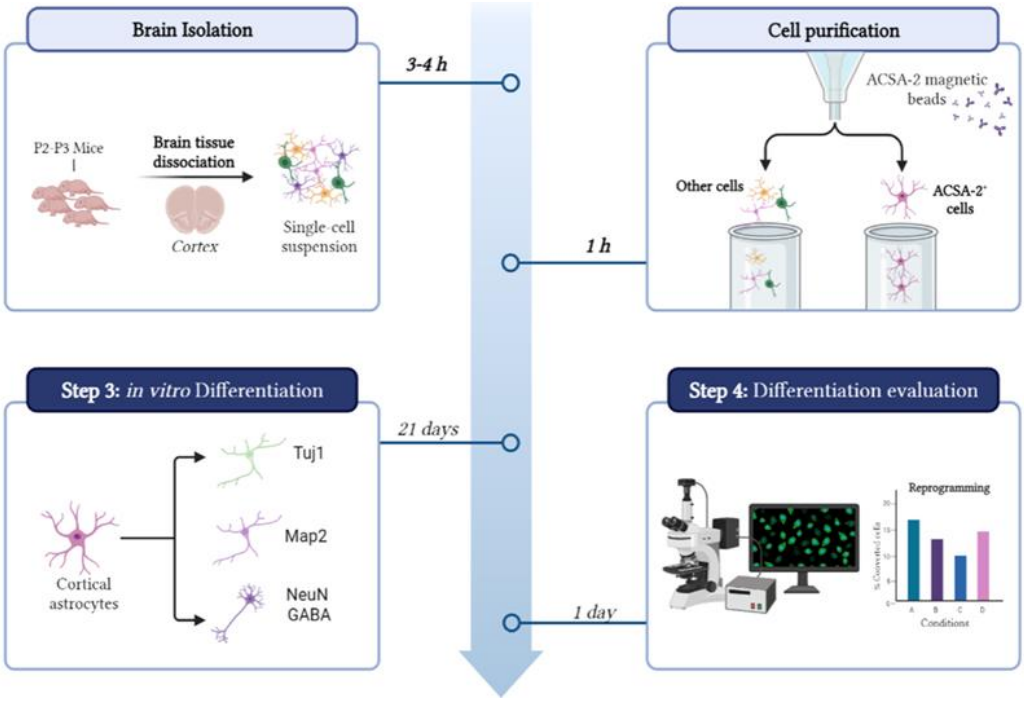

Figure 3. Experimental design Scheme for the in vitro conversion .
Cells are isolated from the cortex of postnatal mice, and purified with ACSA2 antibody. For the in vitro differentiation, astrocytes are first infected with a lentivirus expressing Ascl1. After 21 days iN are characterized by looking at the expression of different neuronal markers by immunostaining and RTqPCR. Electrophysiological properties are also analyzed after 21 days in culture.

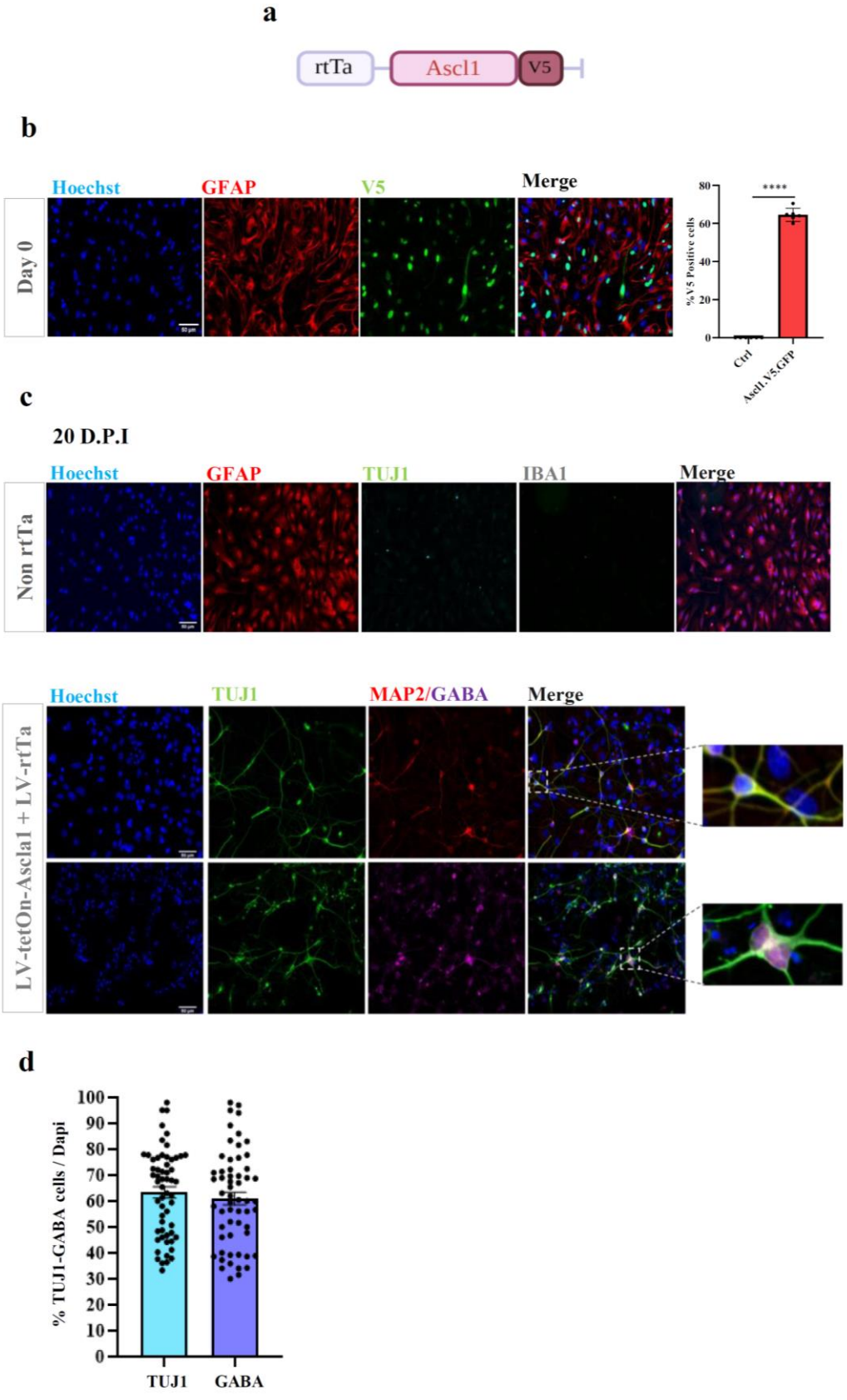
a
rtTa
Ascl1
V5
b
Hoechst
GFAP
V5
Merge
Day 0
%V5 Positive cells
****
Ctrl
Ascl1.V5.GFP
c
20 D.P.I
Hoechst
GFAP
TUJ1
IBA1
Merge
Non rtTa
Hoechst
TUJ1
MAP2/GABA
Merge
LV-tetOn-Ascla1 + LV-rtTa
d
% TUJ1-GABA cells / Dapi
TUJ1
GABA

Figure 3.1. Ascl1 efficiently convert astrocytes into iNs with a GABAergic identity. ***a****. Schematic representation of the inducible rtTA-dependent system lentivirus employed expressing Ascl1.* ***b.*** *Efficiency of infection in culture by immunostaining against V5 and its graphical quantification.* ***c****. Characterisation of the reprogramming of astrocytes 20 d.p.i.. Immunofluorescence images showing astrocyte direct reprogramming upon Ascl1 infection, becoming induced Neurons (iN) positive for several neuronal markers (Tuj1 63,34±2,2%) (****d****).* ***d.*** *Yield neurons tend to acquire mainly a GABAergic-like cells (GABA 60,97±2,3%) (GABA in magenta, Tuj1 in green, scale bar 50μm). n=6 independent experiments. Error bars represent ± SEM. (****p<0.0001) Statistical test: Unpaired Student t-test.*

3.2 Induced neurons present functional properties, eliciting action potentials.

Considering the initial results, a further characterization was carried out. After 10 d.p.i., there was still a significant expression of *Ascl1* by RT-qPCR on infected cells *(Fig. 3.2 a)*. We also observed a significant upregulation in RNA levels of neuronal genes like *Tuj1* and *Map2 (Fig. 3.2 b)*. The success in the conversion process was also measured by the ability of the iN to properly downregulate astrocyte-like genes. Converted cells showed a significant downregulation of some relevant genes for the astrocytic identity (*Gfap, Sox9 and Nfia*) through RT-qPCR after *Ascl1* ectopic expression (*Fig. 3.2 c*).

Moreover, at this time point, iN were characterized for their functionality, showing electrophysiological properties. Indeed, cells reprogrammed with this factor gave rise to functional synapses after 20 d.p.i, being able to elicit and receive action potentials (*Fig.3.2 d*).

Overall, we obtained an efficient reprogramming protocol in accordance to already published studies showing high transdifferentiation of postnatal astrocytes in vitro, presenting distinctive neuronal morphological and functional properties.

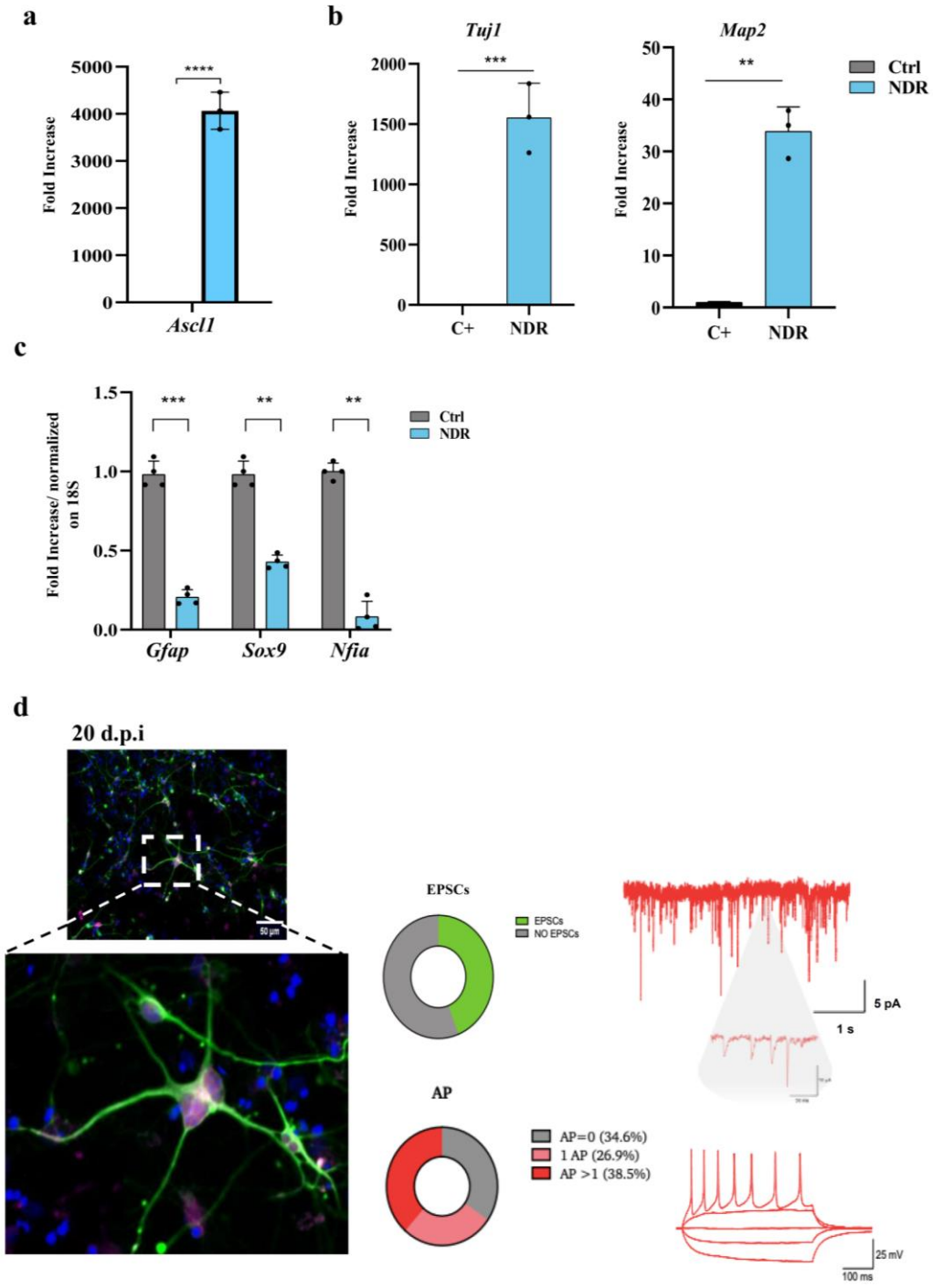
a
Fold Increase
5000
4000
3000
2000
1000
0
****
Ascl1
b
Tuj1
Fold Increase
2000
1500
1000
500
0
***
C+
NDR
Map2
50
40
30
20
10
0
**
C+
NDR
Ctrl
NDR
c
Fold Increase/ normalized on 18S
1.5
1.0
0.5
0.0
***
**
**
Ctrl
NDR
Gfap
Sox9
Nfia
d
20 d.p.i
50 µm
EPSCs
EPSCs
NO EPSCs
5 pA
1 s
AP
AP=0 (34.6%)
1 AP (26.9%)
AP >1 (38.5%)
25 mV
100 ms

Figure 3.2. Induced neurons characterization and electrophysiological properties.

a. *Fold increase of the transcriptional factor Ascl1 RNA expression on infected cells.* ***b.*** *Induced neurons upregulate RNA levels of early and mature neuronal markers at 20 d.p.i.* ***c****. Reprogrammed astrocytes downregulate glia-specific genes, analysed through RTqPCR, normalized with S18 mRNA expression.* ***d****. Electrophysiological properties of the iN after 20 d.p.i. (AP: Action potential; EPSCs: Excitatory postsynaptic potential) n=6 independent experiments. Error bars represent ± SEM. *p<0.05, **p<0.01, ***p<0.001, ****p<0.0001. Statistical test: Unpaired Student t-test.*

3.3 Assessing mature astrocytes transcriptome changes upon *In vitro* maintenance.

To test whether maturation could have an impact on cellular conversion, on top of the aforementioned tests we repeated astrocyte reprogramming directly on adult astrocytes isolated from Aldh1l1:CRE mice *(Supplementary Figure S2)*. To do so, the same protocol used for the pups was used for the isolation step using the miltenyi purification kit (*Fig. S2 a*). After the purification of adult astrocytes with the surface marker ACSA-2, we performed Fluorescence-activated cell sorting (FACS) to check for the purity of the isolated cells acquired at each developmental stage *(Supplementary Figure S2 b)* and plated additional cells to perform immunostaining for the microglia mark IBA1, a cell type commonly presented as a contaminating cell in dissection approaches (*Supplementary Figure S2 c)*. An observation made, is that mature cells greatelly struggle to attach after isolation, however, once they reached confluency manipulating them was equiparable to their immature counterparts. For this reason, before starting the conversion process, we tested whether the infection was equally efficient in both conditions (mature and immature cells). This way, we were able to discard this difference as a cofounding variable in our study *(Fig. 3.3 a)*. After observing no significant differences in their capacity to be infected in vitro, we proceeded with further characterization of the mature isolated cells. Previous studies have shown that upon in vitro culture of postnatal astrocytes, the transcriptome of these changes acquires a more stem-like phenotype (Lattke *et al,* 2021). We, therefore, wanted to test if isolated adult astrocytes also undergo the same change (*Fig 3.3 b*). We checked for several astroglia markers (*Gfap, Slc1a2, Aqp4*) that are upregulated with maturation, and for generic progenitor genes (*Ki67, Sox2 and Nestin*) (Lattke *et al*, 2021). To do this, upon ACSA-2 purification, part of the cells were plated, and the other part was used for RNA extraction and qPCR analysis. When looking at RNA levels of mature and immature genes on the purified and plated adult cells we observed how there was an overall change in the gene expression compared to astrocytes that reside in the brain *(Fig. 3.3 b)*. Whereas mature genes tended to get slightly

downregulated in vitro, immature genes, such as *Ki67* or *Nestin* were upregulated (*Fig 3.3.b*). Moreover, we looked if this loss in maturation profile reached levels comparable to the postnatal astrocytes genetic expression or, if on the contrary, they still presented a more mature status (*Fig.3.3c*). Despite the described changes at the transcriptional level in mature cells that were plated, immature astrocytes still harbor a more progenitor-like gene expression than in vitro *(Fig. 3.3 c).*

These data show how adult astrocytes upon cellular culture conditions change their maturation profile, acquiring a more immature feature expression. However, when comparing postnatal and adult cells, the former ones still present a higher degree of a progenitor profile.

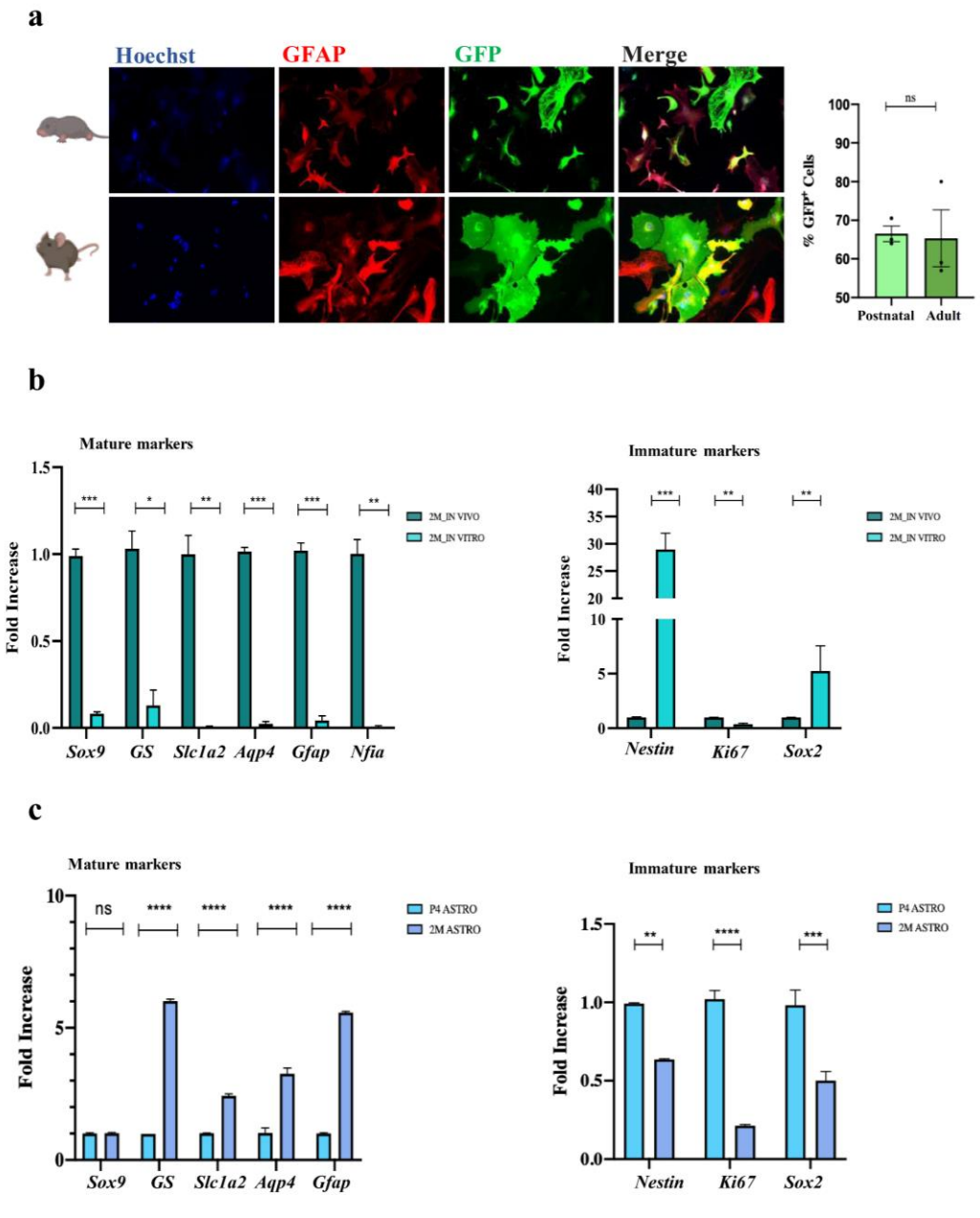
a
Hoechst
GFAP
GFP
Merge
ns
% GFP+ Cells
Postnatal
Adult
b
Mature markers
Fold Increase
2M_IN VIVO
2M_IN VITRO
Sox9
GS
Slc1a2
Aqp4
Gfap
Nfia
Immature markers
Nestin
Ki67
Sox2
c
Mature markers
P4 ASTRO
2M ASTRO
Immature markers

Figure 3.3 In vitro characterization of isolated adult cells.
a. *Adult cells in vitro show equivalent capacity to be infected as postnatal astrocytes with an inducible lentiviral vector expressing GFP.* ***b***. *Change in the transcriptional profile between adult astrocytes isolated from the brain and those maintained in vitro.* ***c***. *Transcriptional profile comparison between in vitro postnatal and adult astrocytes before reprogramming experiments. Fold increase normalized on 18S.*
*n=3 independent experiments. Error bars represent ± SEM. *p<0.05, **p<0.01, ***p<0.001, ****p<0.0001. Statistical test: Unpaired Student t-test*

3.4 During direct reprogramming, mature astrocytes fail in downregulating astrocytic identity.

After characterizing our in vitro model, we carried on and performed the conversion of adult astrocytes in vitro. We employed a CRE inducible lentivirus expressing *Ascl1* on Aldh1l1:CRE mouse derived astrocytes *(Fig. 3.4 a)*.

Following the analysis of conversion at day 7, 14 and 21 post infections, the population of adult astrocytes showed a depletion compared to the same cells in the control condition, an effect we also observed in pararllel experiements performed (*Fig. S1*). Despite the cells that were analyzed presented the capacity to become TUJ1 from the first week they morphollogically resembled astrocytes, or at a transitional stage (*Fig. 3.4 b)*. To understand the underlying cause of this observation, we examined if these cells managed to downregulate their GFAP expression (*Fig. 3.4 c, d*). Interestingly, we observed that during the whole conversion process, adult cells derived iN cells presented a higher and consistent colocalization of TUJ1 and GFAP marks compared to P4 cells (one-way ANOVA, ****$p<0.0001$). On the contrary, converted postnatal astrocytes, managed to overcome this colocalization as early as day 7 (One way Anova, ns, $p>0.0001$) (*Fig. 3.4 d*).

According to these results, immature astrocytes downregulate their starting identity more efficiently than adult astrocytes during transdifferentiation, resulting in a more elaborate neuronal morphological appearance in contrast to what was observed in adult astrocytes.

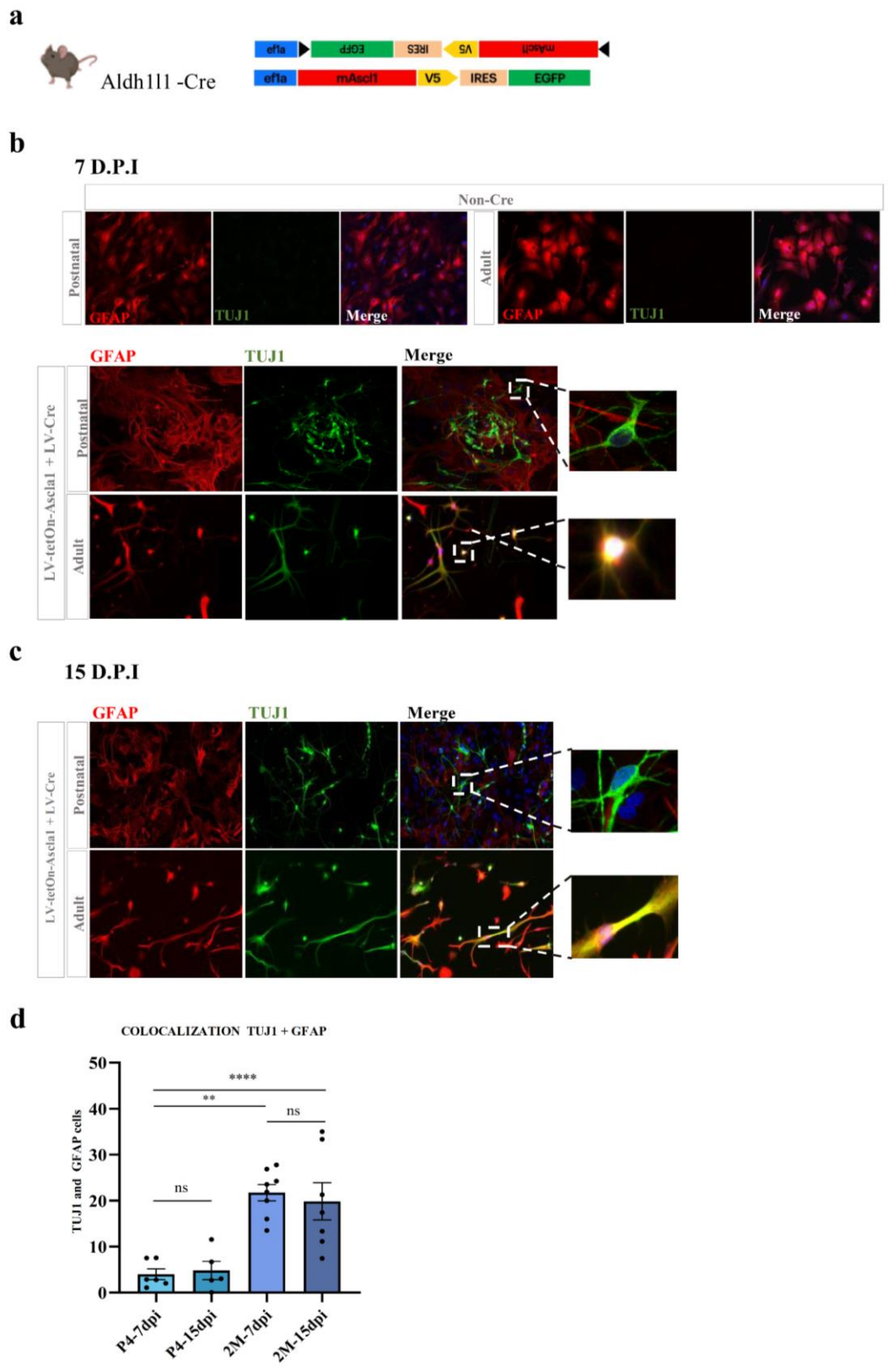
a
Aldh1l1 -Cre
efla
mAscl1
V5
IRES
EGFP
b
7 D.P.I
Non-Cre
Postnatal
Adult
GFAP
TUJ1
Merge
LV-tetOn-Ascla1 + LV-Cre
c
15 D.P.I
d
COLOCALIZATION TUJ1 + GFAP
TUJ1 and GFAP cells
****
**
ns
P4-7dpi
P4-15dpi
2M-7dpi
2M-15dpi

Figure 3.4 In vitro Direct reprogramming of mature and postnatal ACSA-2 isolated cells ***a.*** *Schematic representation of the animal model (Aldh1l:CRE) and the Cre/lox site-specific inducible lentivirus employed expressing Ascl1.* ***b.*** *Immunofluorescence analysis reveal an efficient neuronal conversion of cells expressing Ascl1 after 7 d.p.i.* ***c****. Immunofluorescence analysis reveal an efficient neuronal conversion of cells expressing Ascl1 after 15 d.p.i. (GFAP in red, TUJ1 in green).* ***d****. Quantification showing co-localisation between the astrocytic marker GFAP and the neuronal TUJ1. n=2 independent experiments. Scale bar 50µm. Error bars represent ± SEM. *p<0.05, **p<0.01, ***p<0.001, ****p<0.0001. Statistical test: Unpaired Student t-test.*

3.5 Postnatal cells convert faster and more efficiently than mature cells in vitro.

Next we moved on to characterize further the neurons obtained from mature astrocytes. Indeed, they successfully converted in neurons positive for neuronal marks, such as TUJ1 and even the more mature MAP2 at 21 days post infection *(Fig. 3.5 a, b)*. Additionally, with sholl analysis we analyzed the morphological differences of the iN from postnatal and adult astrocytes. These converted cells failed in reaching the elaborated bipolar shape as those from the postnatal cells, presenting less dendritic arborization and axonal intersections (*Fig. 3.5 b*).

Based on these initial results, initially we quantified the reprogramming outcome by just considering how many induced neuronal cells became TUJ1 (*Fig. 3.5 a)*. We observed a slight, yet statistically significant difference between P4 and 2M astrocytes at day 7 and at day 15 d.p.i. However, when considering the efficiency of the reprogramming based on how many also presented a neuron-like morphology, we observed a delayed and depleted effect on the mature condition (*Fig. 3.5 c*). Whereas 43,66% of postnatal astrocytes at the same time were positive for TUJ1 and acquired a bipolar phenotype from the first week of conversion, only a 6,4% of adult astrocytes presented a similar neuronal morphology at day 7, and 17,82% at day 15. It was only after two weeks when a slight, yet significant increased in adult iN cells with a bipolar morphology was observed. However, reprogramming did not reach 20% of efficiency (*Fig. 3.5 c*). After 20 days in culture, yield neurons presented more mature neuronal markers, such as MAP2 and many presented a neuronal morphology, with some cells completely loosing GFAP signal *(Fig. 3.5 d)*. Interestingly, even when comparing the percentage of cells presenting this mark between the two conditions, we found that adult cells did not reach half the value of postnatal astrocytes *(Fig. 3.5 e),* independently of whether they presented or not a bipolar appearance *(Fig. 3.5 d-f)*. Nevertheless, during the experiement a significant depletion of adult astrocytes was observed after the neuronal induction, increasingly along timepoints as observed from the GFAP immunostainig panels *(Fig. 3.5 a-d)*.

In conclusion, these data show how in this in vitro model using adult astrocytes directly purified from the brain resulted in a delayed and decreased conversion efficiency *(Fig. 3.5 a, b)*.

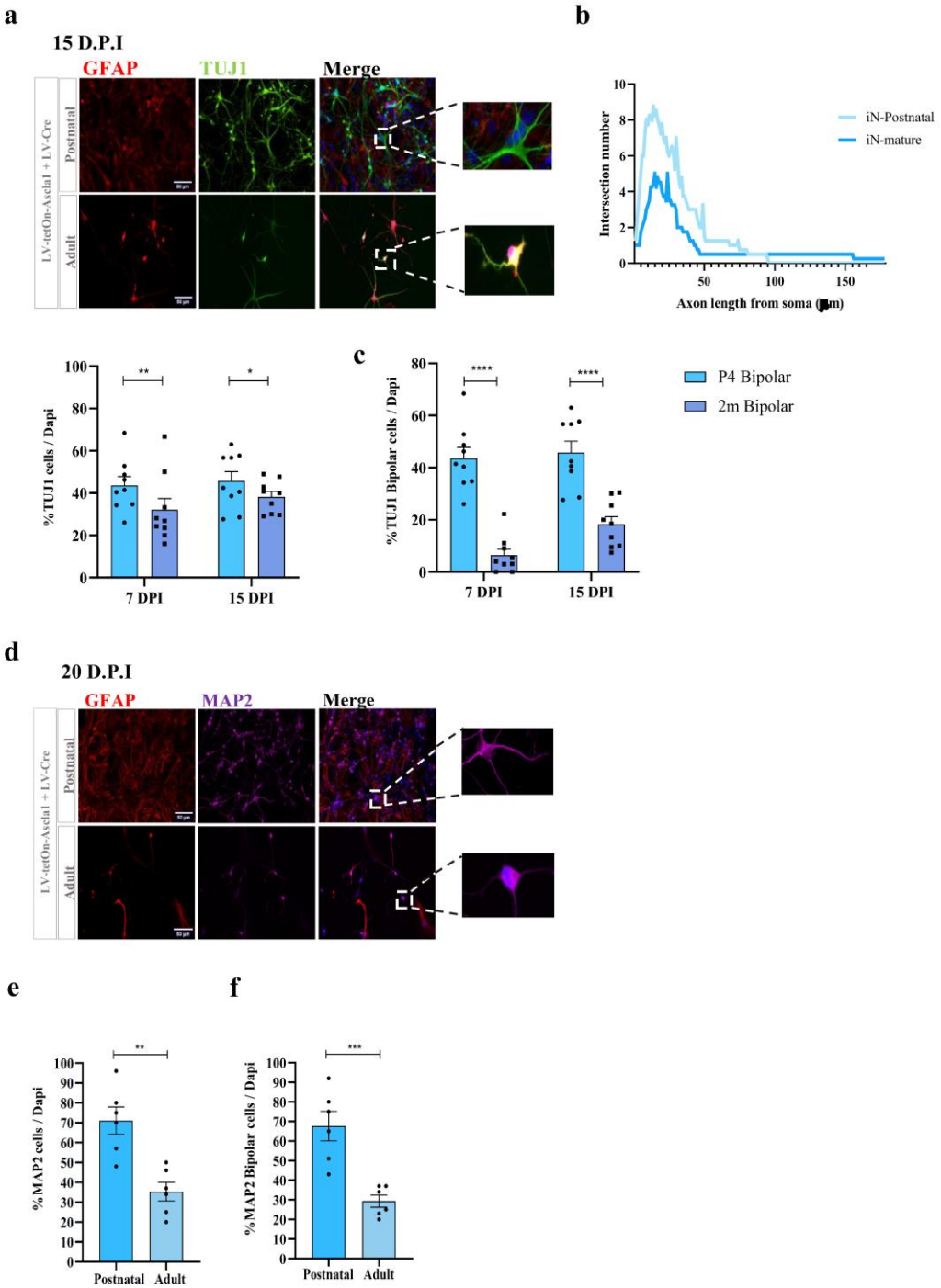
a
15 D.P.I
GFAP
TUJ1
Merge
LV-tetOn-Ascla1 + LV-Cre
Postnatal
Adult
b
iN-Postnatal
iN-mature
Intersection number
Axon length from soma (µm)
c
% TUJ1 cells / Dapi
7 DPI
15 DPI
% TUJ1 Bipolar cells / Dapi
P4 Bipolar
2m Bipolar
d
20 D.P.I
GFAP
MAP2
Merge
e
% MAP2 cells / Dapi
Postnatal
Adult
f
% MAP2 Bipolar cells / Dapi

Figure 3.5 Mature derived neurons present altered morphology and a delayed reprogramming. a. *Quantification of conversion efficiency at 7 and 15 d.p.i. Analysing reprogramming separately based on TUJ1 cells (P4: 43.66±2,2%; 2M: 32.09±2,2%).* ***b****. Sholl analysis on postnatal and mature astrocytes derived iN (P4 vs 2M ****p<0.0001).* ***c.*** *Quantification of conversion outcome on TUJ1 cells with a bipolar neuronal morphology (P4: 43.66±3,7%; 2M: 18,31±3,4%).* ***d-e.*** *Immunofluorescence images and quantification graphs showing astrocyte conversion upon Ascl1 infection 20 d.p.i. (P4: MAP2 70,6±,4%; MAP2-Bipolar 69,8±4,1%) f. conversion of TUJ1 and bipolar cells (2M: MAP2 33±4,1%; MAP2-Bipolar 28,5±4,1%). n=2 independent experiments. Scale bar 50μm. Error bars represent ± SEM. *p<0.05, **p<0.01, ***p<0.001, ****p<0.0001. Statistical test: Two-way ANOVA followed by Tukey's post hoc correction (d). Unpaired Student t-test (a, c, e, f).*

3.6 Postnatal and mature astrocytes present a distinctive chromatin accessibility profile.

Among the mechanisms controlling cellular identity establishment and maintenance, DNA methylation and histone post-translational modification are essential for normal development (Ziller *et al*, 2013), establishing an epigenetic footprint and ensuring cell identity (Mertens *et al,* 2020). Hereof, the distinct chromatin and cellular environment of the cell type of origin certainly can facilitate or impede reprogramming efficiency (Gao *et al,* 2017).

To confirm if indeed the chromatin is different in astrocytes across different developmental stages, we took advantage of available single cell ATAC-seq datasets of postnatal and adult cortex (Zaghi *et al*, 2022 & 10x Genomics). We performed dimensionality reduction analysis on the unified dataset and plotted it. We clearly distinguished 11 different cell populations, and, among them, we found two different clusters that were associated to astrocytes (*Fig 3.6. a*). Moreover, we plotted the predicted expression of key astrocytic markers such as *Gfap* and *Sox9* to validate their identity (*Fig. 3.6 b*). Interestingly, one of the two astrocytic clusters, showed a high level of predicted expression of the progenitor cells markers *Sox2* and *Ki67* (*Fig. 3.6 b*). This indeed was the cluster of astrocytes deriving from the postnatal cortical cells. The other astrocytic cluster showed a high level of predicted expression of more mature markers like *Slc1a2* or *Glu-1,* and a low level of the aforementioned progenitors' markers (*Fig. 3.6 b)*. Hence, this separated cluster will correspond to the adult cells. Thus, these data confirm what has been previously described (Lattke *et al*, 2021), showing that astrocytes have a stage-specific chromatin accessibility profile, in which they go through deep reshaping during differentiation. Despite this, no study has ever considered the contribution that repressive elements of the genome add to the process of cellular specification. We believe that during maturation cells need to repress certain regions to safeguard their identity and avoid the activation of improper gene programs. Hence, we investigated the genome distribution of the main known heterochromatin mark regions upon cell maturation.

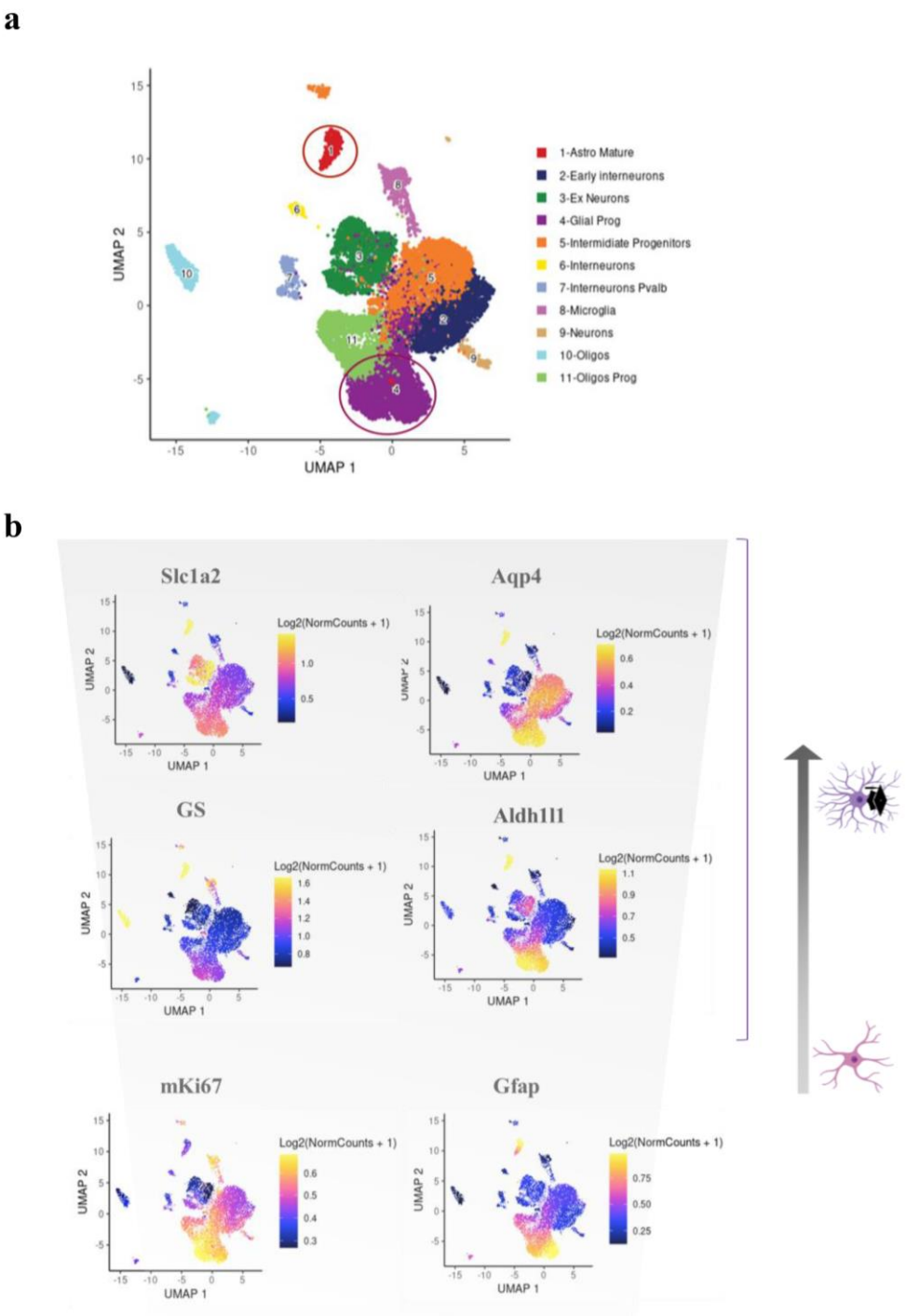

Figure 3.6 scATAC-seq P2-P50 from mice cortex

a. *Dimensionality reduction plot obtained using Uniform manifold approximation and projection (UMAP) algorithm showing different cell clusters population in the cerebral cortex.* ***b.*** *Feature plot of predicted gene expression of key astrocytic markers inside UMAP plot. (Slc1a2: Glutamine transporter; Aqp4: Aquaporin 4; GS: Glutamine Synthetase; Aldh1l1: Aldehyde Dehydrogenase 1 Family Member L1; mKi67: Marker Of Proliferation Ki-67; Gfap: Glial fibrillary acidic protein)*

3.7 Postnatal astrocytes present a permissive chromatin environment.

To efficiently profile the epigenome of cortical astrocytes of C57BL6 mice at P4 and 2 months, we performed CUT&Tag. To implement chromatin profiling by tagmentation (*Fig.3.7*), we first isolated cells as previously explained *(Fig.3; Fig. S2)* and incubated intact permeabilized nuclei with antibodies against lysine-9, 27-trimethylation of the histone H3 tail (H3K27me3, H3K9me3, 3 replicates for each developmental stage), which are abundant histone modification that marks silenced chromatin regions. In contrast, we also incubated cells with a non-specific IgG antibody to measure the untethered integration of adapters.

First, we quality-checked the experiment by performing a principal component analysis (PCA) and Pearson correlation to verify that all replicates had a good level of concordance (*Fig.3.7 a*).

Moreover, to validate the correct distribution of each repressive marker across the genome, we plotted the average signal enrichment of the two markers across a pseudogene, which exemplifies the distribution of the markers around all the genes present in the mouse genome. Indeed, we obtained the expected distribution pattern, with a stronger signal of H3K9me3 at intergenic zones and an enrichment around transcription start sites (TSSs) for H3K27me3. (*Fig.3.7 b*).

Afterwards, we calculated the regions with a significant signal enrichment compared to the IgG control, *a.k.a* peaks, for each replicate (*see methods*). Considering the high correlation between experimental replicates, we merge them together to build a consensus set of peaks per marker & developmental stage.

Next, to simplify subsequent analysis we generated a consensus set of regions containing all the peaks obtained for both markers at each developmental stage. A total of 32.619 peaks were obtained for repressive regions, from which 15420 (47,27%) were enriched for H3K27me3 and 19464 peaks (59,67%) for H3K9me3. Before moving on, we perform another quality check analysis. We plotted the ATAC-seq signal in all those regions and as expected the vast majority

of them resulted completely inaccessible (*Fig.3.7 b*). Conversely, to exemplify the specificity of our experimental approach we show the *Nfia* genomic *locus* (*Fig.3.7 c*). This is a key gene for astrocytic biology and, as shown, it is completely depleted of any of the two repressive markers and presented a high degree of chromatin accessibility as expected.

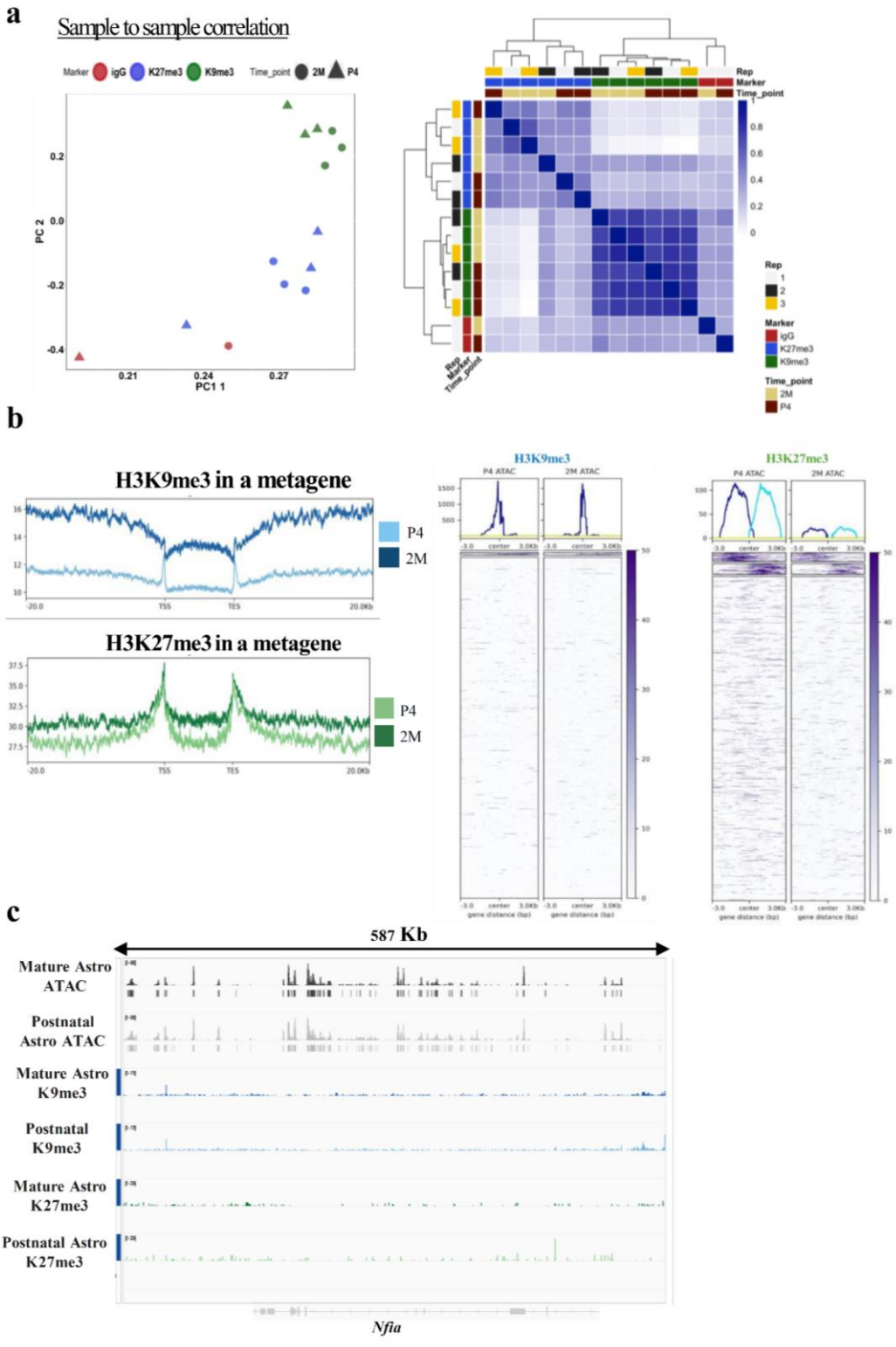
a
Sample to sample correlation
Marker igG K27me3 K9me3
Time_point 2M P4
PC 2
PC1 1
Rep
Marker
Time_point
b
H3K9me3 in a metagene
P4
2M
H3K27me3 in a metagene
P4
2M
H3K9me3
H3K27me3
P4 ATAC
2M ATAC
c
587 Kb
Mature Astro ATAC
Postnatal Astro ATAC
Mature Astro K9me3
Postnatal K9me3
Mature Astro K27me3
Postnatal Astro K27me3
Nfia

Figure 3.7 Heterochromatin characterization of astrocytes upon development.
a. *Principal Component Analysis (PCA) and correlation plot of experimental replicates and IgG controls.* ***b.*** *Metagene profile plot of H3K9me3 and H3K27me3 in the mouse genome. On the right side, heatmaps of ATAC signal inside regions positives for heterochromatinic marks.* ***c.*** *Representative Integrative Genomic Viewer (IGV) tracks of the CUT&Tag for the Nfia locus.*

3.8 Heterochromatin marks signal increase upon development.

Then, we wondered if there was any difference between each marker at the two developmental time points. To do so, we took all the regions that were enriched for each heterochromatin markers at both stages. First, we plotted the signal enrichment (*Fig.3.8 a*) across all the significant regions, and we found that upon maturation, the chromatin seemed to have a higher enrichment of both markers. Then we analyzed more specifically which regions show a significant signal enrichment in both or in only one developmental stage. As shown in the Venn diagrams (*Fig.3.8 a)*, for both markers, a bigger proportion is specific only mature stage, whereas a minor proportion is specific at postnatal stage or common. The genomic position of these subset is in accordance with the general distribution of H3K9/K27me3. Moreover, using the distance criteria, we associated a gene to each one of those regions and performed a functional enrichment analysis (*Fig.3.8 b).* Interestingly, the results showed that among different biological processes, the ones that were associated either with neuronal function or development were significantly and frequently more associated with regions specifically enriched with H3K9me3 or H3K27me3 in mature astrocytes (*Fig.3.8 b).* This concept is paradigmatically exemplified by the genomic *loci* containing *Sema6a* and *Sox11,* two key players in neuronal biology (*Fig.3.8 c)*. As it is shown, these genomic regions tend to acquire a repressive chromatin signal and, at the same time, losing a certain degree of chromatin accessibility, thus resulting in a more repressive environment around those genes.

a

H3K9me3 distribution in the genome

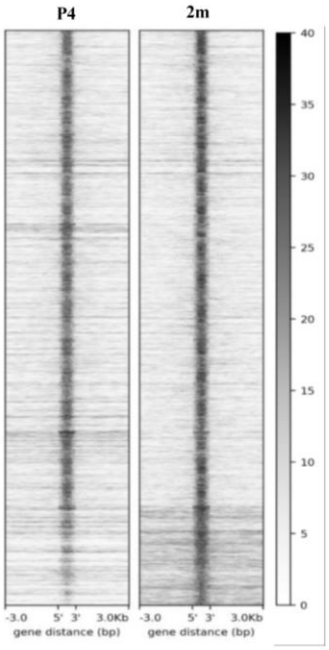

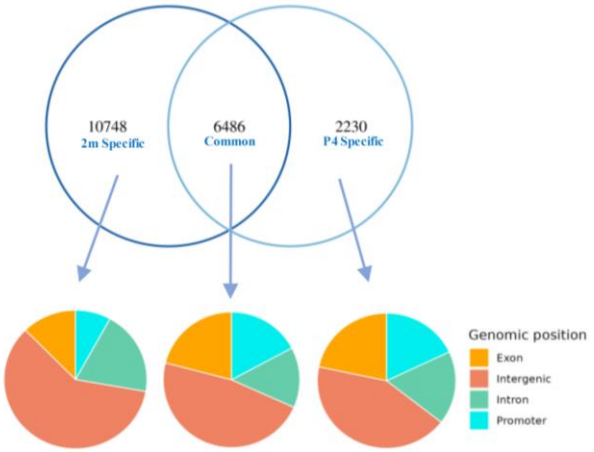

H3K27me3 distribution in the genome

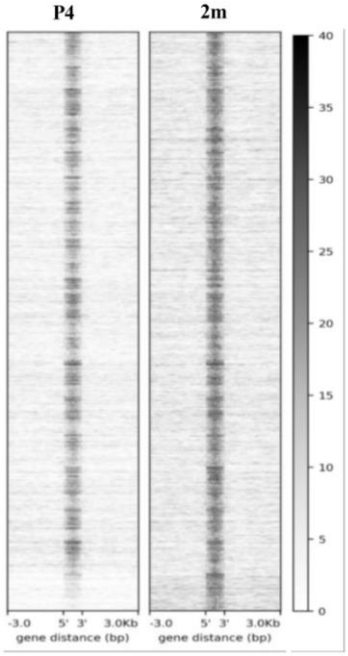

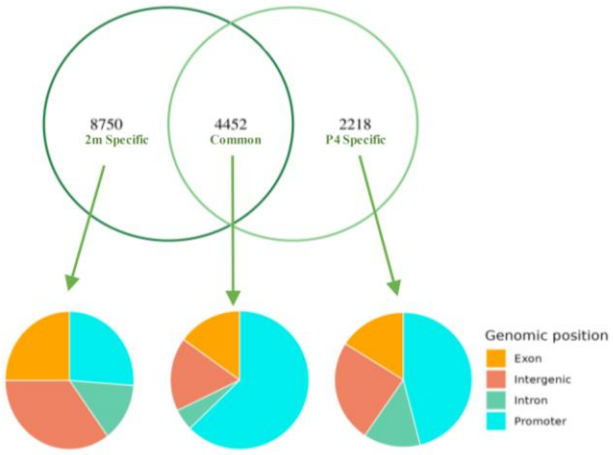

b

Genes associated with H3K9me3 Gene ontology

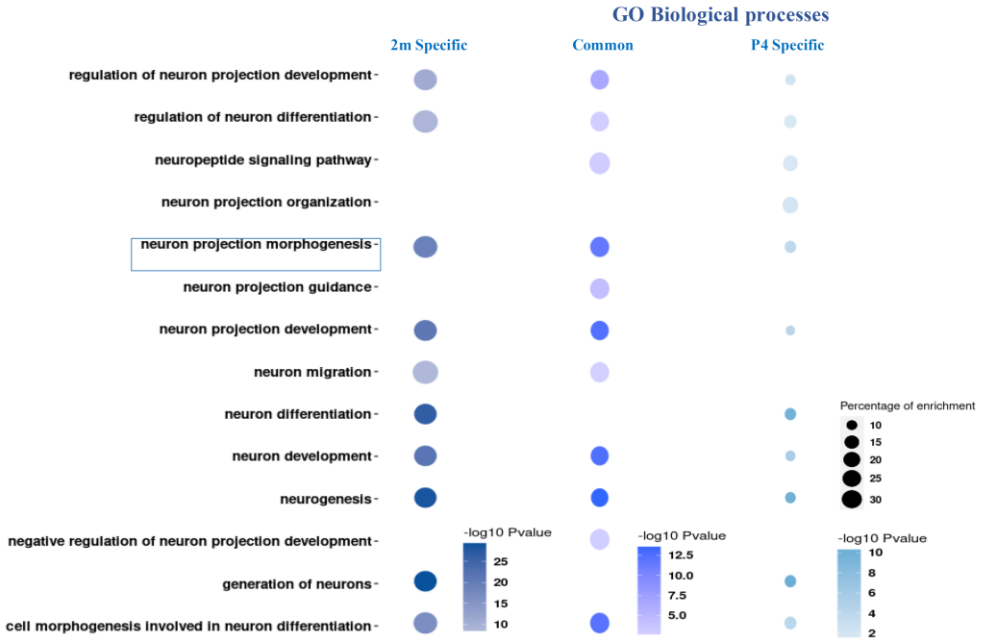

Genes associated with H3K27me3 Gene ontology

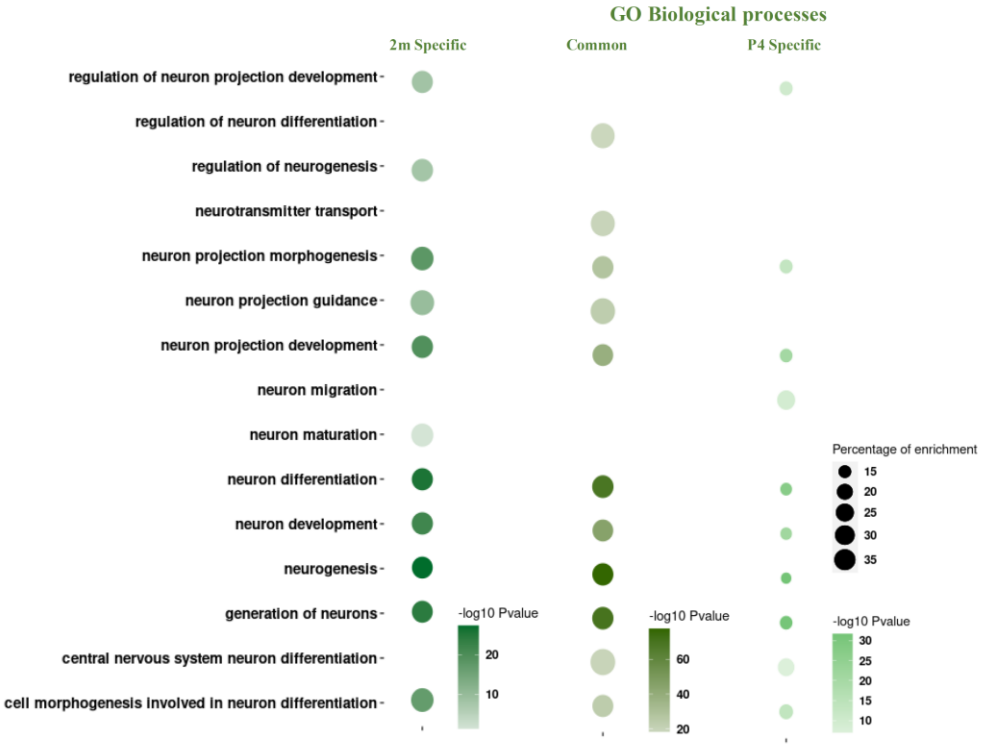

c

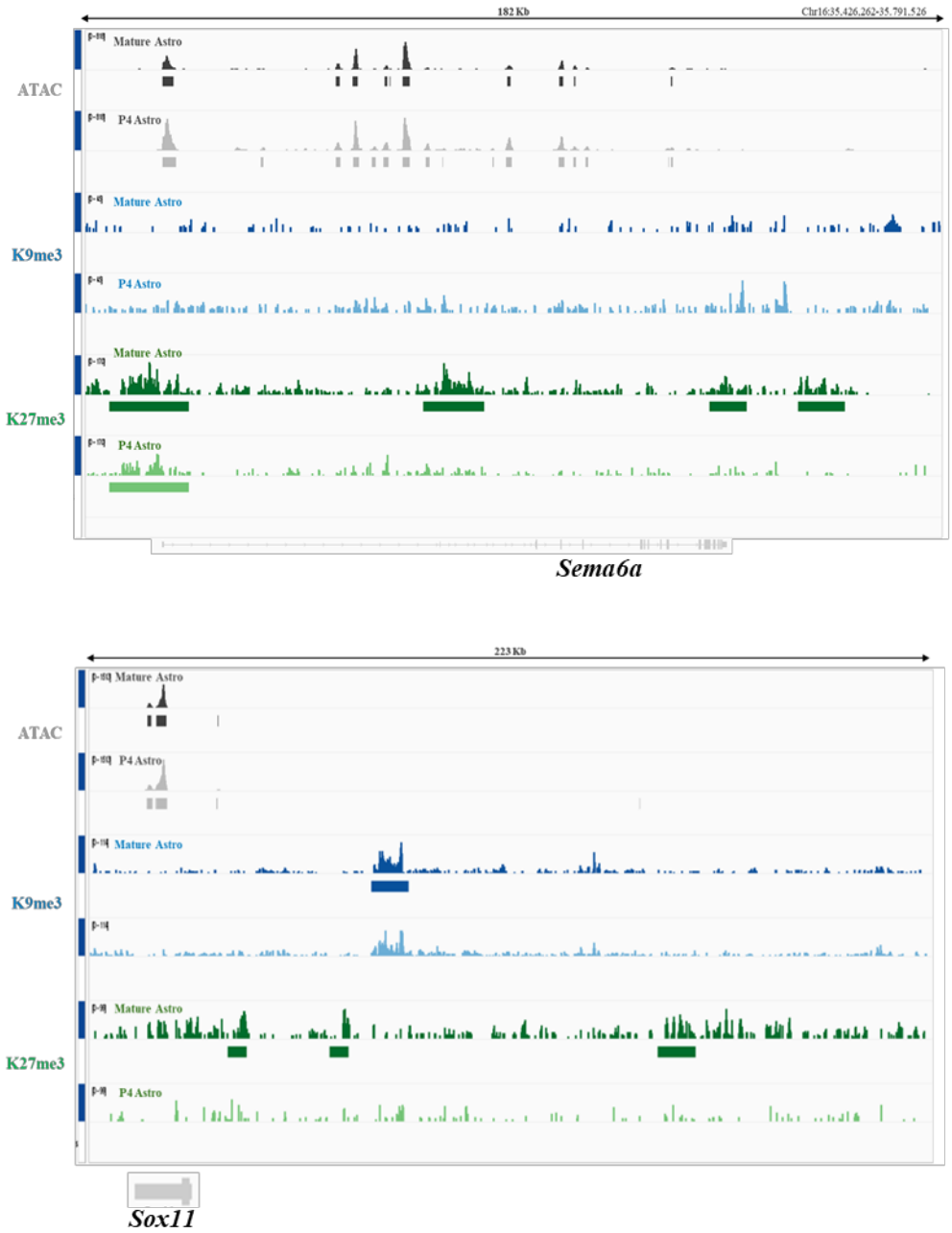

Figure 3.8 Heterochromatin marks increase signal upon development.
a. *Heatmap for the whole genomic distribution of the repressive mark H3K9me3 and H3K27me3 across the genome. Next to each heatmap a Venn diagram showing common marked regions between post-natal and mature cells together with the genomic distribution.* ***b.*** *Functional enrichment results from associating each peak of H3K9me3 and H3K27me3 to its closest gene.* ***c.*** *IGV shot with traces that gained repressive marks in adult astrocytes on the neuronal gene Sema6a and Sox11.*

3.9 The increase presence of H3K27me3 in adult astrocytes has the biggest impact on gene repression.

To further investigate where the most significant differences are located, we divided our data set into three different clusters. We identified that for both marks, cluster 3 contains the biggest number of heterochromatin regions and the ones showing the biggest difference between the postnatal and the mature stage(*Fig. 3.9 a, c highlighted cluster*). Next, we looked again at the most proximal gene to each peak and performed a functional enrichment analysis, showing a prevalence of associated neuronal genes (*Fig. 3.9 b, d*). Considering that there are published RNA-seq datasets from the same developmental stages on astrocytes (Lattke et al., 2021), we analyzed the expression levels of the genes associated with the highlighted functional enrichment categories from cluster 3 *(Fig. 3.9b, d*). This was conducted for both marks, H3K9me3 and H3K27me3. Interestingly, we found that a proportion of them were differentially expressed, as shown in the Venn diagram and heatmaps, indicating a possible direct effect of the differential chromatin marks distribution (*Fig.3.9 b, d*). Again, we put two genomic *loci* as an example, in this case we selected *NeuN* and *Sema5b* (*Fig.3.9 e*). As for *NeuN* we have a strong enrichment of H3K9me3 and slighter of H3K27me3, whereas as for *Sema5b* the strong enrichment is only of H3K27me3. For both genes this result in a decrease of the expression level.

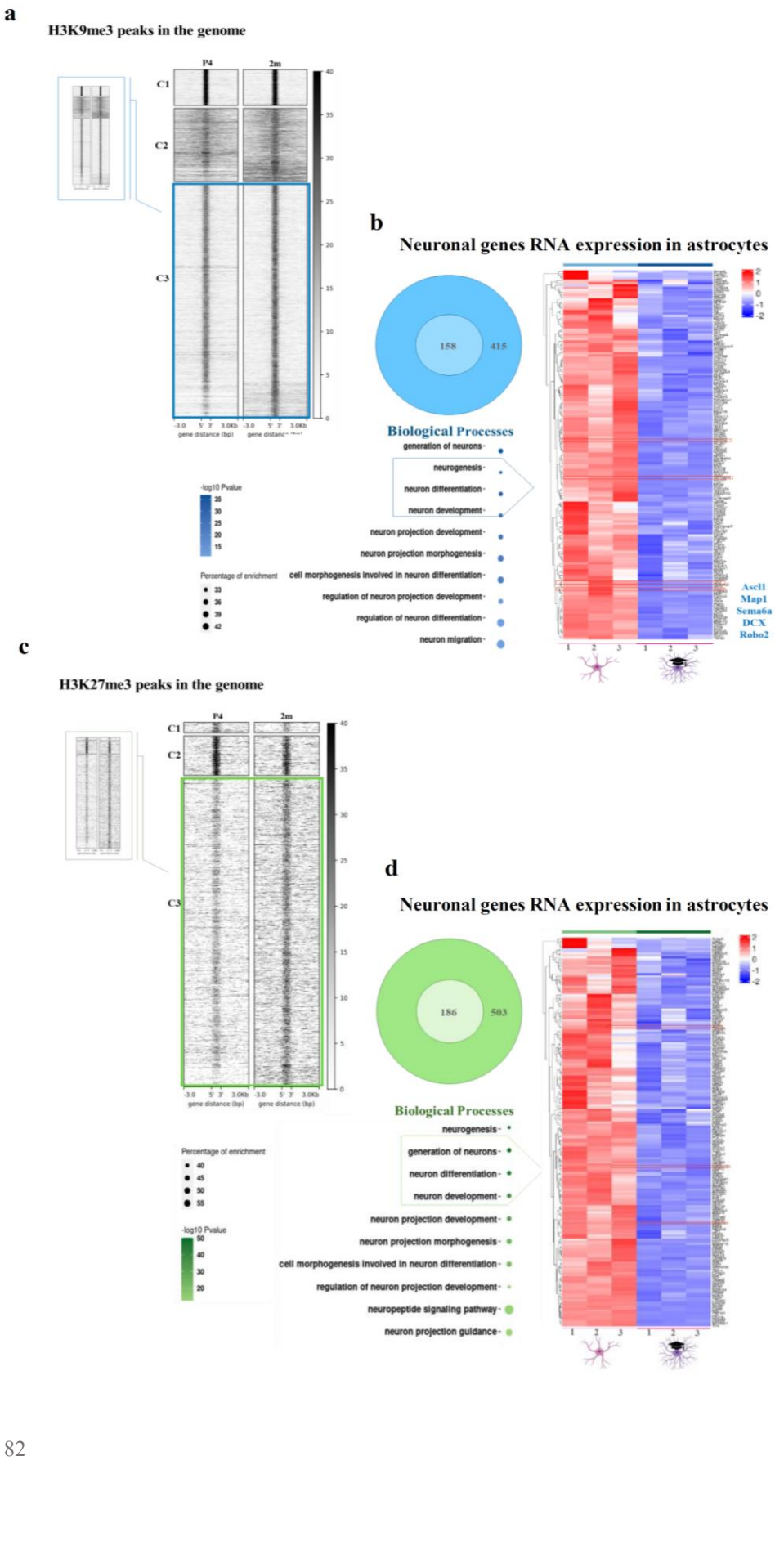
a
H3K9me3 peaks in the genome
P4
2m
C1
C2
C3
gene distance (bp)
b
Neuronal genes RNA expression in astrocytes
158
415
Biological Processes
generation of neurons
neurogenesis
neuron differentiation
neuron development
neuron projection development
neuron projection morphogenesis
cell morphogenesis involved in neuron differentiation
regulation of neuron projection development
regulation of neuron differentiation
neuron migration
-log10 Pvalue
Percentage of enrichment
Ascl1
Map1
Sema6a
DCX
Robo2
c
H3K27me3 peaks in the genome
d
Neuronal genes RNA expression in astrocytes
186
503
Biological Processes
neurogenesis
generation of neurons
neuron differentiation
neuron development
neuron projection development
neuron projection morphogenesis
cell morphogenesis involved in neuron differentiation
regulation of neuron projection development
neuropeptide signaling pathway
neuron projection guidance

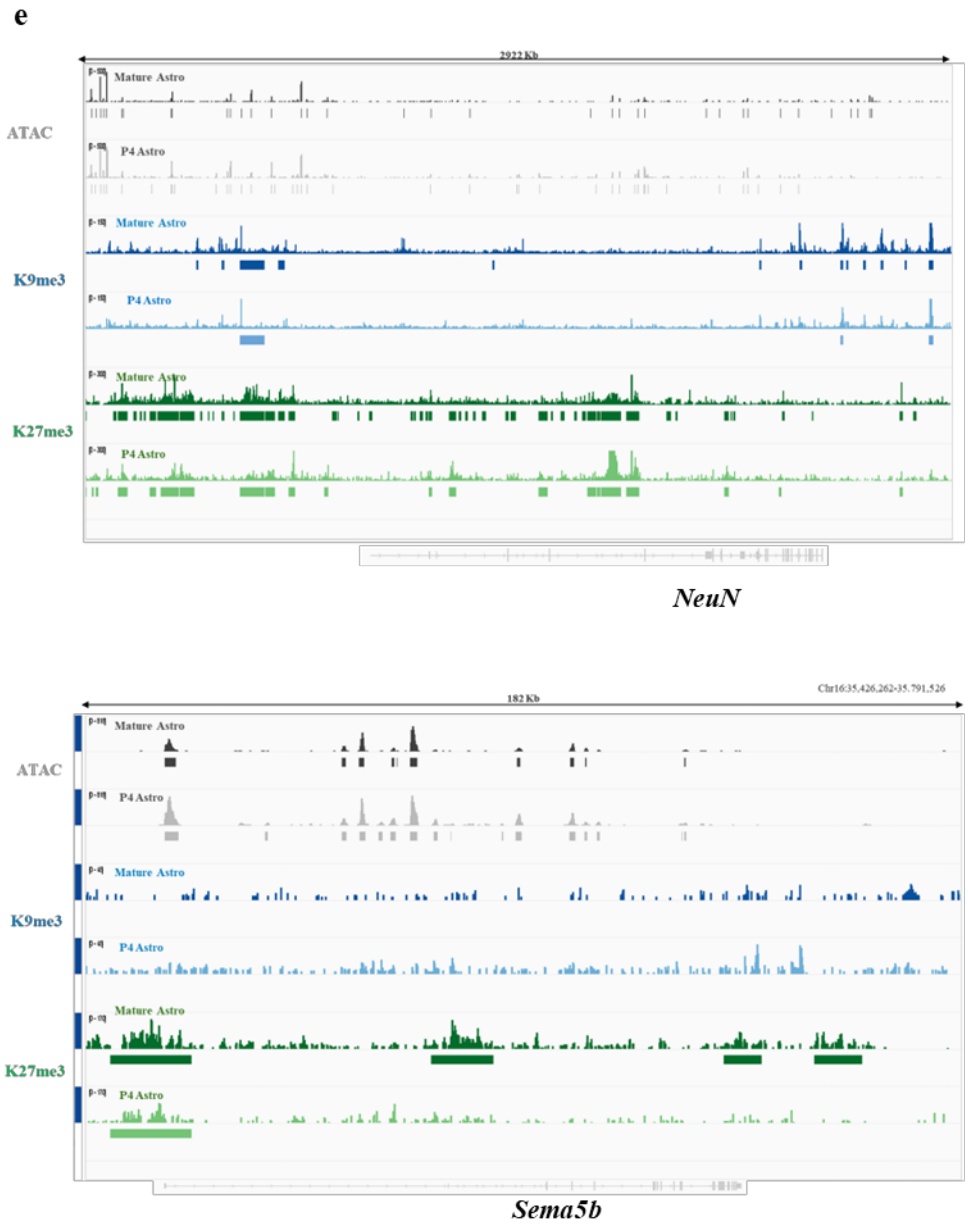

Figure 3.9 Downregulation on neuronal genes on mature astrocytes with an enriched heterochromatin signals.

a. *Heatmap of the H3K9me3 distribution divided in 3 clusters highlighting (blue square) the one with the biggest signal difference between pot-natal and adult astrocytes. Functional enrichment results from associating each peak of cluster 3 to its closest gene; Venn diagram and corresponding heatmap, showing the number of differential expressed genes among the underlined subset.* ***b.*** *Heatmap of the H3K27me3 signal divided in 3 clusters highlighting (green square) the one with the biggest difference between pot-natal and adult astrocytes.* ***e.*** *IGV shot with traces that gained repressive marks in adult astrocytes on the neuronal gene NeuN and Sema5b.*

3.10 H3K27me3 has the biggest impact on gene repression.

Our next goal was understanding if there was any correlation between these changes on gene expression and the differences present at the level of heterochromatinic marks. We therefore focused our attention on neuronal genes that we found associated to regions of the aforementioned 3rd cluster for both markers (*Fig.3.10 a*). We first plotted a Venn diagram to understand how many of those genes were in proximity of cluster 3 H3K9/27me3 marked regions or both. When plotting where in the genome these regions were located, compared to the associated genes, we observed that the H3K27me3 marked regions were more proximal to gene promoters compared to the H3K9me3 marked ones. We then plotted the average gene expression level of those genes (*Fig.3.10 b*), and we found a significant decrease of the average expression of neuronal genes that were marked by H3K27me3 alone or in combination with H3K9me3, like *NeuN*, but not by H3K9me3 alone *(Fig. 3.10 b, c)*.

We investigated if this behavior was also true for the differentially expressed genes present in these subsets. We performed the same identical analysis (*Fig.3.10 d, e*), and again we found a significant difference in the average gene expression level between genes that were marked by H3K27me3 alone or in combination with H3K9me3, and the genes marked by H3K9me3 alone. Together these results seem to indicate a more direct correlation of the H3K27me3 level with gene expression in comparison with H3K9me3.

These data indicate that as an astrocyte undergoes maturation, its chromatin not only becomes more compacted by the presence of more heterochromatin marks and an overall drop in the ATAC signal from P4 to 2m, but that this occurs at genomic regions corresponding to genes important for neuronal identity and function. Moreover, these histone modifications have a preferred genomic distribution, at promoters for H3K27me3 and distal zones for H3K9me3. A curious finding from merging our data set with the RNA-seq, is that postnatal cells, despite presenting some degree of heterochromatin marks, still manage to express in a

higher degree some neuronal-associated genes than mature cells. When looking at the possible effect these repressive marks could have on gene regulation, we found that, especially H3K27me3 has the biggest influence on gene repression. Which goes in accordance with its increased preference for transcriptional starting sites shown in our data and literature *(Cai, Zhang, Loh et al 2021)*. Interestingly, GO terms for neuronal morphogenesis and neurotransmission were among the genes showing this increase in repressive marks and less expression in mature astrocytes.

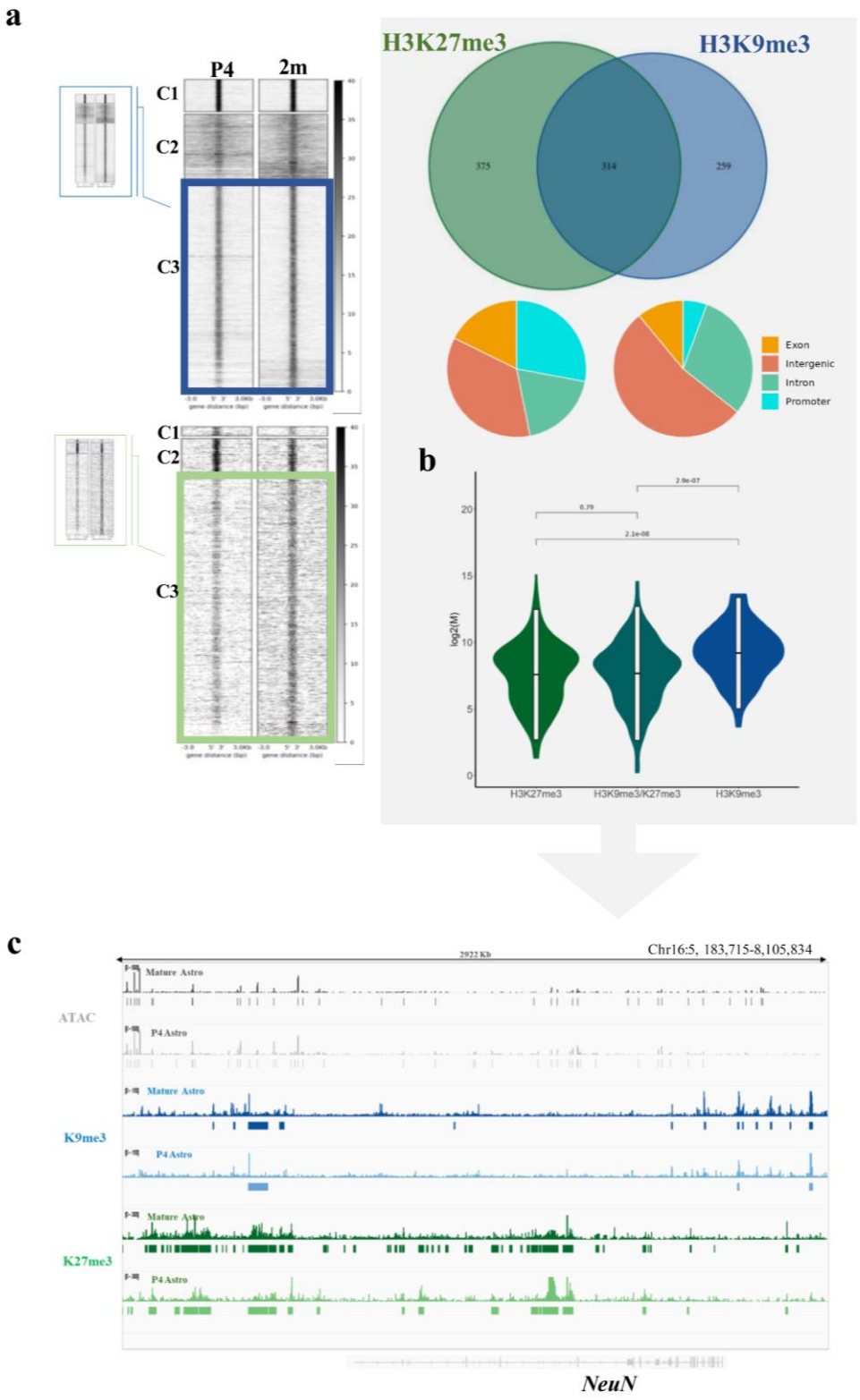
a
P4
2m
C1
C2
C3
C1
C2
C3
H3K27me3
H3K9me3
375
314
259
Exon
Intergenic
Intron
Promoter
b
2.9e-07
0.79
2.1e-08
log2(M)
H3K27me3
H3K9me3/K27me3
H3K9me3
c
Chr16:5, 183,715-8,105,834
2922 Kb
Mature Astro
ATAC
P4 Astro
Mature Astro
K9me3
P4 Astro
Mature Astro
K27me3
P4 Astro
NeuN

d

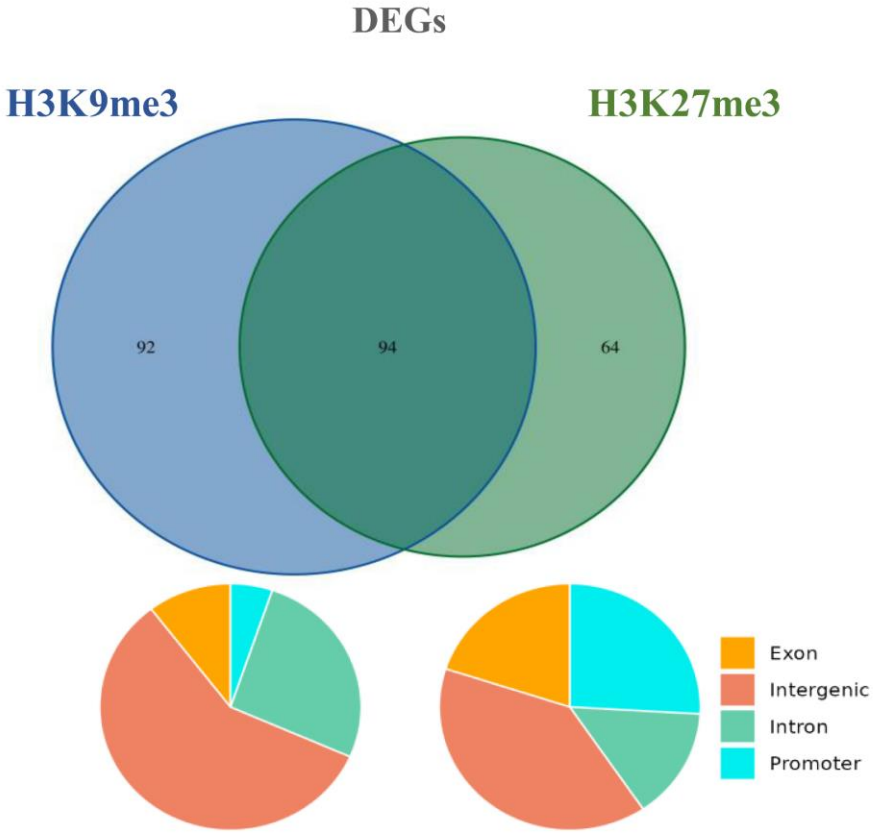
DEGs
H3K9me3
H3K27me3
92
94
64
Exon
Intergenic
Intron
Promoter

e

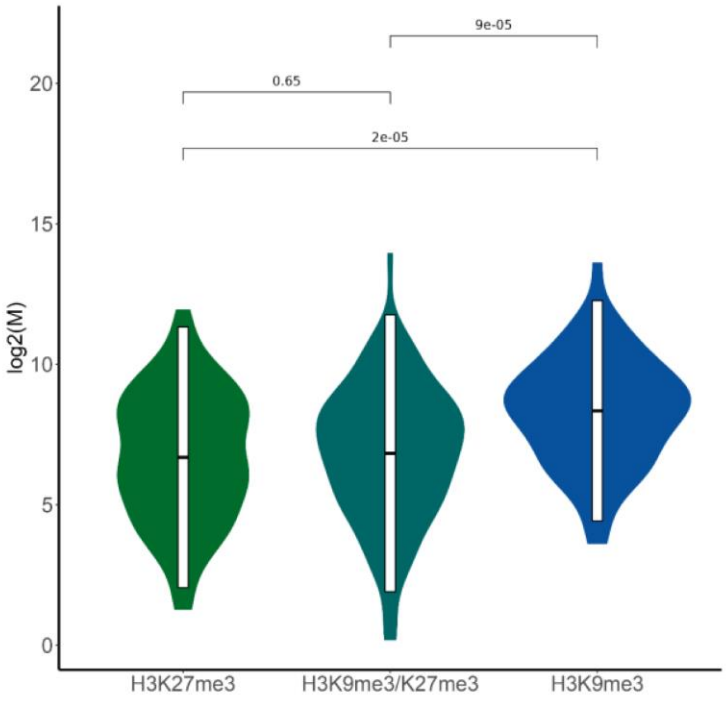
9e-05
0.65
2e-05
20
15
10
5
0
log2(M)
H3K27me3
H3K9me3/K27me3
H3K9me3

Figure 3.10 H3K27me3 repressive marks have the biggest impact on gene repression.

a. *Venn diagram for the genes in cluster 3 containing profiles for double or single repressive mark and its genomic distribution (375 (green) H3K27me3 marked genes ; 259 (blue) H3K9me3 marked genes; 314 double marked genes).* ***b***. *Violin plot showing the statistically significant effect of each profile (H3K27me3 and H3K9me3 alone or double marked genes). Statistic, Anova and Wilcoxon non parametric test (H3K27me3 vs H3K9me3/27me3, P=0.79; H3K27me3 vs H3K9me3, P=2.1e-08; H3K9/27me3 vs H3K9me3, P=2.9e-07).* ***c.*** *IGV shot illustrating a representative trace for the neuronal gene NeuN gaining repressive marks upon maturation and a corresponding loss in chromatin accessibility (grey traces).* ***d.*** *Venn diagram for the differential expressed genes in (a) containing profiles for double or single repressive mark and its genomic distribution (64 (green) H3K27me3 marked genes ; 92 (blue) H3K9me3 marked genes; 94 double marked genes).* ***e***. *Violin plot showing the statistically significant effect of each profile (H3K27me3 and H3K9me3 alone or double marked genes). Statistic, Anova and Wilcoxon non parametric test (H3K27me3 vs H3K9me3/27me3, P=0.65; H3K27me3 vs H3K9me3, P=2e-05; H3K9/27me3 vs H3K9me3, P=9e-05).*

3.11 As an astrocyte matures, heterochromatic marks appear at neuronal-associated loci.

To further analyze these data, we wondered if there were regions that at postnatal stages were free from repressive marks, and later gained heterochromatin signal with maturation *(Fig.3.11 a)*.

We observed that from all 32.619 heterochromatin regions found, 17.890 peaks (54,84%) represented newly acquired marks for H3K9me3, H3K27me3, or both at 2 months *(Fig. 3.11 b)*. Moreover, the ATAC signal for these peaks showed a reduction in the chromatin accessibility signal (*Fig. 3.11 c*). When trying to identify the biological function of these regions, we associated each peak to it closest gene and performed functional enrichment analysis. We found out that the categories were enriched for many neuronal identity properties *(Fig. 3.11 d*), associated with important genes, like *Dcx,* among the genes acquiring this repressive signature as astrocytes mature *(Fig. 3.11 e)*.

To understand the significance of these changes on gene expression, we plotted a Venn diagram comprising of the genes associated with those regions and the neuronal ones that were associated with regions inside cluster 3 *(Fig. 3.9 b, d)* that gained either mark during development *(Fig. 3.11 f)*. A greater proportion of them is present in this subset and we have already shown how these genes present significant changes in their expression level (*Fig.3.10 b*). Thus, these data suggest that the overall gain of repressive marks is somewhat significant in driving the identity changes that is present in astrocytes across development.

In conclusion, our CUT&Tag data shows a transition of the neuronal-associated genomic regions, like for *Dcx,* toward a repressive state in mature astrocytes, indicated by the acquisition of heterochromatin marks, loss in chromatin accessibility and gene expression levels.

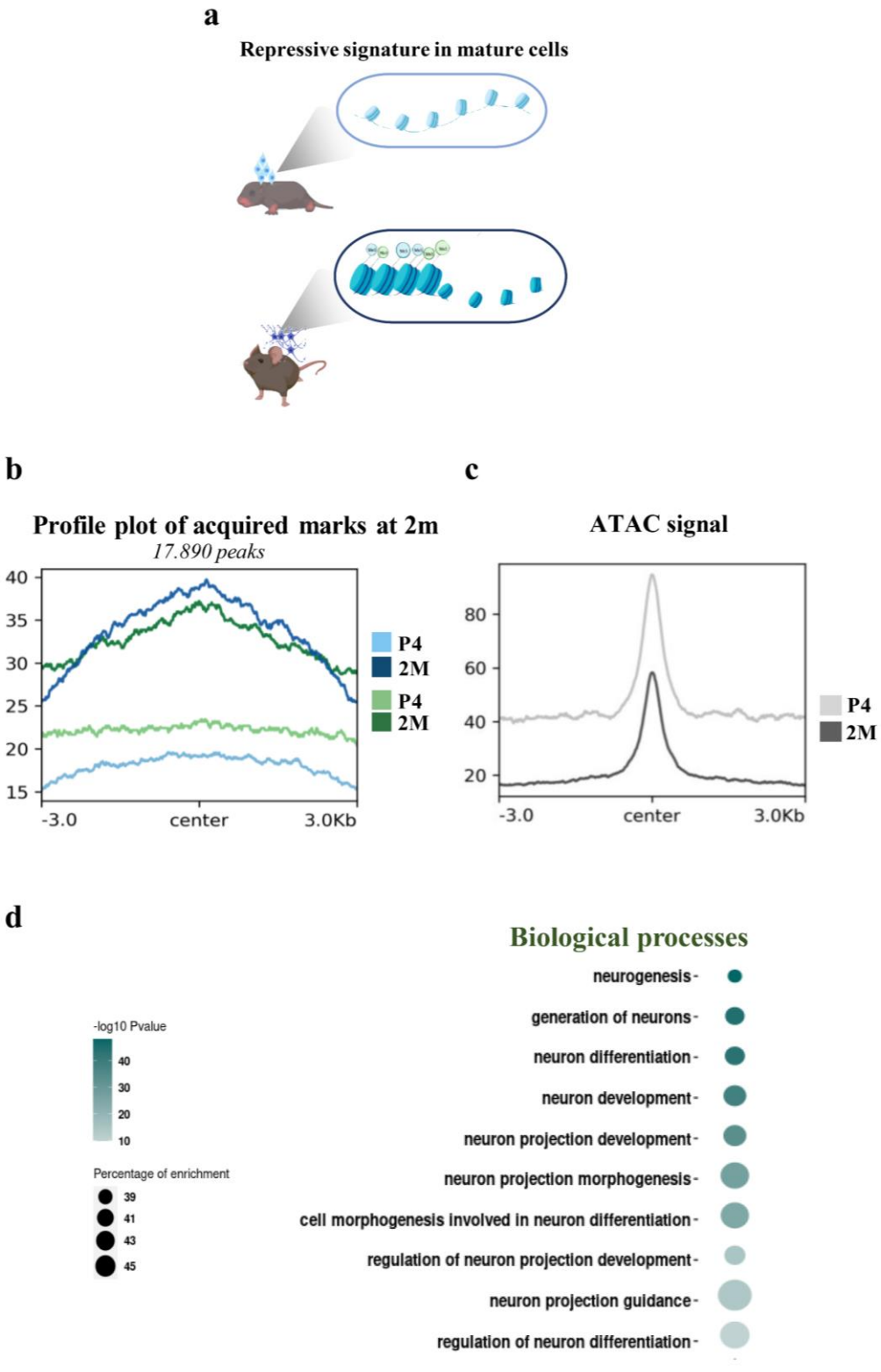
a
Repressive signature in mature cells
b
Profile plot of acquired marks at 2m
17.890 peaks
40
35
30
25
20
15
-3.0
center
3.0Kb
P4
2M
P4
2M
c
ATAC signal
80
60
40
20
-3.0
center
3.0Kb
P4
2M
d
Biological processes
neurogenesis
generation of neurons
neuron differentiation
neuron development
neuron projection development
neuron projection morphogenesis
cell morphogenesis involved in neuron differentiation
regulation of neuron projection development
neuron projection guidance
regulation of neuron differentiation
-log10 Pvalue
40
30
20
10
Percentage of enrichment
39
41
43
45

e

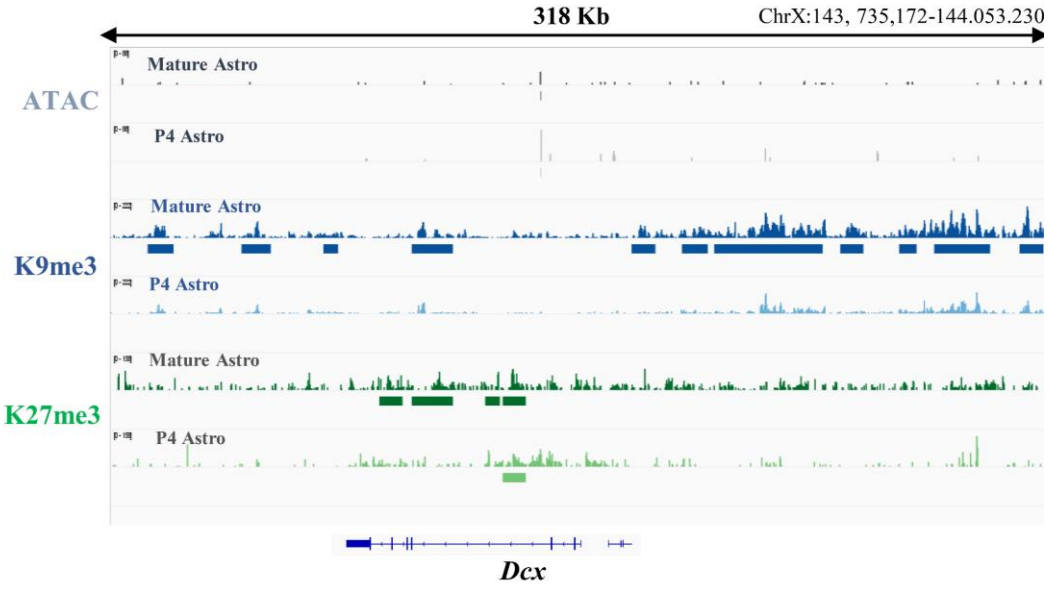
318 Kb
ChrX:143, 735,172-144.053.230
ATAC
Mature Astro
P4 Astro
K9me3
Mature Astro
P4 Astro
K27me3
Mature Astro
P4 Astro
Dcx

f

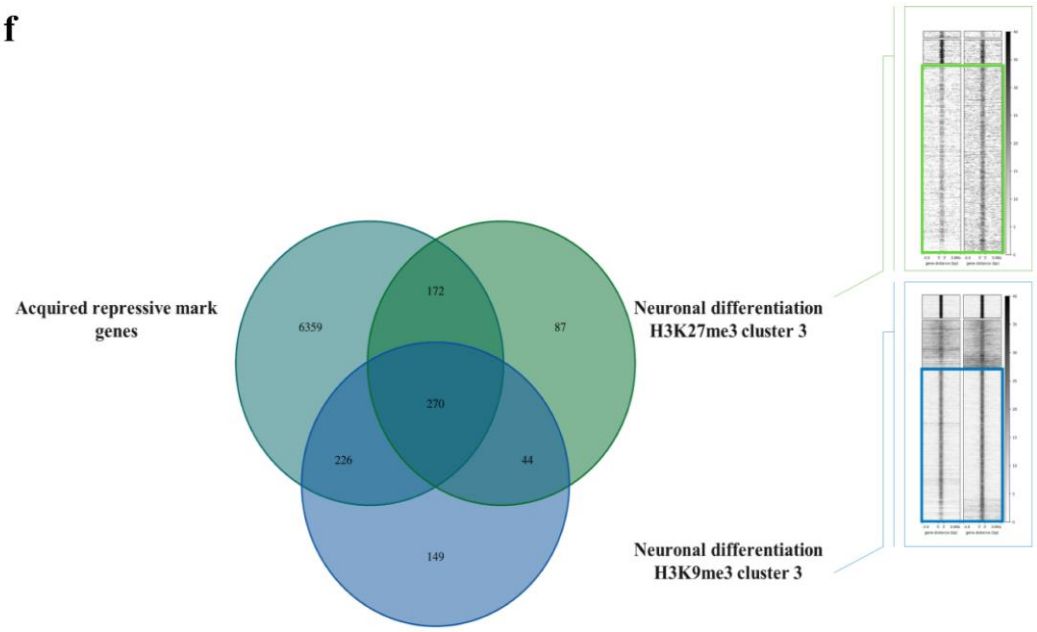
Acquired repressive mark genes
6359
172
87
270
226
44
149
Neuronal differentiation H3K27me3 cluster 3
Neuronal differentiation H3K9me3 cluster 3

Figure 3.11 At postnatal stages, many repressive mark-free regions gain heterochromatin upon maturation.
a. *Schematic illustration showing a gain of the repressive marks with astrocytic maturation.* ***b.*** *Signal profile plot of H3K9me3, H3K27me3, and ATAC (**c**.) inside regions gaining repressive marks in mature astrocytes (17.890 peaks).* ***d.*** *Functional enrichment analysis of the genes associated by distance to the identified peaks in (b).* ***e.*** *IGV shot illustrating a representative trace for the neuronal gene Dcx gaining repressive marks upon maturation and a corresponding loss in chromatin accessibility compared to the postnatal state (grey traces).* ***f.*** *Venn diagram showing the specific heterochromatin signature of these acquired repressed genes upon maturation (172 genes with just H3K27me3; 270 doubled marked genes and 226 genes marked with H3K9me3). Most genes identified associated with neuronal signature belong to cluster 3 of regions showing increased heterochromatin signal in adult cells.*

3.12 With maturation there are higher dense heterochromatin domains.

The increase in the two markers is indicative of heterochromatic regions. Nevertheless, these modifications are also found in euchromatic regions that permit transcription. Indeed, different degrees in chromatin compaction has been described *(Fig. 3.12 a),* with high enriched H3K9me3 regions correlating with tighter chromatin, impeding transcription factor binding and pioneer activity (Becker *et al*., 2017; Mayran *et al*., 2018).

Based on our findings, showing a general enrichment of repressive marks in astrocytes at 2 months, we wanted to go one step further to discriminate regions harboring different degrees of chromatin compaction, rendering more inaccessible certain regions of the genome.

To discriminate different degrees of compaction in the chromatin during astrocyte development we employed SAMMY-seq (**S**equential **A**nalysis of **M**acro**M**olecules accessibilit**Y**). It is a high-throughput sequencing-based method for genome-wide characterization of chromatin dynamics, based on its compaction degree. We were able to isolate and map four different chromatin fractions of postnatal and mature cells separated by solubility and DNase sensitivity. In the first step, we separated all soluble proteins (**S1 fraction**), and obtained a crude intact nuclei extract, from which we further isolated different chromatin fraction by adding different concentrations of DNase and high salt buffers. We obtained the second fraction (**S2 fraction),** as the first released after DNase treatment. To isolate the remaining fractions, first, a high salt buffer helps in the release of high insoluble proteins contained in the third fraction, which are DNase-resistant chromatin (**S3**). Finally, to get the most condensed and insoluble portion of chromatin (**S4 fraction**), we treat with urea (8U). This way we can solubilize the remaining proteins and nuclear membranes (Sebestyén *et al*, 2020). After sequencing of each fraction, to visualize and perform all the subsequent analysis, the SAMMY-seq signal is expressed as a ratio between S3-S2 fractions (S3-S2. S). To check the experimental

quality, we performed Spearman correlation between the SAMMY-seq signal and our chromatin marks, dividing the genome in bins of 1mb (*Fig.3.12 b*). The plot shows a high correlation between the H3K9me3 dataset and the S3-S2. S ratio (*Fig. 3.12 b*), in line with what has been previously described (Mayran *et al*, 2018; Sebestyèn *et al,* 2020).

Consequently, we compared the signal from the SAMMY-seq with our H3K9me3 results and the ATAC signal from P4 and 2M astrocytes, along different chromosomes. This way we can see at the chromosome level a "zoom-in" of the H3K9me3 trace, discriminating among it regions with an enriched S3-S2. S signal, corresponding to more condensed chromatin, (*Fig. 3.12 c, red traces*) or depletion (*Fig. 3.12 c, purple traces*). The latter one corresponding to more euchromatic sites correlating with chromatin accessibility from the ATAC-seq.

When comparing astrocytes at the two different stages, we observed how mature cells tend to present a higher SAMMY signal in enriched H3K9me3 regions compared to the one at P4, despite presenting the histone repressive mark in the same locus. Interestingly, in postnatal cells, the ATAC signal is still present on those regions with H3K9me3, but lesser SAMMY signal compared to the same sites in 2 months astrocytes *(Fig. 3.12 c, Chromosome 10).* This goes in line with our previous results in which, with maturation, there is an overall gain in H3K9me3 and loss in chromatin accessibility.

Using this approach, our preliminary analysis suggests the presence of higher compact regions that are rich in H3K9me3 displaying lower chromatin accessibility that are not present at postnatal stages and are rather gained with time. These data support the notion that during maturation astrocytes develop a more restrictive chromatin environment.

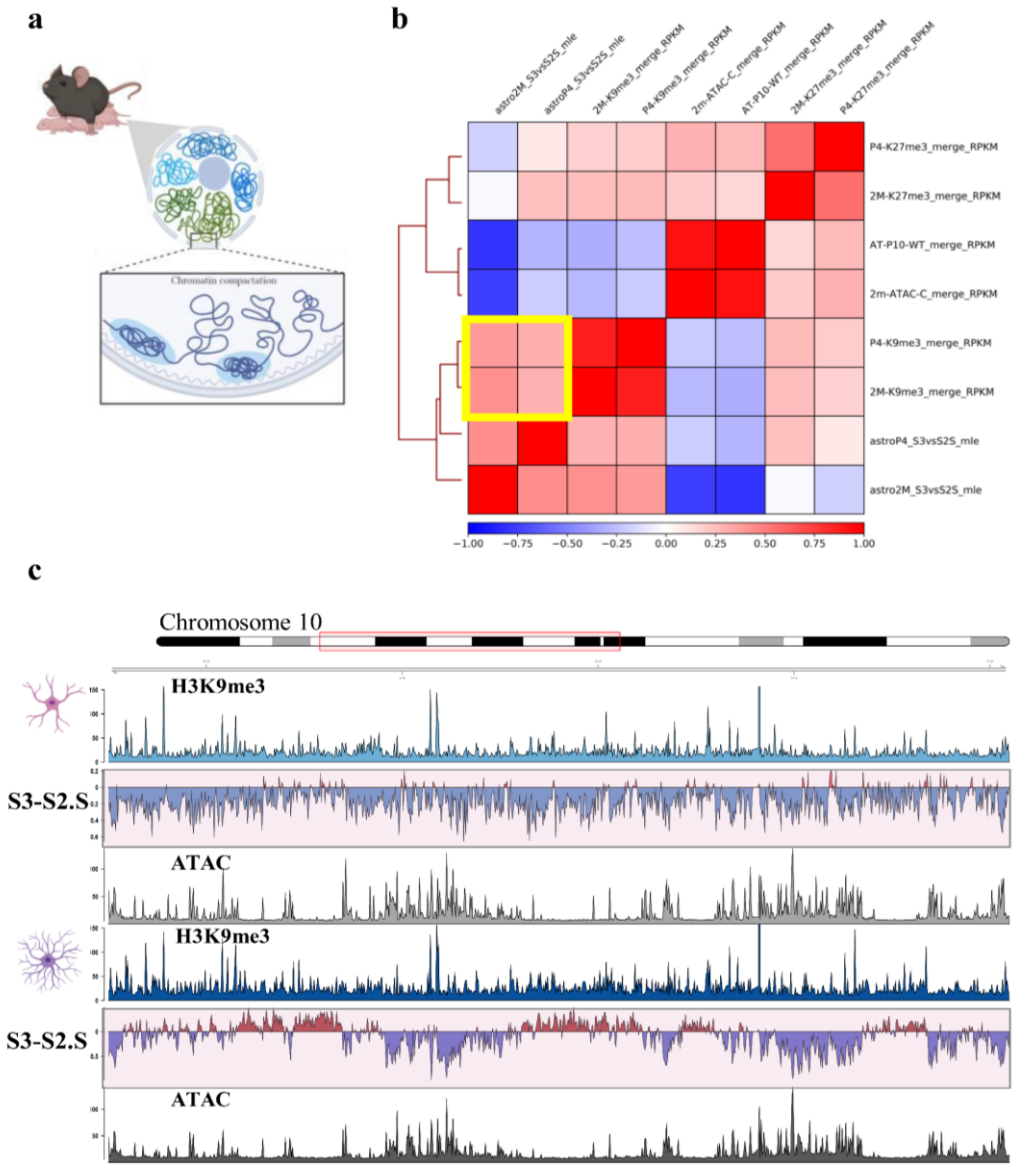

Figure 3.12 Analysing heterochromatin dynamics with SAMMY-seq
a. *Graphical illustration of the different heterochromatin compactation states found within the nucleolus.* ***b****. Correlation plot between SAMMY-seq and all chromatin marks (H3K9me3, H3K27me3, ATAC) in post-natal and adult cells (Yellow box indicating high correlation between H3K9me3 and S3-S2).* ***c.*** *SAMMY-seq signal isolates heterochromatic domains. IGV trace highlighting the SAMMY-seq enrichment signal (S3-S3 ratio) together with the repressive chromatin mark H3K9me3 and ATAC signal (Light blue for H3K9me3; Grey for ATAC signal and red or purple-coloured track for SAMMY-seq S3 vs S2 enrichment or depletion, respectively) on a representative region (Chromosome 10).*

3.13 With maturation there is an increase DNA methylation signal at neuronal genes.

To better understand and further characterize astroglia maturation, we wanted to tackle an additional layer of regulatory information and wondered whether we could see the same effect described so far at the level of the DNA methylation.

To answer this question, we performed methylated-DNA immunoprecipitation sequencing (meDIP-seq) (2 technical replicates and 1 input control for postnatal and mature astrocytes). After performing initial data processing, we identified significant enriched regions over the input conditions. We then merged all the significant regions from each replicate, for each developmental stage, in a unique dataset obtaining a total of 364442 peaks. Then, we plotted the normalized signal of postnatal and mature astrocytes on two heatmaps based on those regions *(Fig. 3.13 a)*. In any case, we did not observe any evident difference in the signal enrichment between the two different developmental stages. Nevertheless, we wanted to understand how the DNA methylation signal was found within the genome between postnatal and mature cells *(Fig. 3.13 b)*. Interestingly, the specific regions identified followed a location pattern concentrated in intergenic and distal zones, similarly to what we observed with the heterochromatin marks. We then associated to each peak its most proximal gene and performed functional enrichment analysis. We noticed that as an astrocyte matures, there was an increase in DNA methylation signal and enrichment on genes important for neurogenesis and its regulation.

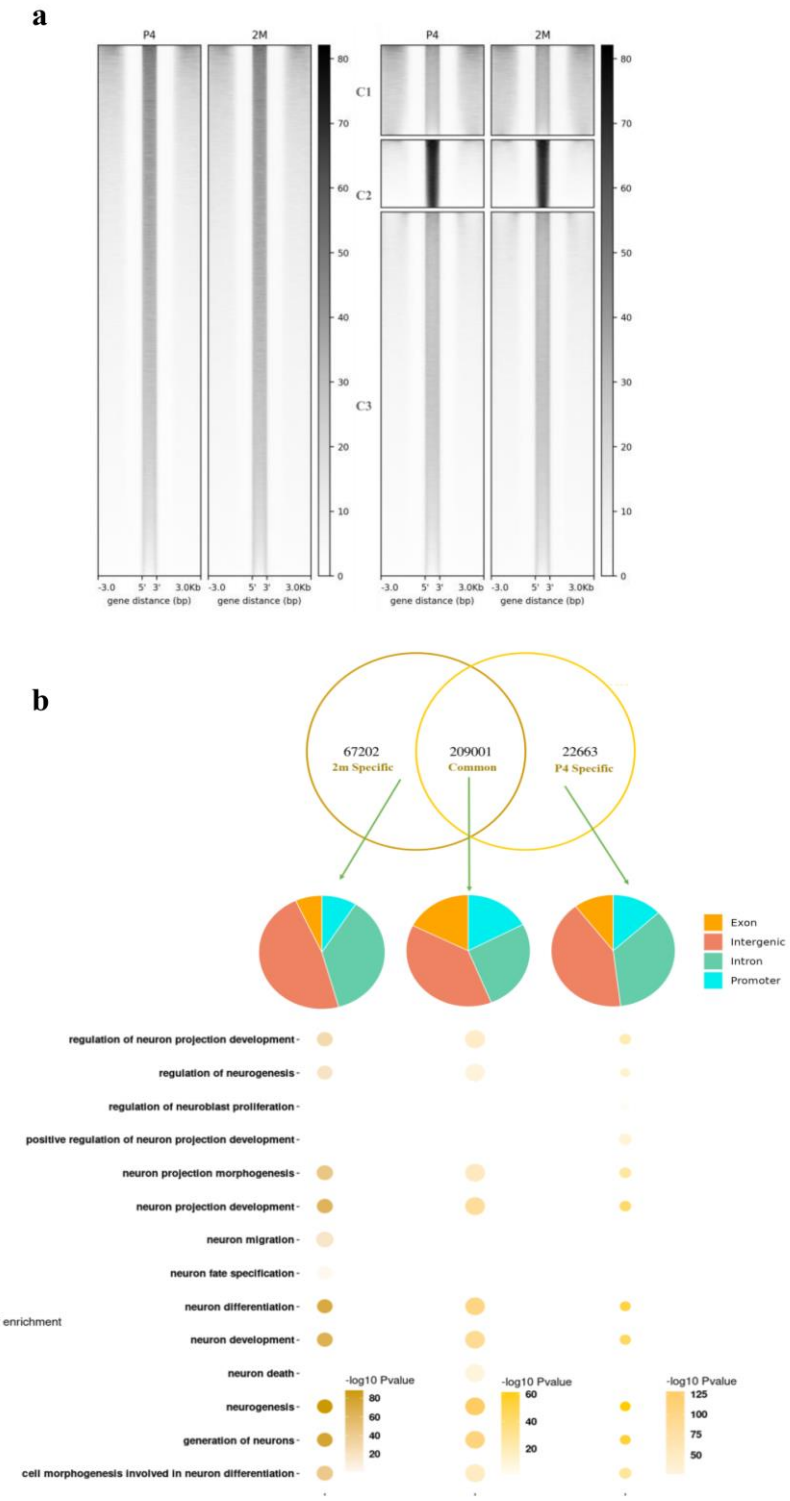

Figure 3.13 Genomic DNA methylation signal in P4 and 2M astrocytes.
a. *Heatmaps for the genomic distribution of the DNA methylation signal in post-natal and adult cells.* ***b****. Venn diagram showing common methylated regions between post-natal and mature cells together with the genomic distribution and functional enrichment results from associating each peak to its closest gene.*

3.14 Mature astrocytes present significantly higher DNA methylation sites and a preference for intergenic regions.

Considering the increase in DNA methylation upon maturation, we wanted to identify the regions that were differentially methylated between the two developmental stages. Therefore, to understand if there were any significant difference in the methylation profile, we used an approach similar to the one used for RNA-seq. In this case, we treated each significant peak as a gene and then we used Deseq2 R package to calculate the statistically different ones (threshold, *padj* <= 0.05, *log2FC* > 0.5). We found a total of 1369 regions in postnatal astrocytes, and 4345 in mature astrocytes showing an increase in DNA methylation level compared to the counterpart *(Fig. 3.14 a).* Again, using the criteria of the most proximal gene, we associated a gene to each one of those regions and performed a functional enrichment analysis *(Fig. 3.14 b).* Interestingly the regions that showed an increased DNA methylation level were significantly proximal to genes noteworthy for the neuronal development and function. This concept is exemplified by the genomic loci containing the two pro-neuronal factors important for neurogenesis during brain development, *Ascl1* and *Ngn2 (Fig. 3.14 c).*

a

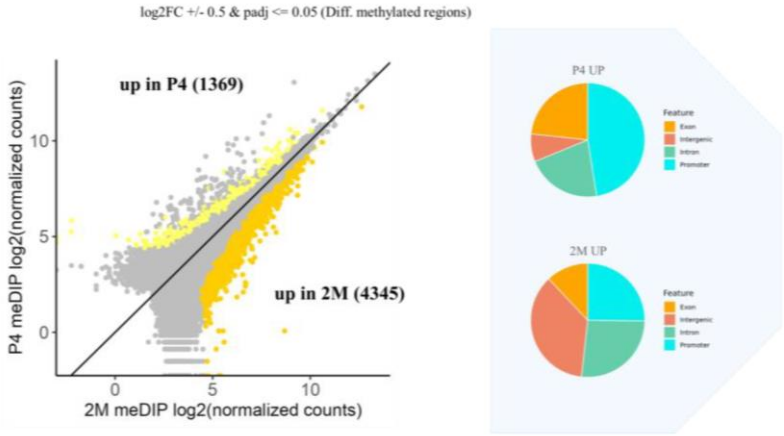
log2FC +/- 0.5 & padj <= 0.05 (Diff. methylated regions)
up in P4 (1369)
up in 2M (4345)
P4 meDIP log2(normalized counts)
2M meDIP log2(normalized counts)
P4 UP
2M UP
Feature
Exon
Intergenic
Intron
Promoter

b

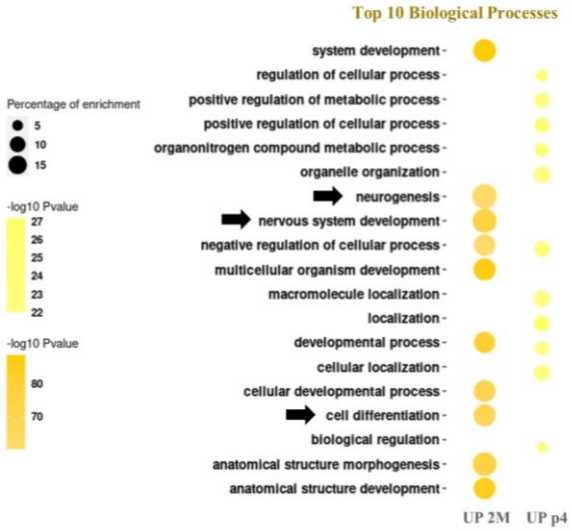
Top 10 Biological Processes
system development
regulation of cellular process
positive regulation of metabolic process
positive regulation of cellular process
organonitrogen compound metabolic process
organelle organization
neurogenesis
nervous system development
negative regulation of cellular process
multicellular organism development
macromolecule localization
localization
developmental process
cellular localization
cellular developmental process
cell differentiation
biological regulation
anatomical structure morphogenesis
anatomical structure development
Percentage of enrichment
5
10
15
-log10 Pvalue
27
26
25
24
23
22
-log10 Pvalue
80
70
UP 2M
UP p4

c

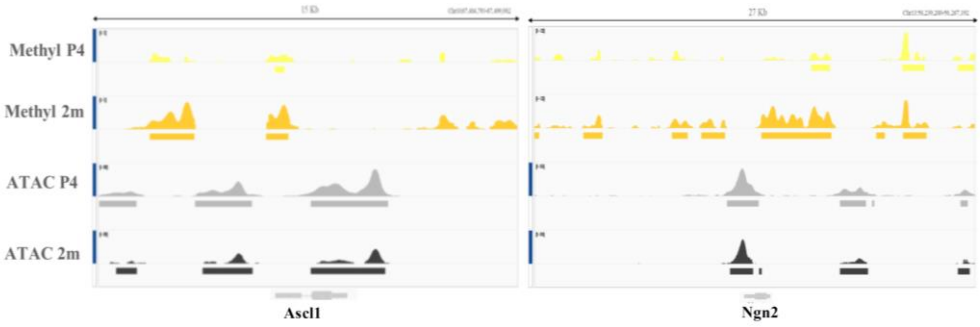
Methyl P4
Methyl 2m
ATAC P4
ATAC 2m
Ascl1
Ngn2

Figure 3.14 Differentially methylated regions during astrocyte maturation
a. *MA plot for the differentially methylated regions between P4 and 2M astrocytes and the distribution of the DNA methylation in the genome.* ***b****. Venn diagram showing common methylated regions between postnatal and mature cells together with the genomic distribution and functional enrichment results from associating each peak to its closest gene.* ***c.*** *IGV shot with the gained DNA methylation traces upon maturation of the pro-neuronal factors Ascl1 and Neurogenin2.*

3.15 Many associated genes methylated with maturation show less RNA levels.

To better investigate the significance of these changes and identify a possible link between methylation and gene regulation, we integrated our data with the RNA-seq data publicly available from Lattke *et al.,* 2021, as previously done. We focused our attention specifically on the regions that showed an increase in DNA methylation at the mature stage. We plotted in a Venn diagram *(Fig. 3.15 a)* the genes related to the neuronal development and we found out that the ones that were significantly different in expression levels (*padj* <= 0.05) were mostly upregulated in the postnatal *(Fig. 3.15 b)*. We therefore observed how DNA methylation negatively correlated with gene expression. Indeed, among genes important for neuronal fate specification, such as Dll1, we found together with a loss in their RNA expression, a gain in DNA methylation and a loss in chromatin accessibility with maturation *(Fig. 3.15 c)*.

Finally, to better define the relation between the different repressive marks that we analyzed so far, we used chromHMM software (Ernst *et al*., 2013). The software takes as an input the binarized genomic signal (200 bp) of the epigenomic data of interest and use a Hidden Markovian Model to understand the relationship between them and determine different chromatin states. In our case, we used our methylated DNA immunoprecipitation (meDIP), H3K9me3 and H3K27me3 dataset (*Fig. 3.15 d)* and we found out that the two tri-methylated H3 marks are distributed separately from each other, with H3K27me3 present in two different states, one with a stronger signal and one with a weaker signal. Overall, the DNA methylation signal is co-occurring together with both H3K27me3 profiles, with an intense signal where the two modifications are stronger and were H3K9me3 is present.

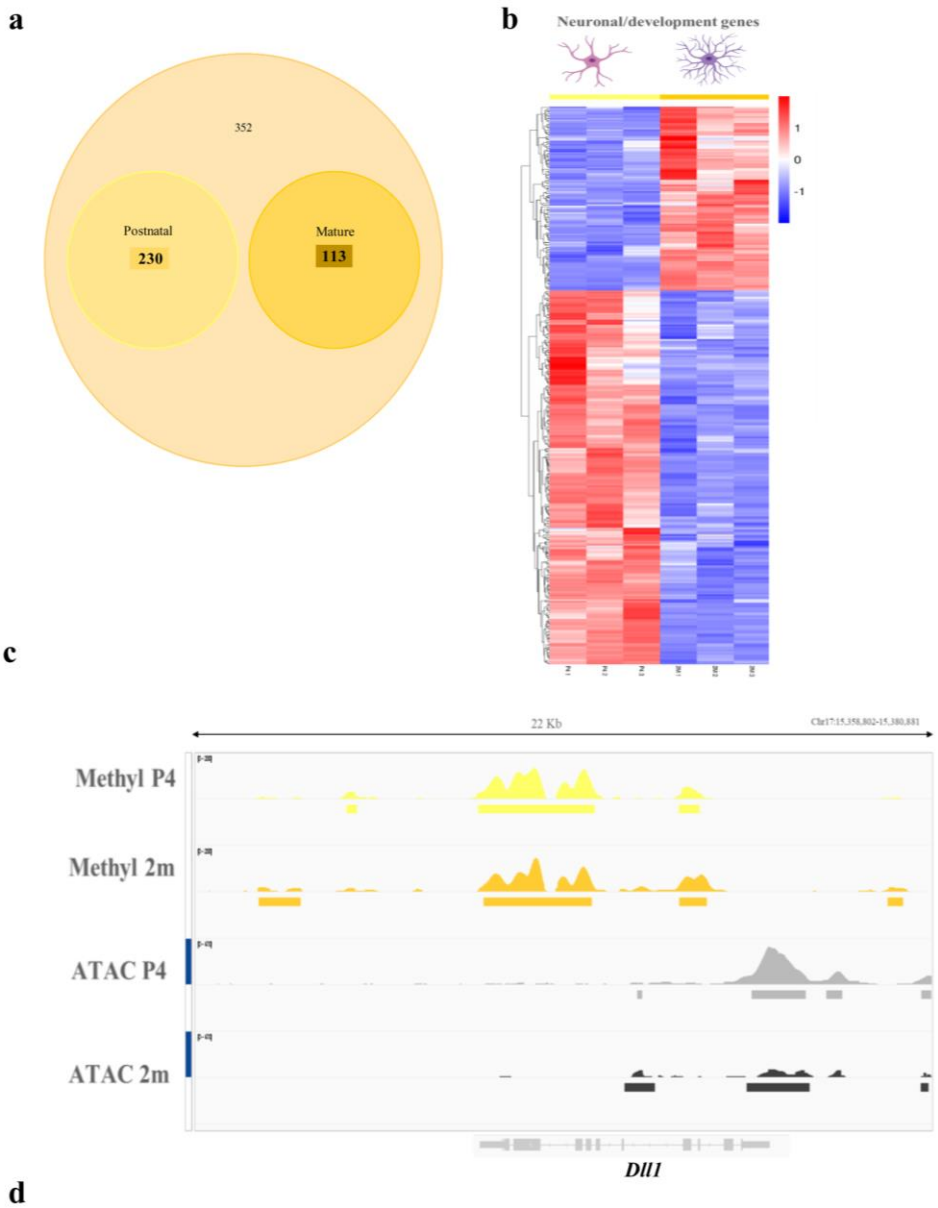
a
352
Postnatal
230
Mature
113
b
Neuronal/development genes
1
0
-1
c
22 Kb
Methyl P4
Methyl 2m
ATAC P4
ATAC 2m
Dll1
d
Chromatin State
1
2
3
4
5
6
H3K9me3
meDIP
H3K27me3
Marks

Figure 3.15 Methylated genes upon maturation show less RNA levels.
a*. Venn Diagram showing the proportion of differentially expressed genes among neuronal/development genes subset associated with DNA methylated regions and relative heatmap (b.).* ***c****. IGV trace for the neuronal fate specification gene Dll1 showing an acquisition of DNA methylation throughout the gene body and surrounding.* ***d.*** *ChromHMM results showing the different chromatin states (1-6) identified in postnatal and adult astrocytes based on the signal of different chromatinic and DNA methylation marks.*

3.16 Mature developmental stages impact on Ascl1 binding pattern.

Having observed that astrocytic maturation brings about a global restructuring of the chromatin architecture in regions involving alternative cell fate identities, we hypothesized that this chromatin state change might have an impact on the general molecular activity of Ascl1 in promoting neurogenesis.

To address this, we examined cortical astrocytes isolated from Aldh1l1:Cre/tdT mice at early postnatal stages (P4), when astrocytes are mainly immature and still proliferating, and at a later stage, when astrocytes have achieved full maturity (2 months). Following the collection and dissociation of the brain tissue, target cells were purified using magnetic-activated cell sorting (MACS) with the astrocyte surface antigen ACSA2 (Fig. S2a). To perform the in vitro conversion at the same time, for the two different developmental stages, we performed the purification of adult cells 10 days before than the postnatal animals, this was done considering mature astrocytes takes around 10 to 14 days to properly attach and reach confluency before any conversion process. Once properly attached, for each stage, $1x10^6$ cells were plated and infected with a Cre inducible lentivirus encoding for *Ascl1.V5*. Passed 3 days from infection, we performed CUT&Tag to map the interaction between Ascl1 and DNA to identify its binding sites on postnatal and adult astrocytes during conversion towards a neuronal phenotype *(Fig. 3.16 a).* Throughout the 3 days in culture, the medium was serum/small molecule free, to properly analyze the effect of the factor and avoid any external cue influence *(Fig.3 16 a).* We performed immunoprecipitation and library preparation from a total of 200.000 postnatal and $1x10^5$ adult nuclei from three independent preparations.

After sequencing and first preprocessing steps, we identified regions with a signal enrichment significantly above the one of IgG control for all replicates of every experimental condition. Afterwards, we merged all the peaks from every experimental replicate, for each condition. We obtained a total of 38223 Ascl1 bound genomic loci in postnatal and 37516 in mature astrocytes. We first analyzed their genomic distribution *(Fig.3 16 b),* finding no major differences between the

two stages, confirming the already described tendency of Ascl1 to bind preferentially far from TSS either intergenic or intronic (Wapinsky *et al*., 2013; Raposo *el at*., 2015). After this initial assessment, we proceeded to perform a qualitative analysis of the binding in the two developmental stages. For both the experimental conditions, we clustered the bound regions based on the normalized signal value (Strength in binding). Then, for each obtained cluster, we mapped its position across the genome *(Fig.3 16 c, d)*. In this initial data there is already a glimpse of some differences in the binding action of Ascl1, showing that especially in the first 2 clusters from the mature astrocytes there is a changed preference for the factor to bind preferentially to promoter proximal regions. At the same time, we also linked each peak to the proximal gene and performed functional enrichment analysis *(Fig.3 16 c, d)*, showing how overall, in both cases, Ascl1 target genes revealed an enrichment of biological processes linked to neuronal differentiation and neuronal activity. Nevertheless, it was noticeable how in mature cells Ascl1 binding was less significant and enriched on genes pertaining to cluster 1, where the strongest signal in its binding was found *(Fig.3 16 c, d).*

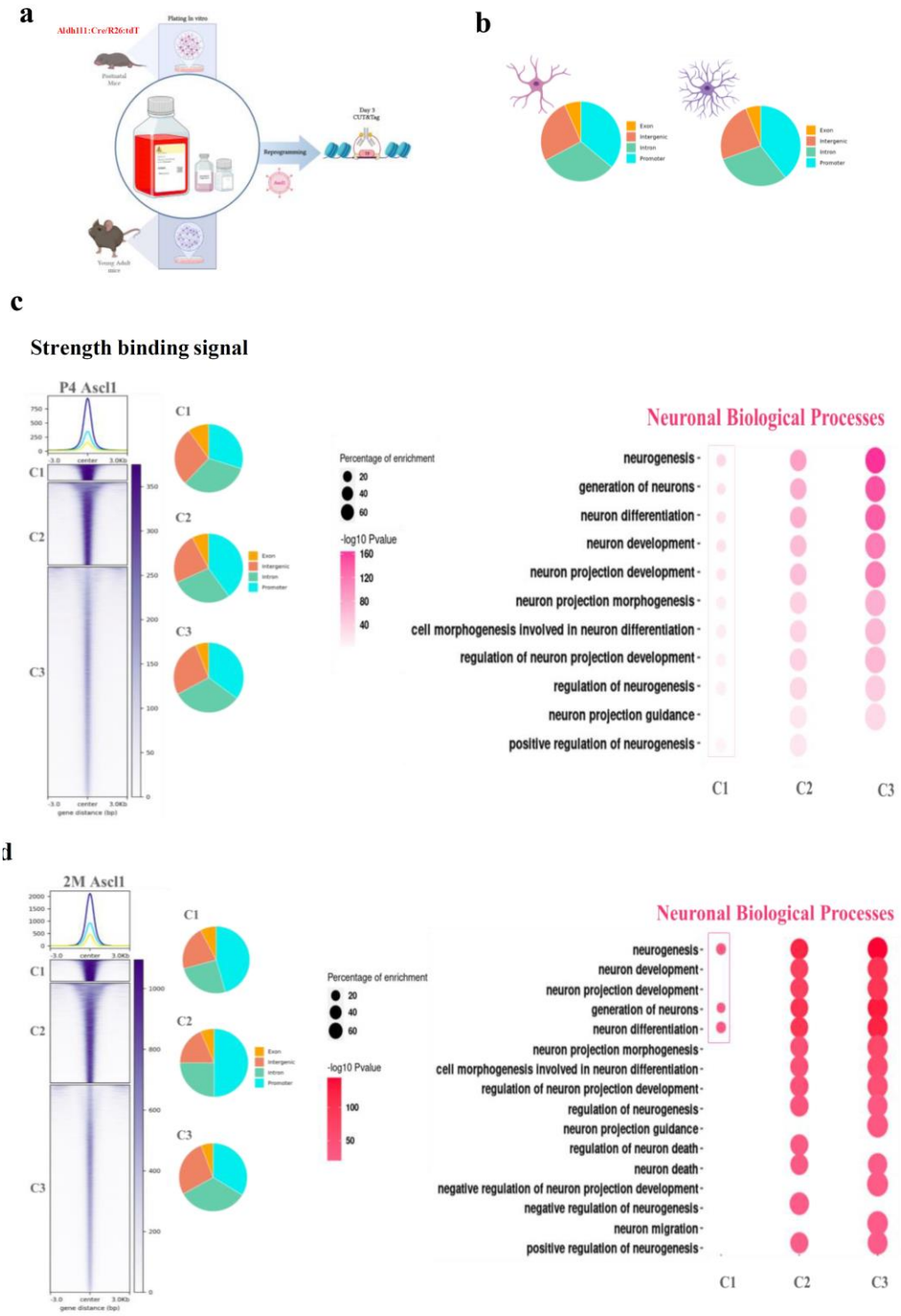
a
Aldh1l1:Cre/R26:tdT
Plating In vitro
Postnatal Mice
Young Adult mice
Reprogramming
Day 3 CUT&Tag
b
Exon
Intergenic
Intron
Promoter
c
Strength binding signal
P4 Ascl1
C1
C2
C3
gene distance (bp)
Neuronal Biological Processes
Percentage of enrichment
20
40
60
-log10 Pvalue
160
120
80
40
neurogenesis
generation of neurons
neuron differentiation
neuron development
neuron projection development
neuron projection morphogenesis
cell morphogenesis involved in neuron differentiation
regulation of neuron projection development
regulation of neurogenesis
neuron projection guidance
positive regulation of neurogenesis
d
2M Ascl1
100
50
regulation of neuron death
neuron death
negative regulation of neuron projection development
negative regulation of neurogenesis
neuron migration

***Figure 3.16 Ascl1 binding profile in postnatal and adult astrocytes in vitro. a**. Graphic scheme of the experimental rational (n=4 Adult mice, n=6 Postnatal mice). **b.** Genomic distribution of Ascl1 in postnatal and adult astrocytes. **c**. Heatmap for Ascl1 binding, clusters (C1, C2, C3) showing binding sites ordered by their signal strength in postnatal **(c)** and adult mice **(d)**. Next to each figure functional enrichment results obtained by linking each peak with the closest gene.*

3.17 Ascl1 binds to more genomic regions at P4 than at 2M astrocytes In vitro.

To better understand the different action Ascl1 has between postnatal and mature astrocytes we performed a differential binding analysis using Deseq2 R package. First, we generated a consensus set of Ascl1 bound regions merging the peaks from the postnatal and the mature stage, obtaining a unique set of 48562 regions. After running the analysis, to obtain the differentially bound regions (DBRs), we filtered (*padj*<=0.05, *log2FC* > 0.5) 11223 peaks that were more bound to the postnatal stage and 8681 more bound to the mature astrocytes *(Fig. 3. 17 a).* We then wanted to identify where in the genome these DBRs were located, finding how at postnatal stages the TF does not change its binding towards intergenic regions, whereas in adult astrocytes there is an acquisition of many promoter sites *(Fig. 3.17 a).* We then identified how the majority of DBRs were associated with genes enriched for GO terms related to the regulation of neuron differentiation and the morphological changes involved in neuron differentiation *(Fig 3.17 b, c).* Additionally, we wondered if these differences in Ascl1 binding were also located at genes regulating the functional properties of neurons during differentiation, such as *Shank3*. Gene Ontology analysis of the DBRs of Ascl1 revealed an enrichment of biological processes linked to synaptic properties, including synapse assembly, synaptic signaling or chemical synaptic transmission *(Fig. 3. 17d, e).*

Ascl1 genome binding has been described in few other cellular types, always showing a preference for intergenic regions, in line with our current results. Interestingly, when looking at mature cells differential binding sites, we found an increase at promoters *(Fig. 3.17 a, f*). Ascl1 seems to bind new 1509 additional promoters on mature cells *(Fig. 3.17 f, g)* which were associated to many genes regulating a variety of biological and cellular processes. However, we identified a group of promoters, related to the regulation of the nervous system development that was only present on postnatal astrocytes *(Fig. 3.17 h).* This suggests that besides the gain in binding sites on mature cells at promoter sites, only at a postnatal

stages Ascl1 binds specifically to a set regulating the development of the nervous system.

Overall, these results are indicative of a significant difference in the number of regions that are bound by Ascl1 between postnatal and adult cells, with a loss, or delayed binding to genomic sites associated with genes regulating the process of neuronal induction in vitro.

a

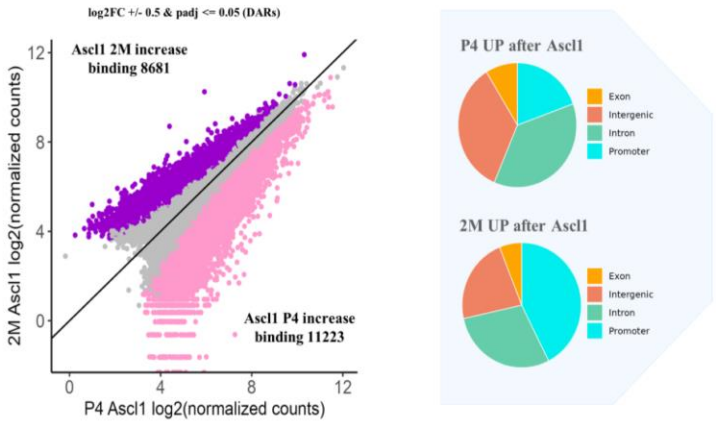
log2FC +/- 0.5 & padj <= 0.05 (DARs)
Ascl1 2M increase binding 8681
Ascl1 P4 increase binding 11223
2M Ascl1 log2(normalized counts)
P4 Ascl1 log2(normalized counts)
P4 UP after Ascl1
2M UP after Ascl1
Exon
Intergenic
Intron
Promoter

b

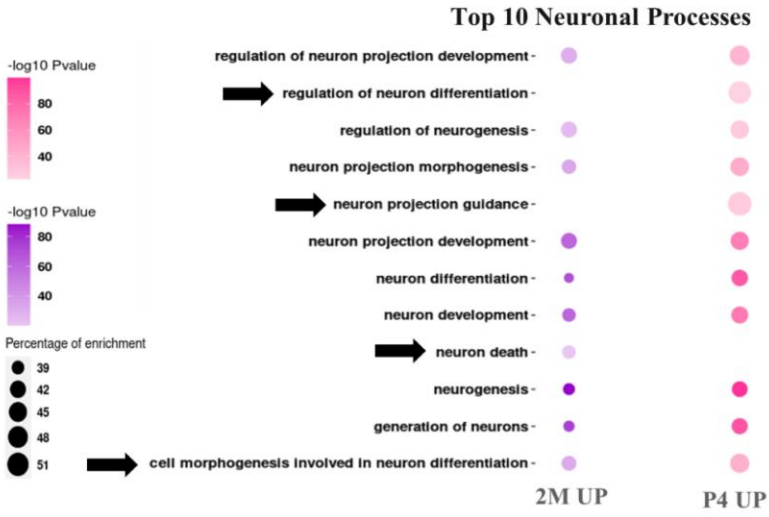
Top 10 Neuronal Processes
-log10 Pvalue
Percentage of enrichment
regulation of neuron projection development
regulation of neuron differentiation
regulation of neurogenesis
neuron projection morphogenesis
neuron projection guidance
neuron projection development
neuron differentiation
neuron development
neuron death
neurogenesis
generation of neurons
cell morphogenesis involved in neuron differentiation
2M UP
P4 UP

c

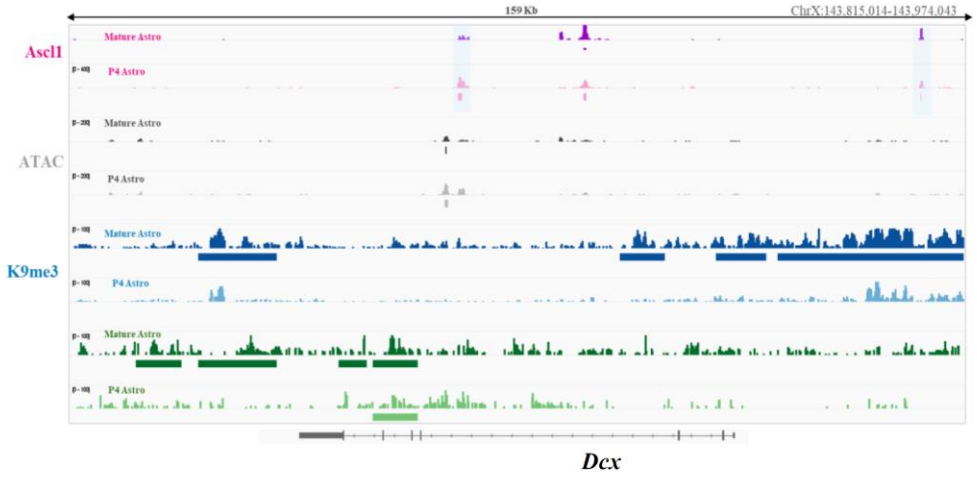
159 Kb
ChrX:143,815,014-143,974,043
Ascl1
ATAC
K9me3
Mature Astro
P4 Astro
Dcx

d

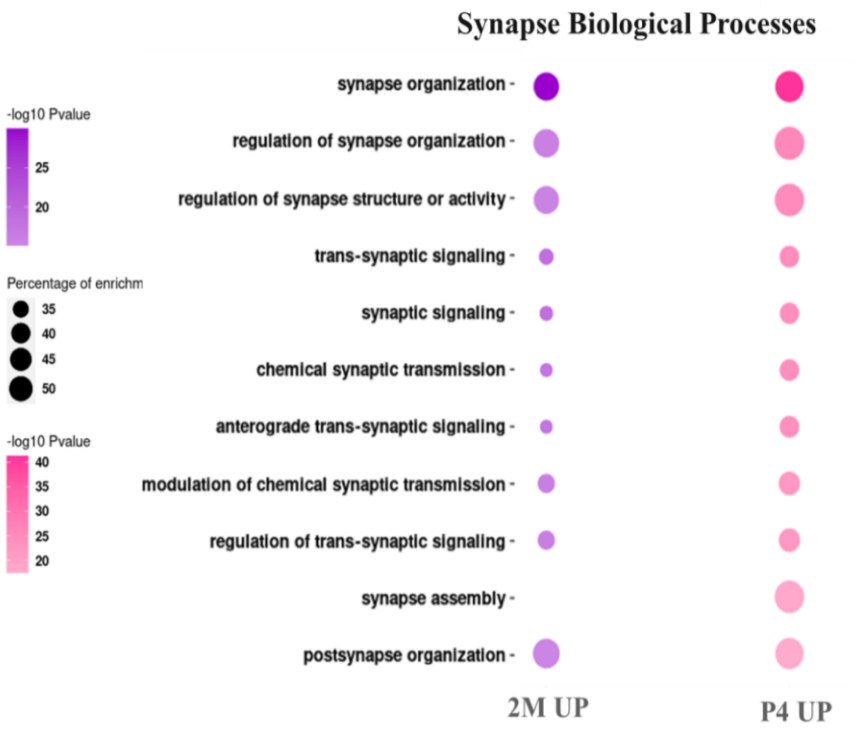
Synapse Biological Processes
-log10 Pvalue
25
20
Percentage of enrichm
35
40
45
50
-log10 Pvalue
40
35
30
25
20
synapse organization
regulation of synapse organization
regulation of synapse structure or activity
trans-synaptic signaling
synaptic signaling
chemical synaptic transmission
anterograde trans-synaptic signaling
modulation of chemical synaptic transmission
regulation of trans-synaptic signaling
synapse assembly
postsynapse organization
2M UP
P4 UP

e

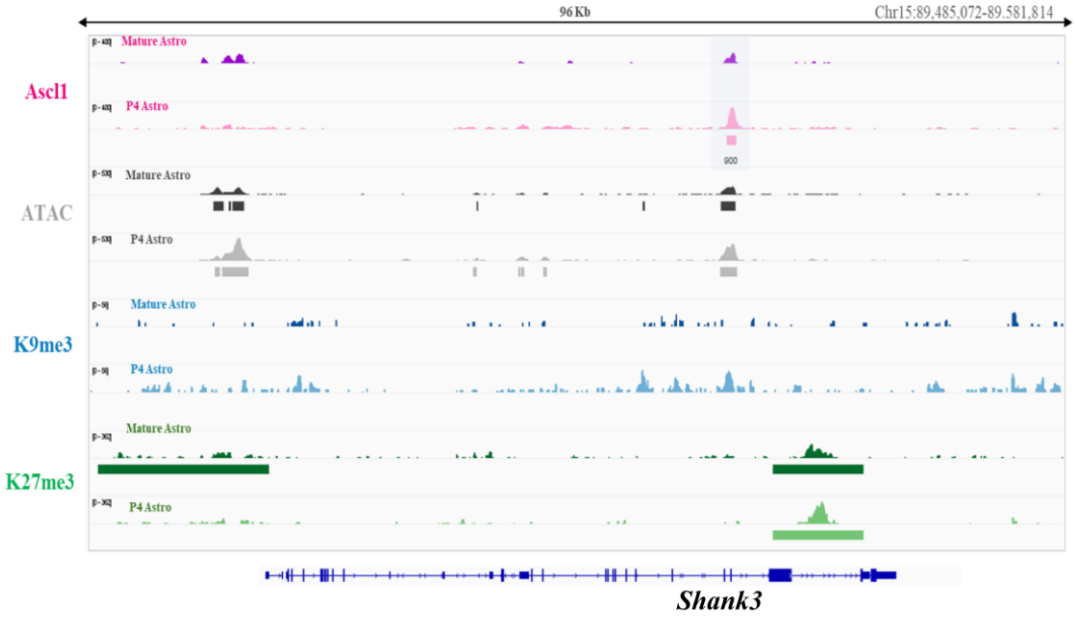
96 Kb
Chr15:89,485,072-89,581,814
Ascl1
ATAC
K9me3
K27me3
Mature Astro
P4 Astro
Shank3


f
P4 UP after Ascl1
2182
Exon
Intergenic
Intron
Promoter
2M UP after Ascl1
3690
Exon
Intergenic
Intron
Promoter
g
DBRs at promoters
Mature
3056
293
Postnatal
1585
h
Top 10 Biological processes
-log10 Pvalue
50
45
40
35
Percentage of enrichment
12
15
18
21
-log10 Pvalue
100
75
50
25
system development
regulation of multicellular organismal process
regulation of cellular process
regulation of biological process
positive regulation of lipid localization
positive regulation of cellular process
positive regulation of biological process
organonitrogen compound metabolic process
nervous system development
negative regulation of cellular process
multicellular organism development
developmental process
biological regulation
animal organ development
anatomical structure morphogenesis
anatomical structure development
2M UP
P4 UP

Figure 3.17 In vitro comparison differential bound regions at promoters.
a. *MA plot for the Ascl1 differential bound regions between P4 and 2M astrocytes and their genomic distribution.* ***b.*** *Functional enrichment results for the top 10 neuronal processes were obtained by linking each peak with the closest gene.* ***c.*** *IGV trace for the neuronal gene DCX. Highlighted the lost Ascl1 peaks in adult astrocytes.* ***d.*** *Functional enrichment results for the top 10 synaptic processes were obtained by linking each peak with the closest gene.* ***e****. IGV trace for the neuronal gene regulating synaptic assembly and activity Shank3. Highlighted the lost Ascl1 peaks in adult astrocytes.* ***f.*** *Upregulated promoters after Ascl1 infection in P4 and 2M astrocytes.* ***g****. Venn diagram with specific and shared promoters that are differentially bound regions (DBR) of Ascl1 in both developmental stages.* ***h****. GO terms for the differentially bound promoters in astrocytes.*

3.18 An increasing number of genes driving neuronal differentiation are lost targets of Ascl1 in mature astrocytes.

We next sought to identify the regions that were more specifically bound by Ascl1 at each stage. With this purpose, we decided to filter regions not only by the Deseq2 filters, but we also plotted on a Venn diagram the regions that were found to be significant peaks in one or the other timepoint *(Fig.3.18 a)*. We ended up obtaining 5201 peaks that were stage specific at postnatal stage and 3375 peaks that were specific in the mature astrocytes *(Fig.3.18 a)*. A set of 23334 peaks were found to be in common between the two conditions. We then associated to each specific peak the closest gene and use the RNA-seq data previously mentioned to understand how the transcriptional landscape surrounding these subsets of bound regions is shaped. We plotted in a histogram for each subset the number of differentially expressed genes (DEGs) based on the log2 fold change between postnatal and mature astrocytes *(Fig.3.18 b)*. These data seem to indicate that a more favorable transcriptional landscape is present around those genes in the juvenile astrocytes. Interestingly, this effect was also observed even in the subset of targets that are specific in the adult stage *(Fig. 3.18 b)*. In accordance with our previous results, the genes identified within these Ascl1 binding stage-specific sites are regulating the overall process of neuronal identity *(Fig. 3.18 c)*. Among the gene targets that are loss in mature astrocytes, we identified the transcriptional repressor *Myt1l*, a known cofactor of Ascl1 during conversion that represses the starting cells' transcriptional program *(Fig. 3.18 c, d)*. On the contrary, some neuronal targets are only identified later in development, like the *Isl1*, which plays an essential role in neuron differentiation and cholinergic neuron identity *(Fig. 3.18 e)*.

Overall, these results suggest that despite no big differences are found between the pattern in Ascl1 binding between the two developmental stages, there is however an important set of genes relevant for the conversion towards a neuronal fate that are lost in mature astrocytes.

a

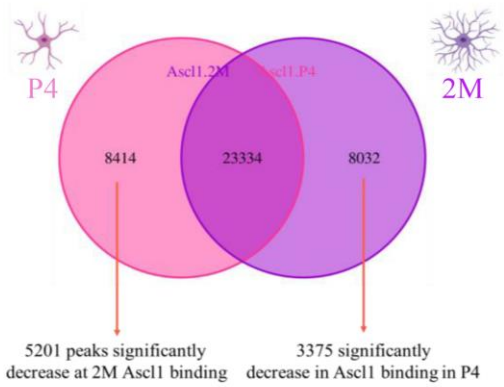
P4
Ascl1.2M
Ascl1.P4
2M
8414
23334
8032
5201 peaks significantly decrease at 2M Ascl1 binding
3375 significantly decrease in Ascl1 binding in P4

b

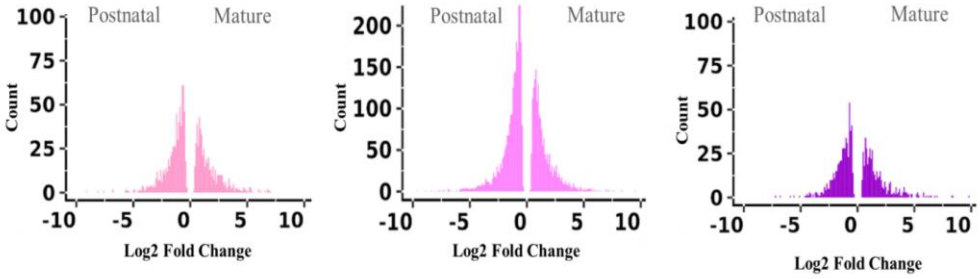
Postnatal
Mature
Count
Log2 Fold Change

c

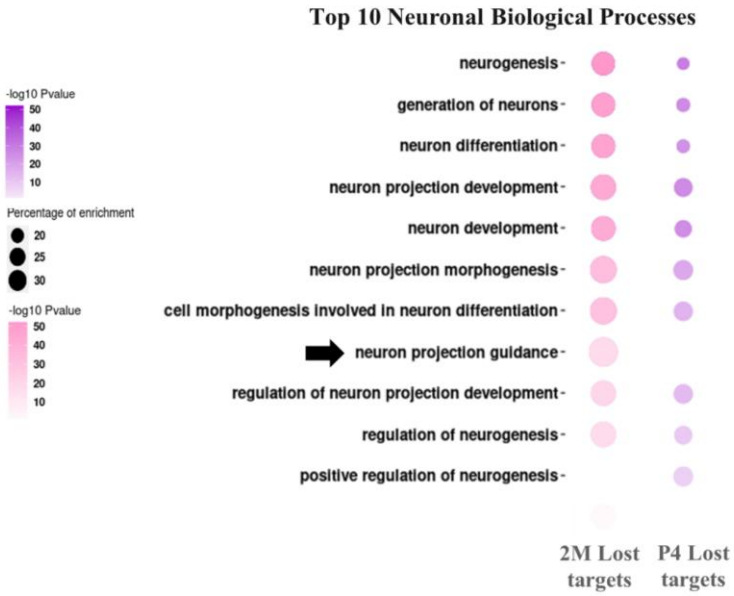
Top 10 Neuronal Biological Processes
-log10 Pvalue
Percentage of enrichment
neurogenesis
generation of neurons
neuron differentiation
neuron projection development
neuron development
neuron projection morphogenesis
cell morphogenesis involved in neuron differentiation
neuron projection guidance
regulation of neuron projection development
regulation of neurogenesis
positive regulation of neurogenesis
2M Lost targets
P4 Lost targets

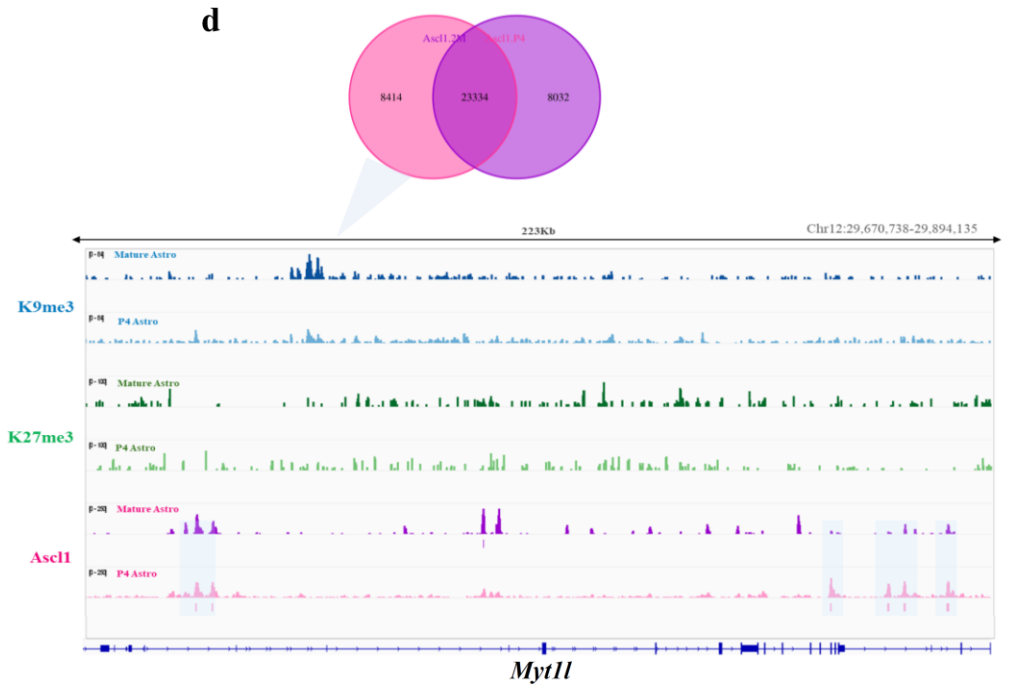
d
8414
23334
8032
223Kb
Chr12:29,670,738-29,894,135
K9me3
K27me3
Ascl1
Mature Astro
P4 Astro
Myt1l

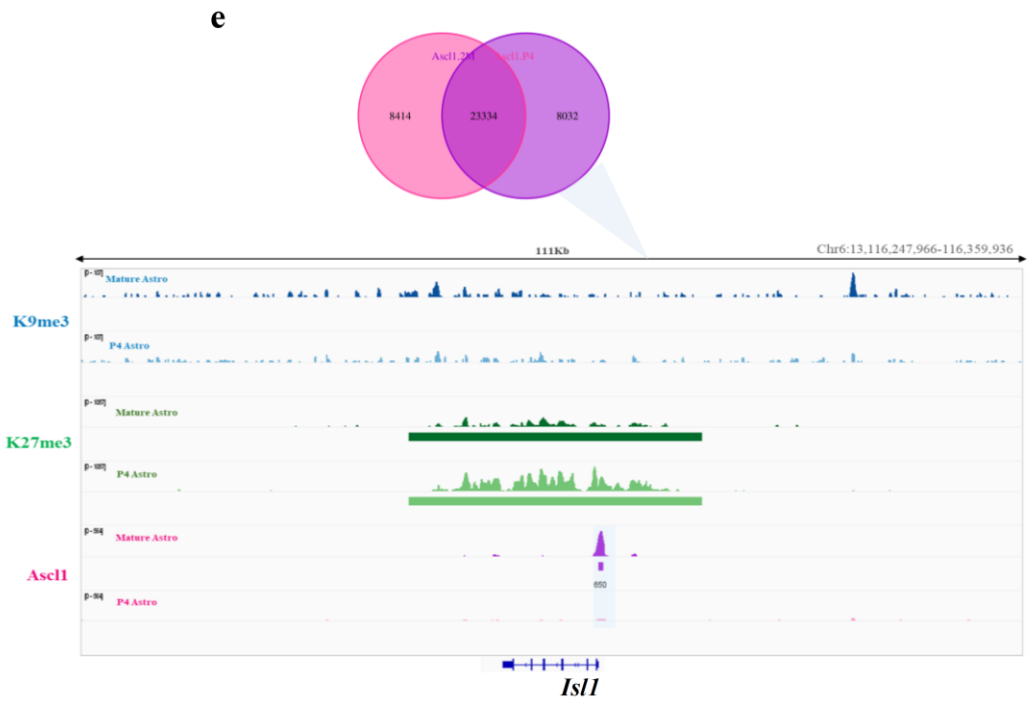
e
8414
23334
8032
111Kb
Chr6:13,116,247,966-116,359,936
K9me3
K27me3
Ascl1
Mature Astro
P4 Astro
Isl1

Figure 3. 18 Ascl1 specific peaks for each astrocytic developmental stage.
a. *Venn diagram illustrating the statistically significant specific peaks for P4 and 2M astrocytes.* ***b.*** *Histogram plot, showing the number of differentially expressed genes targeted by Ascl1 at different developmental stages ordered by the log2 fold change between the post natal and mature stage.* ***c.*** *Functional enrichment results for the top 10 neuronal processes obtained by linking each peak with the closest gene for the lost targets at each stage.* ***d****. Venn diagram illustrating the statistically significant specific peaks for P4 and a representative IGV tracing shot for the transcriptional repressor Myt1l, lost in mature cells.* ***e****. Venn diagram illustrating the statistically significant specific peaks for 2M and a representative IGV tracing shot for the neuronal Isl1 gene, lost in mature cells*

3.19 Target genes important for neuronal functionality are lost in mature astrocytes

Based on the general goal of cell conversion to produce a mature, and subsequently functional neuron, we sought to analyze how certain genes in this regard are found in postnatal and adult astrocytes. Considering our in vitro results, postnatal cells as early as 20 days post infection already presented electrophysiological properties. Unfortunately, mature cells in vitro at the same time point fail to reach the confluency required for induced neurons to generate contact and promote these properties. However, with the genomic analysis, we are able to gain a better understanding on whether there are any differences by examining further these *Ascl1* binding sites that were lost as a result of maturation. Accordingly, we looked for genes regulating the acquisition of synaptic properties in the converted cells. Following our in vitro observations, postnatal cells displayed an enhanced and significant proportion of specific target genes involved in synaptic development. On the contrary, many of these regions, like *lrrtm4* which regulates synaptic assembly, were lost with maturation *(Fig. 3. 19 a, b)*. These results indicate that in our model, *Ascl1* binds to a lesser extent to neuronal identity genes, and more specifically to genes that are important in the determination of a mature and functional neuron.

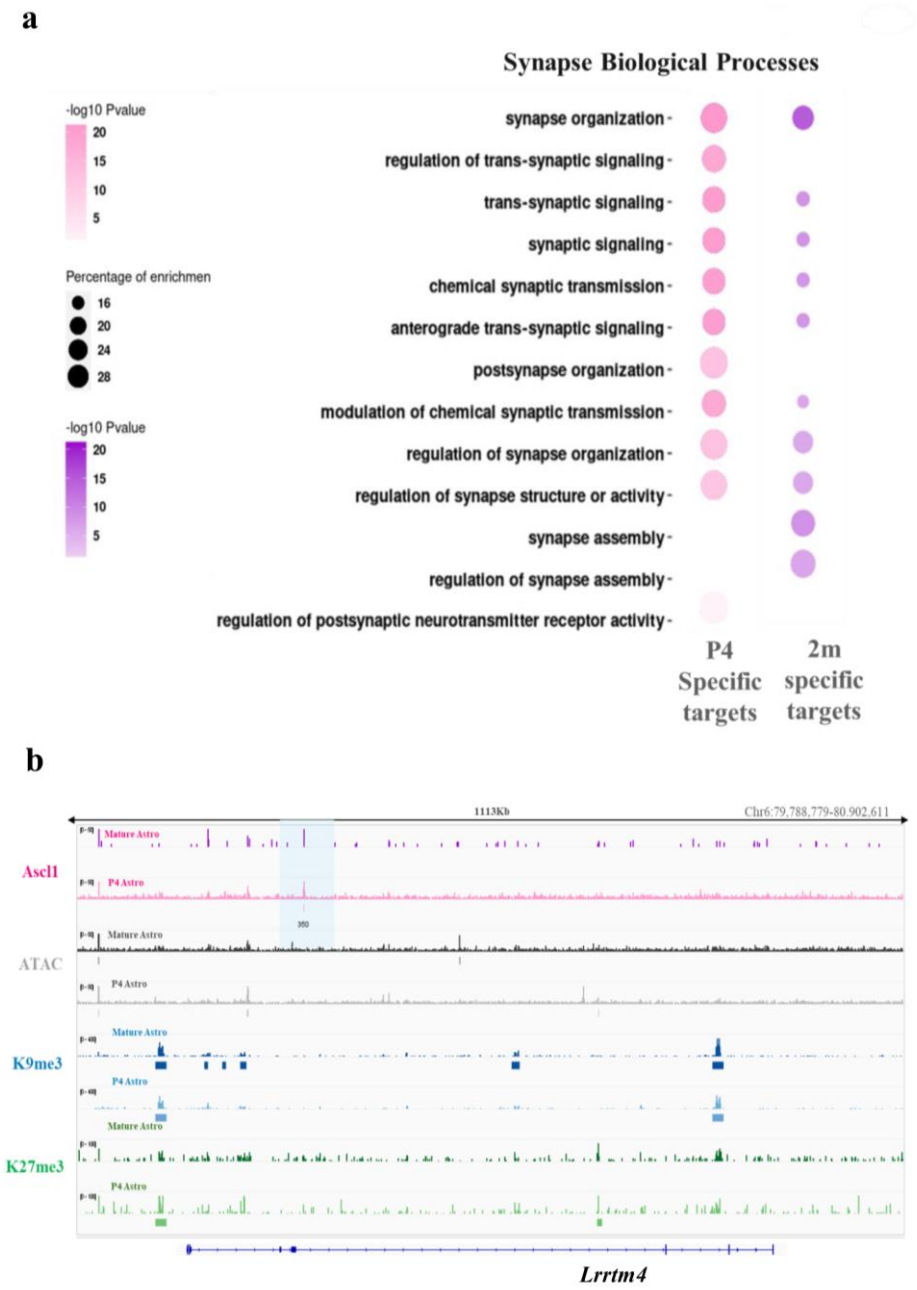

Figure 3. 19 Target genes important for neuronal functionality are lost in mature astrocytes.

a. *Functional enrichment results for the top 10 synaptic processes obtained by linking each peak with the closest gene in P4 and 2m specific Ascl1 binding sites.* ***b.*** *IGV tracing shot for the gene regulating synaptic assembly LRRTM4, lost in mature cells*

3.20 Ascl1 preferentially binds to already accessible chromatin.

Ascl1 is well established as a pioneer transcription factor, with evidence demonstrating its capacity to bind closed chromatin and promote local DNA accessibility (Wapinski *et al*., 2013; Raposo *et al.,* 2015; Park *et al*., 2017). However, how this factor behaves in different developmental stages has not been described yet. What it has been shown is how a permissive chromatin environment allows for a promiscuous binding of Ascl1 to the chromatin (Woods *et al*., 2022) and how a highly compacted chromatin environment blocks the pioneer activity of some proteins (Mayran *et al.,* 2018). Considering how we have described an acquisition of a more restricted environment with maturation in astrocytes, and the difference in the binding preference, we wondered how Ascl1 might deal with such a difference.

Consequently, to gather further evidence for Ascl1 pioneer activity at the identified binding sites we used chromHMM again to understand which chromatin states were predominantly in the regions bound by the factor *(Fig. 3. 20 a)*. As it shown in the figure, the preference goes toward a chromatin which is in active state, as indicated by a strong presence of active marks such as H3K27ac and open chromatin. In both cases, there is also a very mild co-occurrence in regions that present some degree of DNA methylation and H3K27me3, indicating that Ascl1 might also bind to a portion of poised/mildly repressed regions. The preference for active chromatin is also underlined by the heatmaps *(Fig. 3. 20 a)* which shows that the stronger the factor signal is, the higher the degree of chromatin accessibility and H3K27ac is. Indeed, when looking at the chromatin state among the specific bound regions previously identified, we can see how this is the case also when looking at the mature-specific sites, where Ascl1 is binding in chromatin slightly more accessible and active than at postnatal one. Overall, these results are indicating that, at least in our model, Ascl1 binds at already open and active DNA, representing permissive environments.

To conclude, this work provides strong results proving how during astrocyte maturation there is an increase presence in repressive marks and DNA methylation on genes regulating neuronal identity. The direct repression of many genes important for neuronal differentiation, maturation and function seems to be mainly polycomb mediated; whereas the heterochromatin mark H3K9me3 correlates with higher chromatin condensation in mature stages but seems to not affect directly Ascl1 binding. Moreover, we provide the first in vitro characterization of Ascl1 binding profile in mature astrocytes with many unknown effects. Initially, we described how this protein binds more genomic regions regulating conversion at postnatal stages than for adult astrocytes. Interestingly, we also observed a shift in Ascl1 genomic binding preference towards promoters in more mature cells, and despite this, there is a loss of many targeted promoters associated with genes regulating the nervous system development. Additionally, in adult astrocytes, we could see that Ascl1 targets in a lesser extent neuronal identity associated genes and despite this transcriptional factor is regarded to have a pioneer activity, in astrocytes, Ascl1 preferentially binds mostly on accessible chromatin.

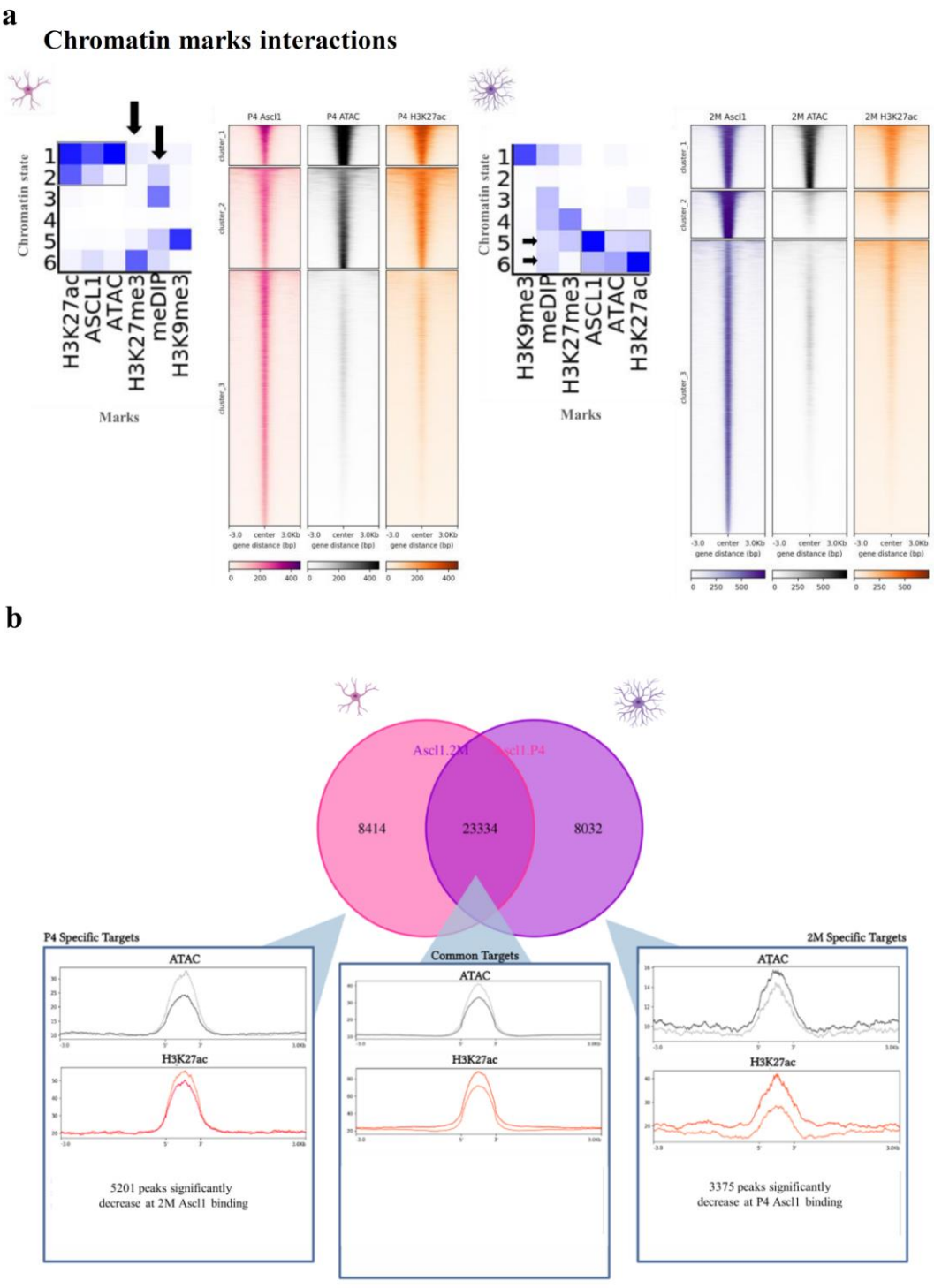

Figure 3.20 Ascl1 preferentially binds to already accessible chromatin.
a. *ChromHMM results showing the different chromatin states identified in post-natal and adult astrocytes based on the signal of different chromatinic marks. On the side heatmaps showing the signal enrichment of Ascl1, ATAC, H3K27ac in Ascl1 peaks at post-natal (38.223 regions) and mature astrocytes (37.516 regions).* ***b.*** *Scheme illustrating the chromatin accessibility and active mark H3K27ac for P4, 2m and common peaks.*

4 On-going work.

Currently, looking at the relationship found between all the omics performed *(Fig. 3.20 a)* we are trying to understand the realtionship between DNA methylation dataset, the described Ascl1 results in vitro, and the presence of the repressive mark H3K27me3.

To further characterize the chromatin landscape during astrocyte maturation we are looking at the overall arrangement of distal regulatory regions, to test if at this level there are differences among the two developmentals stages *(Fig. S3)*. Preliminary data, done by mapping the active histone mark H3K27ac, indeed goes in accordance with this idea, showing a rearrangement in some cluster groups of CREs during maturation (*Figure 4.1*). Additionally we have performed the same experimental approach, but on postnatal and adult mice infected with an AAV expresing *Ascl1* (Fig. S3). Here we intend to study the impact Ascl1 has in vivo on these regulatory regions and on chromatin accessibility. This way we aim to describe the whole enhancer-Superenhancer reorganization during maturation and reprogramming. This will enable us to study how cell heterogeneity affects differently astrocytes capacity to initiate reprogramming, even from cells within the same brain region, as astrocytes do still show a level of idiosyncrasy (Siletti *et al*, 2022).

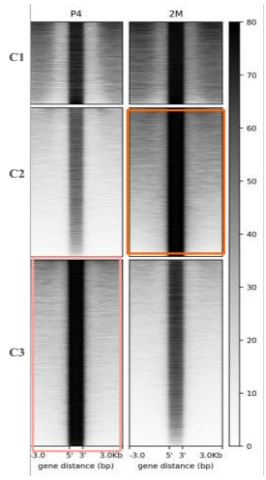

Figure 4.1 H3K27ac signal across the genome during astrocyte maturation.

5. Discussion

The perspective of cellular identity and plasticity has evolved from early reprogramming studies using somatic cell nuclear transfer (SCNT) to enucleated vertebrate eggs (GURDON *et al.*, 1958; Wilmut *et al.*, 2002; Takahashi & Yamanaka, 2006). Nowadays, not only is cell fate reprogramming possible starting from a fully differentiated cell, but it is aimed towards an application to human disease, by restoring and replacing the structure and function of an affected brain network (Barker *et al.*, 2018; Leaman *et al.*, 2022). The potential benefits of direct reprogramming for regenerative medicine are in addition to increasing our understanding of cell fate specification and plasticity (Fang *et al*, 2018; Wang *et al*, 2021a). Indeed, countless in vitro and in vivo studies on mice and in human cells have shown how cell fate can be manipulated, albeit with varying and relatively low efficiency, especially when employing it directly in the brain. However, this field is currently looked with skepticism as recent studies have shown limited to no neuronal conversion *in vivo,* questioning the lack of proper tracing and delivery methods, overall challenging the field (Xiang *et al*, 2021; Wang *et al*, 2021b; Leib *et al*, 2022), and further incrementing the discrepancies found up until now.

Despite these methodological problems recently highlighted (Xiang et al, 2021), for the past two decades, a plethora of studies have been published, elucidating numerous factors that can both, enhance and diminish the outcome of the conversion of specific cell types into neurons (Bocchi et al, 2022). Direct reprogramming applied for the repair of the CNS has the major advantage of the use of endogenous cells as a source of cell-based replacement for neurons lost due to an insult or neurodegeneration (Bocchi et al, 2022; Leaman et al, 2022). In this sense, astrocytes, a peculiar star-shaped cell, are regarded as the ideal candidate cell type for this purpose. This is not only due to their numerosity in the CNS or their closer ontogenetic relationship with the terminal cell, the neuron, but because of their functional heterogeneity across the nervous system and the fact that they share

a common progenitor with them. Indeed, developmentally related cells allow for a more feasible conversion (Leaman et al, 2022). Due to their regional identity, astrocytes differ from other glia, in their shared gene regulatory networks with neurons residing within the same brain region (Herrero-Navarro et al, 2021). Fundamentally, these cells bear, to a certain degree, a similar transcriptional program with neurons, hence making them great candidates for ease of transdifferentiation.

Besides the close developmental relationship, other variables have shown to influence the amenability of cellular reprogramming. The developmental stage, that is, the maturation state of the starting cell can highly impact the proneness of a cell to change its identity (Jorstad et al, 2017). The most successful transdifferentiation experiments done in vitro have, indeed, used cortical astrocytes from postnatal mice, yet when replicating the procedure in vivo, the animals used are at a young adult age. Thus, at two distinct stages of development. While astrocyte heterogeneity has been documented at the morphological, functional, and, more recently, at the single-cell level, little is known about their cellular specification and maturation process. A recently published study by Lattke and colleagues in 2021, describes how astrocytes undergo significant transcriptional and chromatin changes from postnatal to mature stages in the brain. More intriguingly, it also reveals that in vitro models using these cells fail to mimic the in vivo astrocytic phenotype (Lattke et al, 2021). The differences between the transcriptional profiles of astrocytes in these two environments, increase exponentially, with astrocytes failing to recapitulate in vitro the maturation state found in the living brain even at postnatal stages (Lattke et al, 2021).

All in all, this study strongly indicates that the mechanisms identified so far hardly account for the astrocyte maturity in vivo. This paper, without a doubt, constitutes a valuable resource for future research. Therefore, when looking at the

field of direct reprogramming, a major limitation is still encountered when aiming to reveal the molecular changes driving conversion or even the molecular signature of the factors ectopically employed to rewrite cell identity. So far, the currently available results are from studies performed mainly on in vitro conditions and on cells which, apparently, are not completely representative of those in the adult brain (Tiwari *et al*, 2018).

Therefore, we believe that despite the encouraging results supporting glia-to-neuron, there is, however, an important limitation this field encounters, which regards the proper understanding of the starting cell.

Consequently, our research rises upon a simple question: are the cells employed for in vitro conversion studies resembling those from the brain? At first glance, it would appear that this is not the case. Accordingly, and to broaden these findings and their application in reprogramming, we performed in vitro astrocyte-to-neuron conversion from astrocytes isolated from the mice cortex at two different developmental stages (postnatal day 4, P4 and at 2 months mice, 2M), an approach that has never been attempted before.

First, we aimed to develop an efficient protocol for generating induced neurons (iN). Thus, we first tested and characterized already published protocols to postnatal cells to generate a proper control condition (Heinrich *et al*, 2010). As expected, our in vitro immature astrocytes started to change morphologically after only a few days post-infection and began expressing the early neuronal marker β-Tubulin III (TUJ1). When iN were characterized, converted cells were positive for more mature markers like NEUN, GABA, and MAP2. Additionally, cells presented electrophysiological properties, such as the capacity to elicit and receive action potentials, indicating that our induced neurons were mature and functionally active.

Overall, as expected, over 60% of in vitro postnatal cortical astrocytes were efficiently reprogrammed into neurons with the sole expression of an inducible lentivirus expressing *Ascl1 (Fig. 3.1 d)*. We then applied our initial conversion protocol on adult cells and wondered if this impacted conversion in the maturation state. Thrillingly, this difference in cell state already led to a noticeable perturbation in conversion efficiency throughout reprogramming, with adult astrocytes conversion averaging half of that from postnatal cells *(Fig. 3.5)*. Interestingly, the morphological changes of many converted cells were altered, displaying mixed phenotypes representing an intermediate state supported by the expression of neuronal and astrocytic markers *(Fig. 3.4)*. Overall, already with this in vitro characterization, we reported a delayed and decreased conversion of adult cells in vitro. Nonetheless, it is noteworthy to mention, that, after isolation, mature cells struggled in attaching compared to postnatal ones. Therefore, when examining whether moving them from the brain to the dish significantly changed their transcript profiles, results proved that this environmental change has an effect rendering them more immature, the same way Lattke and colleagues reported in postnatal astrocytes *(Fig. 3.3)*. This result is indicative that, in general, when experimenting with cells in vitro these are not representing completely the in vivo behavior.

In this regard, when comparing the morphological differences of the iN in the two conditions we observed significant differences. With mature astrocytes presenting a less elaborated neuronal appearance and a prevalence of an astrocytic phenotype (*Fig. 3.5 b*). Despite many functional neurons can have different shapes, considering that postnatal and adult astrocytes shared identical experimental conditions, brain origin, and overexpression of the same transcriptional factor, we did not expected for the differentiation to produce alternative neurological morphologies. However, the drastic transcriptional and morphological changes of adult astrocytes in vitro before conversion, could be a plausible influential variable in determining the iN morphology. This, indeed, accounts for a limitation in the

study, as the experimental environment itself alters greatly the status of the mature astrocyte. Thus, the conversion effect observed, not only is showing an effect of the developmental state, but also an environmental change effect, which can potentially alter the cells chromatin organization, a factor important when aiming to manipulate cellular identity. Overall, these results reinforce the belief that although mature astrocytes harbor the potential to be reprogrammed, they might need more assistance.

Naturally, as cells differentiate and commit to a specialized cell fate, different molecular layers safeguard their cellular identity (Brumbaugh *et al.*, 2019). Besides the proper control of genetic programs, the 3D chromatin organization, occupancy of nucleosomes, and histone modifications are controlled by a diversity of chromatin factors and transposable elements, which regulates and maintains cell identity and genome integrity (Brumbaugh *et al.*, 2019). Consequently, choosing the most suitable cell for conversion is essential. As previously indicated, many variables influence the extent to which the target cell is optimally achieved. Consistent with our in vitro results, immature and intermediate phenotypes challenge the objective of obtaining a fully terminal and mature cell, even if an intermediate pluripotent state is skipped during direct cell conversion (Kelaini *et al*, 2014). It has been explained how the conflict between the donor and the target cell can prevent full maturation of the iN, which implies the acquisition of electrophysiological activity and complete neuronal morphology. Without doubt, this is a pivotal goal, as the gain of functional properties is essential for proper integration and interaction within the local tissue in which reprogramed cells are grafted. Therefore, one can consider whether is it possible that the differences between postnatal and adults' astrocytes genomic architecture could affect, first, the proneness of these cells to transdifferentiate efficiently and secondly, to reach a maturation state of the iN.

Considering all this, we wanted to start by focusing on the diverse chromatin landscapes in astrocytes. Accordingly, we wanted to corroborate the sustantial differences between mature and immature cortical astrocytes in their chromatin landscape during development. This can be done by merging available data of dynamics in accesible chromatin of cortical cells during development at the single cell level. This way, we could identify how astrocytes form two distinct and separated cellular clusters depending on the expression of progenitor or mature astrocytic marks (Preprint: Zaghi et al, 2022 & 10x Genmics dataset). Interestingly, we noticed how postnatal astrocytes resembled more to neuronal stem cells *(Fig. 3.6)*. However, we aimed to understand not only how the active portion of the chromatin help the cells to reach its final stage of maturation. As a matter of fact, we wanted to shed light on the process allowing the cells to inhibit and repress different molecular programs that are related to other fates. A process that is essential to reach its final identity, but many times overlooked. Therefore, for chromatin profiling, we opted to perform Cleavage Under Target and Tagmentation (CUT&Tag), which efficiently reveals regulatory information in the genome (Kaya-Okur *et al*, 2019). Chromatin profiling of repressive marks and/or DNA methylation, unlike RNA sequencing, allows for the identification of silenced genome regions, which, as exhaustively explained, is crucial for establishing cell fates in development and acts as a barrier for reprogramming. Therefore, with this technique, we mapped the general distribution in the genome of the two best described heterochromatin marks, H3K9me3 and H3K27me3, in astrocytes at two different maturation states, P4 and 2M.

Initially, we found that upon cell maturation, there is a global enrichment in heterochromatin marks and loss in chromatin accessibility in astrocytes, suggesting that chromatin is found in a more repressive state as these cells mature and adapt to the requirements of the developing brain *(Fig. 3.7).* Probably, this is a mechanism to safeguard their identity and hence their functionality for the proper homeostasis of their environment. Interestingly, at both developmental stages, we found that the

general distribution of the heterochromatin marks tends to locate at distal regulatory areas and, to a lesser extent, at promoters or in the gene body (*Fig. 3.7)*. Specifically, each mark showed its expected pattern, with H3K9me3 distally distributed and H3K27me3 highly enriched at transcription start sites (TSS) (*Fig. 3.7 b)*. This fact prompted us to examine where precisely in the genome these marks were enriched, especially upon maturation. Additionally, to better understand what these regions are controlling we aimed to identify genes associated to these repressive signals. When associating the repressive peaks with their most proximal genes, many regions corresponded predominantly to genes involved in neuron determination and function *(Fig. 3.8)*. This enrichment was mainly observed on genes when cells are on a mature stage. Therefore, to determine whether these alterations of the repressive marks have a direct effect on gene expression, once we associated each region a gene (based on distance), we found that postnatal cells, despite having heterochromatin marks, can express some neuron-associated genes more strongly than mature cells *(Fig. 3.9)*. Interestingly, mature astrocytes exhibit less expression of genes associated with neuronal morphogenesis and neurotransmission *(Fig. 3.9 e).* This latter function is of interest as astrocytes, the more they differentiate, the more synaptic functions they acquire (Lattke *et al*, 2021). It appears that essential genes regulating neuronal morphological properties and neuronal maturation functions are, somehow, more repressed and less accessible than their postnatal counterparts. Considering these early results, it may be a plausible explanation for why under the same conditions in vitro, 2-month-old cells have a more challenging time acquiring the same morphological changes than postnatal cells during conversion. In accordance with this, we further found how some neuronal-associated genomic regions, like for *Dcx or MeCP2*, transition from a non-marked state toward a more repressive one in mature astrocytes compared to postnatal cells *(Fig. 3.11e)*.

We went one step further and looked at the relationship between these marks and gene regulation. Interestingly, when looking at the differential expression of

genes gaining a repressive signature upon maturation, only those harbouring H3K27me3 alone or together with H3K9me3 had the biggest repression *effect (Fig. 3.10)*. This can be explained as H3K27me3 is located near promoter regions. Alternatively, it is well described how H3K9me3 is associated with constitutive heterochromatin, therefore we did not expect such a difference or strong effect on gene regulation. Certainly, to better elucidate the real effect that H3K9me3 has on gene regulation, 3D chromatin organization data will be helpful, especially considering its genome distribution and, in this regard, how our annotation system (gene association based on distance) does not account for the real effect it may have.

To better analyze how during development this increased in repressive signal occurs, and its impact in cell identity, we selected regions showing a progressive acquisition of repressive marks upon maturation. Interestingly, we identified over 17.000 sites with a heterochromatic signature that were not present at immature stages or to a lesser extent *(Fig. 3. 11)*. This gained heterochromatin signal was accompanied by a decline in the chromatin accessibility and RNA expression on regions associated to genes regulating neuron differentiation and functions.

So far, these results are in line with the notion that heterochromatin is integral to cell identity maintenance by impeding the activation of genes for alternate cell fates. Moreover, heterochromatic regions are associated with histone 3 lysine 9 and 27 trimethylation, but these modifications are also found in euchromatic regions that permit transcription. In this regard, Kenneth Zaret work has helped in revealing how highly enriched H3K9me3 regions correlates with higher compacted chromatin domains and how these have shown to impede direct reprogramming (Soufi *et al*, 2012; Becker *et al*, 2017). Along this line, different levels of chromatin compaction have been described (Becker *et al*, 2017), with heterochromatin regions, despite having repressive marks, revealing euchromatin properties. These, known as sonication-resistant regions, show diverse biochemical properties, which

will partially explain why at P4, some repressive marked areas still present a higher degree of transcriptional activity compared to 2M cells. To better understand if in our cells, these strongly marked regions at a mature state are more present, we performed SAMMY-seq to, literally, untangle heterochromatin properties of the different astrocytes' populations (Sebestyén *et al*, 2020). Our preliminary results indicate a difference within heterochromatin regions, at the chromosomal level, in astrocytes during their maturation process *(Fig. 3.12)*. This suggest that, in accordance with published studies, within repressive sites, identified by the presence of H3K9me3, there are high chromatin compacted regions, and that these are mainly present on mature astrocytes. Interestingly, there are studies reporting a correlation in the gain of repressive marks in adult cells and a coincidence with more compacted regions that tend to be at LADs, modifying the whole 3D chromatin architecture (Sebestyén *et al*, 2020). It would be interesting to perform a Lamin-B genomic mapping in our cells, to see whether this is the case in astrocytes, and perform deeper analysis on where in the genome these differentially highly compacted regions are.

Overall, this approach could entail a powerful tool to potentially identify important targets driving neuronal reprogramming. These different fractions can represent a more accurate measure than the histone marks alone in predicting transcriptional silence and resistance of alternate fate genes to activation during direct cell conversion.

With this result we could observe that, even if at each cell stage the heterochromatin pattern is similar, the presence of a different level of chromatin compaction, demonstrated by different biochemical properties, and the increased presence of the marks themselves, suggest a different level of plasticity at each cell state. This might be especially true for the neuronal-associated loci, as many of them, although proximal to repressive marks, show a higher degree of

transcriptional activity at the postnatal stage compared to the adult one. Recently, it has been suggested that active transcription determines the chromatin state rather than being a consequence of it (Wang *et al*, 2022). Therefore, if we follow this lead, we can speculate that these loci might be more prone to be fully activated, hence more transcribed and probably defining the distinct epigenetic landscape between the two developmental stages. Without a doubt, further analysis in this regard will be needed to generate robust conclusions in the future.

As an additional layer of regulatory information, we wondered if in terms of DNA methylation, we could identify the same effect as described so far for the chromatin compaction. This idea stems from previous work highlighting the role of DNA methylation as key player during the developmental process of various cell types in the cerebral cortex (Moore *et al*, 2013). Moreover, DNA methylation is possibly the first step of a chain of modifications that leads to the silencing of different genomic loci, guiding both the deposition of H3K27 and H3K9 methylation (Moore *et al*, 2013; Jeltsch *et al*, 2018; Methot *et al*, 2021).

To profile DNA methylation on mature and immature astrocytes we applyed meDIP. Our data show that the global pattern of DNA methylation is quite preserved between postnatal and mature astrocytes *(Fig. 3.13)*. This comes to no surprise, considering that we are comparing the same cell type at two different stages of maturation. Despite this, some interesting differeces are present and among the few genomic regions presenting a differential methylation level, we see that at the mature stage there is an increase in DNA methylation proximal to important neuronal genes, such as *Ngn2* and *Ascl1* itself *(Fig. 3.14)*. Moreover, it seems that this alterations seems to lead to a significant loss in chromatin accessibility and a decrease in the gene expression level on some of those genes *(Fig. 3.15)*. Still, we observed that many of those differential methylated regions are located, in many cases, far from a TSS. Therefore it is not always possible to

precisily link those alterations directly with gene expression. More specific analysis on the promoter-enhancer network are needed in the future to solve this issue.

When talking about cells identity manipulation and the conversion process, several intrinsic variables, such as metabolic shifts (Gascón et al, 2016), epigenetic memory, and missing environmental conditions, have significantly impacted how well the differentiation process occurs and how well cells can undergo complete differentiation (Hörmanseder, 2021). Equally important, transcriptional factor dynamics matter. A large body of literature has examined the molecular dynamics of pioneer factors alone, in combination, and with downstream targets to understand how they behave in various cell types to induce neural phenotypes (Aydin *et al*, 2019). Indeed, several reprogramming barriers for transcriptional factors are reported (Cheloufi *et al*, 2015; Masserdotti *et al*, 2015; Gascón *et al*, 2017; Brumbaugh *et al*, 2019). Nevertheless, one basic limitation this field still faces is that many studies aimed at revealing the molecular changes driving conversion and the binding pattern of the factors employed have been conducted mainly in vitro and on cells that are not completely representative of those from the adult brain. By doing so, the reprogramming process overlooks both the effects of the environment as well as the developmental stages at which it is intended to be used. Thus, the direct binding and molecular activity of Ascl1 on astrocytes to date has left unanswered questions, and the variety of results reported in vivo suggests that it is not yet clear to what extent the molecular diversity of the targeted astrocytes as well as the specific environment affect the outcome of reprogramming.

Thus, the lack of understanding about astrocytic chromatin environment together with the literature available showing how the activity of the same factor changes in other models of reprogramming to induce conversion, illustrate that despite the identification of the mechanisms by a specific factor, differential environmental cues can have an impact on their induction properties (permissive or restrictive)

(Woods *et al*, 2022), cofactors availability, and possibly changes in the DNA binding affinities (Lee *et al*, 2020). Among the plethora of possibilities, one we considered is the fact that the underlying epigenetic variation in the donor cell, can also influence.

Having observed that astrocytic maturation brings about a global restructuring of the chromatin architecture in regions involving alternative cell fate identities, we hypothesized that this change in chromatin state might have an impact on the general molecular activity of Ascl1 in promoting neurogenesis.

In our attempt to study how the different maturation state could affect reprogramming, we opted to characterize, for the first time, the binding profile of Ascl1 in vitro on immature and mature astrocytes with CUT&Tag. When manipulating only one variable, such as the cell stage, this provides a proper controlled mean to compare its effects. Therefore, we overexpressed Ascl1 for three days, under a controlled medium condition to avoid any extrinsic influence *(Fig. 3.16)*. Initially, when comparing the results, we observed how the protein follows a similar action plan in tuning the new cellular identity. However, with further analysis, we could observe how specifically on mature cells, it significantly bonds milder to high affinity regions associated with neuronal genes and how it reshaped its genome binding locus on high affinity sites *(Fig. 3 16 c, d),* targeting many additional promoter sites. Nevertheless, when comparing in the two condition this promoter difference, we found that despite the gain upon maturation, only in immature cells the protein specifically bound to promoter regulating nervous system development *(Fig. 3. 17 f-h)*. Moreover, Ascl1 not only suffers a reshape in its genome distribution, but when looking deeper these results, we also found how this happened within some targets like *Dcx*, presenting some level of binding rearrangement within the gene body and at its surrounding. The idea that this could be related with the different chromatin environment previously described, is

supported by the observation that this alteration change cooccurred with an increase in repressive marks at this site upon maturation *(Fig. 3.17 c)*.

Taking together all the information known until now, one can argue that P4 cells share a more similar transcriptional program to a neuron, even presenting a less hostile environment for the action of chromatin remodeling proteins. Thus, they might find the path to generate fully mature neurons smoother as their chromatin environment seems to be somehow permissive. In accordance with this, we show that among the differential binding profile of Ascl1 during astrocyte specification, there a is a significant number of genes regulating neuronal maturation and functionality that are lost *(Fig. 3.17 a-e)*. Hence, we found how genes like *Lrrtm4* or *Shank3,* playing a role in synapse assembly and formation, and dendritic spine maturation, are only targeted at postnatal stages *(Fig. 3.17 e; Fig. 3.19 b)*. These finding are interesting, as in our in vitro model observed that conversion of mature cells give rise to neurons presenting shorter axonal extensions and less dendritic arborization, possible consequences of a blocked or delayed differentiation process. Alternatively, among the specific subset of genes associated to Ascl1 binding in mature cells, we identified new target genes promoting alternative subtype neuron differentiation, like *Isl1* promoting a cholinergic neuron identity *(Fig. 17 e; Fig. 18 e)*.

Despite, the repressive signature astrocytes seem to gain during development, there is evidence supporting *Ascl1* role as a pioneer transcription factor, capable of binding closed chromatin and increasing local DNA accessibility. By doing so, factors with different pioneer activity can interact, and cell fate can be regulated, bypassing the hustle of a more compacted astrocytic chromatin (Chanda *et al,* 2014; Park *et al*, 2017; Raposo *et al,* 2015; Wapinski *et al,* 2013). However, our results provide evidence on how, in our model, Ascl1 mainly binds to already active and open chromatin even at a mature state *(Fig. 3.20)*. A fact also supported by the

rearrangement of the binding sites Ascl1 has on some genes acquiring a heterochromatic environment in adult cells. Which, considering how at this point the chromatin presents a more restrictive environment, shown with our SAMMY-seq data, it could explain the loss in many targets present at postnatal stages. This different pioneer effect we describe, can additionally be explained since whereas we use cells closely related with the terminal fate, previous studies describing Ascl1 prominent pioneer activity have employed cells from a distant ontogenetic relationship, such as fibroblast (Wapinski *et al,* 2013).

We have also tried to assess the relationship between DNA methylation and the binding profile of Ascl1 in the context of astrocytes-to-neuron conversion, as we observed a co-occurrence between the two *(Fig. 3.20a)*. So far, there is clear evidence that a subset of the genomic sequences targeted during neuronal reprogramming are found to be methylated, especially on mature cells. Further analysis on this subject is needed to understand if and how this is impacting the reprogramming process. It has been shown how in fibroblast undergoing conversion, Ascl1 alone is able to rewire the methylome of the starting cell towards the acquisition of a particular methylation profile found in mature neurons (Luo et al, 2019). Interestingly, they also described how with the addition of synergic factors enabled a more efficient a precise way in doing so. With our results, we can speculate that just the diverse chromatinic environment could already change the rewiring activity of the factor, alone or when in combination. With this data obtained from in vivo astrocytes, we provide a meaningful tool to better understand changes at this layer, underlying neuronal induction.

Taking all together, in our case, even the slightest difference in the chromatin rearrangement and epigenetic signature, which we observed just from the developmental age, could potentially influence the fate switch trajectory astrocytes undergo. Following this argument, an interesting approach will be to study the

synergic effect cofactors may have in improving the chromatin remodeling during cell conversion. However, some cofactors or indirect targets may have a double knife effect, probably also due to these genomic differences. So, for instance, whereas Ascl1 is thought to bind closed genomic regions, this is not the case for many of its identified cofactors. Therefore, *Brn2*, who forms a complex to ease neuronal induction and elicits a downstream molecular cascade, ultimately could be altered by some epigenetic barrier, such as DNA methylation or histone modifications (Parkinson *et al*, 2022).

Currently within the field, it is becoming more apparent that adult cells, especially astrocytes, have different requirements for conversion in vivo. Indeed, new research is covering this issue, even with no previous characterization of the cells, together with the specificities of the factor selected. Hence, some groups are approaching this by examining Ascl1's phosphorylation status and how it improves neuronal conversion in vivo and in vitro (Galante *et al*, 2022; Ghazale *et al*, 2022; Woods *et al*, 2022). So far, whereas some groups have shown an increase in the yield of iN in adult cortical astrocytes in vivo, showing an enhanced capacity of *Ascl1* to downregulate the donor identity and acquire a more mature neuronal phenotype with elaborate dendritic arbors (Ghazale *et al*, 2022). However, these results do not tackle the recent problems regarding the no specificity of the delivery methods to induce conversion when using AAVs (Xiang *et al*, 2021). On the other hand, other studies have reported, with the same approach, a propensity of Ascl1 to create additional new binding sites depending on the chromatinic environment it encounters (Woods *et al*, 2022) and when increasing its activity further (via phosphorylation sites mutations) it aberrantly activates alternative pathways such as myogenesis, and interestingly, on cells not undergoing conversion, Ascl1 potentially promotes an oligodendrogliogenic fate (Galante *et al.*, 2022). These studies, are in line with other papers (*see introduction 1.7.1*) showing this alternative direction of *Ascl1* (Kim *et al.*, 2010; Mall *et al.*, 2017; Hersbach *et al.*, 2022). Consequently, it has been previously reported, that the addition of the

repressor *Myt1l*, the neuronal reprogramming is improved, highlighting the idea that cofactor and additional molecular interventions might be required for conversion on adult cells in vivo (Mall *et al*, 2017). Interestingly, in this regard, our findings show how upon maturation, Ascl1 is no longer able to bind and activate the gene encoding for *Myt1l*, a factor known to guide the fate-specific activation of Ascl1 (Rao *et al*, 2021). This further supports how on adult cells, some molecular mechanisms underlying neuronal conversion are lost.

An important aspect we consider relevant, is the fact that the environmental context (*in vitro vs. in vivo*) can highly affect TFs chromatin sensitivity. This is supported by some data, showing that whereas the factor Hepatocyte Nuclear Factor 4 Alpha *(Hnf4a*), when in vitro, is highly sensitive and does not bind to nucleosomes; in vivo has been shown to open closed chromatin when highly expressed (Isbel *et al*, 2022; Hansen *et al*, 2022). However, according to new research questioning the pioneer activity hypothesis, the pioneer activity of transcription factors may be more dependent on their cis-regulatory context, as well as on the synergistic co-expression of multiple factors to activate genes not otherwise activated (Hansen *et al*, 2022). This may lead to the idea that despite Ascl1 can induce neuronal phenotype and downregulate the donors' identity genes, this does not preclude the possibility that a restrictive environment or a significant change in chromatin accessibility may, on the contrary, limit these affinities. Actually, we show how a difference just on the developmental state brings about a global restructuring of the chromatin architecture in regions involving alternative cell fate identities, and how an alteration in Ascl1 binding occurs upon astrocytic maturation. Probably, this can be a product of Ascl1 binding to alternative regions of lower affinity or an alteration of its chromatin sensitivity and specific affinities to different cofactors or heterochromatin marks, directly modifying the availability of some chromatin remodelers. Indeed, during development, it has been recently described how Ascl1 interacts with the chromatin remodeling complex mSWI/SNF at distal regulatory elements to regulate neural differentiation (Păun *et al*, 2022) and when

looking at how the repressive signature during astrocytic specification happens at distal regulatory regions, this accounts for a plausible explanation for the modified binding of the factor.

Overall, when looking at the literature and the diversity in the results, cells employed, and experimental conditions (living brain or dish), it is clear, that many variables can influence conversion. Although some groups have shown that the intrinsic properties of a cell play a very important role in how a specific factor behaves, our study is the first one providing clear evidence on how a difference in the developmental time of a cell can highly shape the reprogramming course. We believe that this apparent interaction between cellular developmental age and transcriptional factors action may assist in the understanding of how cells safeguard their identity and unravel molecular candidates for improving engineering strategies. Indeed, as these preliminary results indicate, numerous complex layers of epigenetic organization exist in establishing cell identity and controlling transcriptional access to DNA.

When analysing the interactions between multiple regulatory layers in the maturation process in astrocytes from the mouse cortex, we can build a better rationale for the elements enabling lineage decisions and identity specification. The general take-home message from this work is that mature astrocytes, despite having the ability to be differentiated, they may take a longer time and struggle to acquire a fully functional mature neuron phenotype. When carefully applying this to the field of direct conversion we consider it to be of relevance, as the goal is not only to obtain a cell resembling a neuron, but a functional one, able to integrate to a pre-existing network and fundamentally, to survive in it. Considering how the different developmental stage seems to alter the general activity of the proneuronal factor Ascl1, probably due to the more hostile environment it encounters once the cell matures, it would be interesting to search ways in which this landscape could

become less restrictive on alternative fates, when the goal is to manipulate it (*Image 4*).

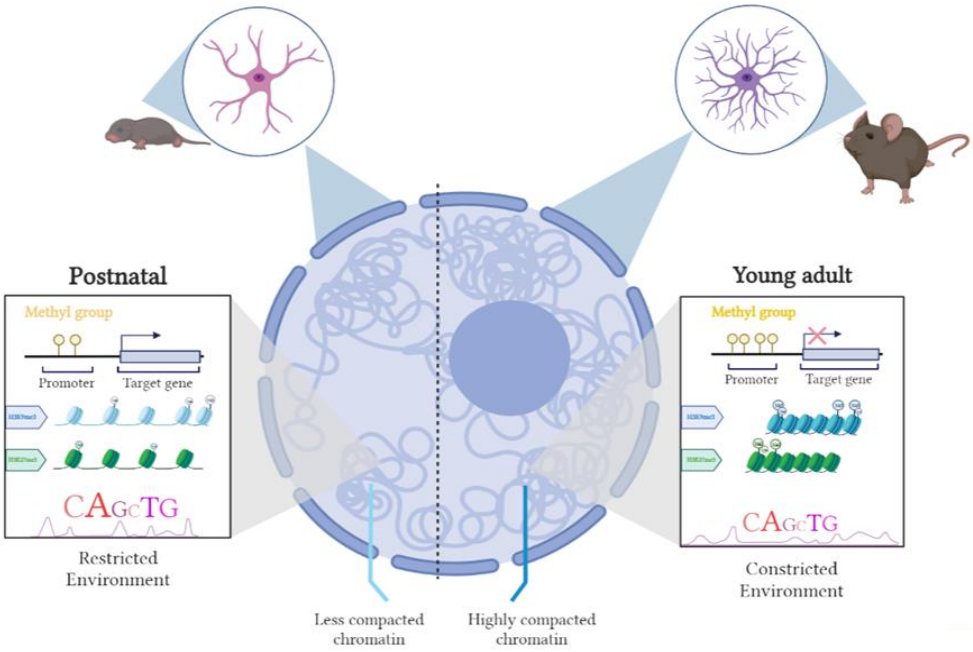

To put it in a nutshell, considering our preliminary results, we think that for conversion, it is essential (i) to determine and analyze the stage of development and the intrinsic chromatin landscape that cells might have before and during conversion, (ii) the environment in which studies are performed (living brain or culture dish), and (iii) the interplay with the transcriptional factor of election. All in all, astrocytes are considered suitable cells for in situ reprogramming goals to overcome neuronal phenotypic conversion, and differences in chromatin landscapes due to different developmental stages and transcriptional programs could explain how reprogramming becomes a challenge in vivo. Ultimately, as a cell becomes more specialized and reaches its terminal fate, additional strategies probably are helpful to compensate for the loss in cellular plasticity upon cell maturation (Jorstad *et al*, 2020; Sun *et al*, 2021). We hope these findings may also provide valuable insight into how these intrinsic properties may affect the mechanisms by which other fate-determinant factors operate.

Overall, direct reprogramming is, in its essence, a holistic procedure that requires attention at every step, with a particular emphasis on the more basic molecular principles of cellular identity. Therefore, by understanding the cellular basis of identity manipulation, we can be one step closer towards an improved neuron conversion in the living brain. In this regard, our preliminary study is the first one providing strong insight into the differences in the chromatin environment of astrocytes at different developmental stages that can potentially impact the mediated conversion process of different transcriptional factors.

5 Material and Methods

5.1 Lentivirus preparation

- LV-Ef1α-Ascl1.V5-ires-GFP
- LV- Ef1α - GFP
- LV-Tet-On-Ascl1.V5
- LV-Tet-On- Rorβ
- LV-Tet-on-Fezf2

For the generation of LV, I followed a general protocol from our laboratory provided by Dr. Serena Giannelli. Lentiviral replication-incompetent were produced by co-transfection of different plasmids (third generation vector): transfer construct, packaging construct, Rev-encoding construct and envelope construct. The packaging constructs mix is made of pMDLg/pRRE, important to package third generation vectors; pRSV - REV, Rev-encoding constructs and pMD2.VSV-G, for the envelope construct.

Vector stocks were prepared by calcium phosphate transfection and concentrated by ultracentrifugation. Briefly, vectors were produced by transfection of HEK293T cells in 150mm dishes. To produce LV, a transfection mix was first prepared with H_2O SALF, containing 30ug of the packaging constructs and the construct with the gene of interest. Finally, 125µl of 2.5M CaCl2 were added, following the widely used transfection procedure. The precipitate was formed by the addition of 1250µl, drop wise, of 2X HBS solution to the total 1250µl DNA-TE-CaCl2 mixture while vortexing at full speed. The precipitate was added to 293T cells immediately following addition of the 2X HBS and cells were incubated at 37°C overnight. After 14-16 hours post- transfection, the medium was replaced. After 30 hours the produced viruses found in the supernatant were collected, filtered through a 0.44µm Stericup GP cellulose acetate (Sigma-Aldrich), placed on the ultracentrifuge special tubes, and ultra-centrifugated for 2 hr at 20°C at 20.000 rpm. Afterward, medium was removed, and the ultracentrifuge tube properly cleaned. The pellets containing the vector were re-suspended in 80ul of sterile PBS. The

concentrated vector preparation was then divided into small aliquots and stored at –80°C.

5.2 Animals

For in vitro and in vivo experiments C57BL6N wild type and ALDH1^{ert2}::CRE mice were bought from Jackson laboratories. Mice were maintained at the San Raffaele Scientific Institute Institutional mouse facility, and experiments were performed in accordance with experimental protocols approved by local Institutional Animal Care and Use Committees (IACUC).

5.3 In vitro studies

5.3.1 MACS-based astrocyte purification.

To obtain a pure populating of postnatal and adult astrocytes for in vitro and in vivo genomic studies brain tissue was obtained from C57BL/6Jaz mice at postnatal day 4 and 6-10 weeks (2 months). First, animals were anesthetized with CO_2 and perfused through the heart with Sodium Chloride 0,9% (S.A.L.F) to ensure removal of blood cells form the brain tissue. The skull was removed, and brains were carefully extracted and dissected to isolate the cortex. Afterward, Isolation and purification of young and adult astrocytes was done using the "Anti-ACSA-2 MicroBead Kit, mouse" (Miltenyi, Biotec) following the manufacturer protocol for adult astrocytes,elsewhere explained (Lattke *et al*, 2021). Briefly, once dissected the tissue was cut to small pieces and dissociated with the Neural Tissue Dissociation Kit (P) (Miltenyi Biotec) in a C Tube. Afterward, tissue was dissociated while incubated for 30 min at 37 °C using the OCTO-dissociator machine. To remove the remaining tissue that did not dissociated, we filtered the tissue using a 70 µm cell strainer. All subsequent steps and centrifugations were performed at 4 °C with pre-cooled reagents. The cells were collected by centrifugation (300 × *g*, 10 min, 4 °C) and resuspended in proper quantity of cold

DPBS, depending on tissue mg processed (3.1-6.2 ml respectively) and (900ul-1.8 ml) 'Debris removal solution' (Miltenyi Biotec). The suspension was carefully overlaid with 4 ml DPBS, and centrifugated at 3000 × *g*, 10 min, 4 °C with maximum acceleration and no deceleration. This allowed for the formation of three layers, with a middle ring of debris. Next, the upper two gradient layers were removed and extra cold DPBS is added reaching 15ml centrifugated at 1000 × *g*, 10 min, 4 °C. Afterwards, the supernatant is removed, and cell pellet is resuspended in 80 µl of MACS buffer (1x PBS, 0,5% BSA, 2mM EDTA) and 10 µl of Fc-Block from the ACSA2-Kit for incubation for 10 min in the dark at 4ºC. Then, further incubation with 10 µl of magnetic-bead conjugated Anti-ACSA2-antibody for 15 min was performed at 4ºC. To collect and clean cells, the suspension was centrifugated and resuspended in 500 µl of MACS buffer. Meanwhile, the magnetic separator (OctoMACS, Miltenyi 130-042-109) was set up, and a MS column (Miltenyi 130-042-201) pre-equilibrated with 500 µl of MACS buffer. Then, the cell suspension was passed through a 70 µm cell strainer. The column was then washed twice with MACS buffer before its removal from the separator and wash out the purified astrocyte preparation with a flush of 1ml of buffer. Cells are purified and ready to perform genomic experiments.

5.3.2 Flow cytometry

To estimate the number of ACSA-2 positive cells after isolation and purification, cells were further incubated with ACSA-2 antibody (1:50) for 10 minutes at 4ºC. Then, samples were immediately analyzed with Fluorescence-activated cell sorting (FACS) Canto II (BD) flow cytometer at the San Raffaele hospital, and the number of ACSA positive cells was analyzed using FCS Express 7 Flow (De NovoSoftware) and presented it as a percentage value.

5.3.3 Cell culture

After astrocytes isolation, once 90% confluency was reached astrocytes were incubated with 0.025% trypsin (Gibco) at 37ºC for 10 minutes to detach them. Cells were centrifuged at 1200 rpm for 5 minutes and counted using Countess™ II Automated Cell Counter (ThermoFisher Scientic). Astrocytes were seeded on a previously treated with Poly-L-Lysine/Laminin/Fibronectin (all from Sigma-Aldrich, 100 µg/ml, 2 µg/ml, 2 µg/ml) 24 well plate (Cornig) at a confluency of 7-8x10^4 cells/cm^2. Cells initially are always resuspended in AstroMACS medium (Miltenyi Biotec, 130-117-031), composed of the MACS neuro medium (130-093-570), supplemented with MACS NeuroBrew-21 and a AstroMACS Supplement, lyophilized. This is an optimized serum-free cell culture medium developed for the cultivation of primary astrocytes from both neonatal and adult mouse neural tissue. For the first 3 days it was complemented with 10% of Gibco Fetal bovine serum (FBS) (ThermoFisher scientific) to ensure proper attachment. After 3 days half of the medium was changed once or twice a week, without FBS.

5.3.4 Profiling of Ascl1 binding in vitro

After isolation and purification of astrocytes as previously described, once astrocytes reached confluency, 1x10^6 cells were plated in a 6 well plate coated with Matrigel, in 3 replicates. After 24 hours, ectopic expression of *Ascl1* in a CRE inducible lentivirus was added for 20 hours. After 3 days, the conversion was stopped, and cells were employed for genomic experiments. To ensure during the conversion process that the binding is solely due to Ascl1 alone and no other signal contained in the medium, cells were always in AstroMACS medium (Miltenyi Biotec, 130-117-031).

5.3.5 Maturation induction

After dissection of Postnatal cortical astrocytes, cells were infected with the two inducible lentiviruses expressing *Rorβ* and *Fezf2*. After 20 hours the medium was replaced with fresh AstroMACS medium complemented with antibiotic selection (Puromycin 1µg/ml) cells for 48h and Doxycycline (2 µg/ml) for an additional week. Afterwards cells were characterized via RTqPCR and others undergo reprogramming with LV expressing *Ascl1*.

5.3.5.1 Directed Neuronal conversion

To induce glial directed neuronal conversion, astrocytes were plated at a confluency of $8x10^4$ cells/well and transduced with a Tet-On lentiviral vector expressing *Ascl1* as the pro-neural factor in AstroMACS medium. After 24 hours post-infection, the virus was removed and cells were then replaced with fresh induction media containing DMEM-F12 with 1% of P/S, Glutamine supplemented with Doxycycline (2µg/ml), B27 (1X), BDNF & GDNF (Peprotech, 20 ng/ml), Forskolin (10 µM) overnight. The procedure was the same for al conversion experiments in vitro. Doxycycline was maintained for all the experiment; afterwards half of the medium was replaced with fresh Neuronal induction medium twice a week**.**

Different control conditions will be set up by adding lentiviral vectors without Tetracycline-Controlled Transcriptional Activation (tTA), or lentivirus expressing *GFP*. Various controls will be established also for the process over time, as cells with induction medium containing DMSO as well as astrocytes just with the full maturation medium to see whether this is sufficient to induce neurons and normal astrocytes with its specific medium to check sporadic differentiation into neurons. Secondly, some cover glasses are tested in parallel to validate the purity of the cell population by performing immunostaining for glial markers (GFAP) and for immature cells, (SOX2) for neural stem cell markers. Moreover, during direct reprogramming and when neurons are starting to be observed, we perform immunostaining to check for neural markers MAP2 and BIII tubulin along with the

astrocyte marker GFAP and SOX9(Heinrich et al., 2010) at three different timepoints (Day7, Day 14 and Day 20). During differentiation, the proliferative and pluripotency marker KI67 and SOX2 are used to make sure cells don't require passage through a pluripotent state.

5.3.5.2 Sholl Analysis

Neuron morphological properties of induced neurons derived from postnatal and mature astrocytes was performed by transducing with a lentiviral vector expressing *GFP* (EF1a-GFP) at low titer 10 d.p.i of differentiation for 1 hour. This way we can obtain sparse GFP cell-labelling. After 20 d.p.i, cells were processed for immunofluorescence analysis as previously described. Images of the dendritic tree of double positive GFP^+/TUJ1 or MAP^+ cells were analyzed using Sholl Analysis plugin in ImageJ software (NIH, USA). The graphical representation and the two-way ANOVA statistical analysis was performed using GraphPad Prism 8.

5.3.6 Electrophysiology of iN

For the electrophysiological characterization of induced neurons, the experiment was performed following previous studies from our laboratory (Mattia *et al*, 2022), it was performed clamp recordings in whole cell configuration. Cells were superfused with ACSF containing (in mM): 125 NaCl, 4KCl, 10mM HEPES, 1.3$MgCl_2$, 2$CaCl_2$, 10mM Glucose, (pH 7.3 with NaOH). Patch pipette (2-4 MΩ) were filled with internal solution containing (mM): 125 KH_2PO_4, 2 $MgCl_2$, 10NaCl, 10 HEPES, 0.5 EGTA, 2 NaATP and 0.5 NaGTP (pH 7.25 with KOH).

Current step protocols were used to evoke APs, injecting 500-ms-long depolarizing current steps of increasing amplitude (Δ 5 pA, max 400 pA). Recordings were acquired using a Multiclamp 700A amplifier (Axon Instruments, Molecular Devices) and a Digidata 1550 (Axon Instruments, Molecular Devices)

D/A converter combined with Clampex (Axon Instruments, Molecular Devices). Signals were filtered at 10 kHz and digitized at 50-100 kHz. Passive properties were calculated using Clampfit (Axon Instruments, Molecular Devices) from the hyperpolarizing steps of the current-clamp step protocol. capacitance was calculated in the current-clamp hyperpolarizing step as follows. First, the resistance was determined as voltage derivative (dV)/DI (voltage/current), and then the cell time constant (tau) was obtained, fitting the voltage changing between baseline and hyperpolarizing plateau. Capacitance was calculated as tau/resistance. Capacitance is the time constant of the voltage between the baseline and the plateau during a hyperpolarizing step. An event was detected as an AP when cross 0 mV and when the rising slope was more than 20 mV/ms. Threshold was defined as the voltage at which the first derivative (dV/dT) reach 10 mV/ms.

For EPSCs/IPSCs recording cell were voltage-clamped at -70 mV. EPSCs were recorded using the same solution used for firing profile characterization. The cell capacitance and series resistance (up to about 75%) were always compensated. Currents were low-pass filtered at 2 kHz and acquired on-line at 5–10 kHz with Molecular Devices hardware and software. Synaptic events were analyzed using MinyAnalysis (Synaptosoft).

5.3.7 RNA extraction and qRT-PCR

To quantify gene expression we followed an established protocol in our laboratory (*Banfi el al, 2021*), cells were collected for RNA extraction using the TRI Reagent isolation system (Sigma-Aldrich) according to the manufacturer's instructions. In all experiments, 500 nanograms of RNA was reverse transcribed into cDNA using the ImProm-II Reverse Transcription System (Promega). Thereafter quantitative real time polymerase chain reaction (qRT-PCR) was performed in duplicates or triplicates with custom-designed oligos using the CFX96 Real-Time PCR Detection System (Bio-Rad, USA). Then, the obtained cDNA was amplified in a 16µl reaction mixture containing 2 µl of diluted cDNA, 1× Titan Hot

Taq EvaGreen qPCR Mix (Bioatlas, Estonia) and 0.5 mM of each primer. 18S rRNA as housekeeping gene for each experimental condition. The quantitative analysis of the relative fold expression was performed using the CFX Manager software (Bio-Rad, USA) and the ΔΔCt method.

5.3.8 Immunostaining

The procedure for IF is done with a shared protocol from (Mattia *et al*, 2022). Briefly, cells were seeded on PLL-coated glass coverslips, and they were fixed for 60 minutes on ice or 30 minutes at room temperature in 4% paraformaldehyde (PFA, Sigma-Aldrich), solution in phosphate-buffered saline (PBS, Euroclone). Afterwards, they were washed with PBS and permeabilized for 45 minutes in blocking solution, containing 0.1% Triton X-100 (Sigma-Aldrich) and 10% donkey serum (Sigma-Aldrich), and incubated overnight at 4 °C with the primary antibodies diluted in blocking solution (see table 1). The following day, cells were washed in fresh PBS 3 times for 3 minutes and then incubated in blocking solution for 1 hour at room temperature with Hoechst 33342 (ThermoFischer Scientific) together with the proper secondary antibodies (ThermoFIsher Scientific). Images were acquired with epifluorescence microscope Nikon DS-Qi2 and analyzed with ImageJ software.

Antigen	**Species**	**Company**	**IF**
GFP	Chicken	ThermoFisher A10262	1:1000
V5	Rabbit	Abcam ab15828	1:500
GFAP	Chicken	Abcam ab4674	1:1000
GFAP	Rabbit	Millipore MAB360	1:1000
Tuj1	Rabbit/Mouse	Covance PRB-435P	1:500
Map2	Chicken	Abcam ab92434	1:1000
NeuN	Rabbit	Abcam AB104225	1:500
GABA	Rabbit	Sigma-Aldrich A2052	1:400-1000

Sox2	Mouse	R&D ab59776	1:200
Iba1	Rabbit	Abcam ab48004	1:1000
ACSA 2 PE-Vio 770	Mouse	Miltenyi Biotec 130-116-246	1:50
Secondary			
488	Mouse	Thermo-Fisher A21202	1:1000
546	Rabbit	Thermo-Fisher A10040	1:1000
647	Chicken	Thermo Fisher A21449	1:1000

Table 1. Antibodies

5.3.9 Statistics for In vitro Reprogramming

For in vitro studies regarding reprogramming conditions, all values are expressed as mean ± standard error (SEM) of at least 3 independent experiments. Statistical analysis and graphs were prepared in GraphPad Prism 8. Normality of distribution was assessed using Shapiro-Wilk test and the significance of the differences between groups was analyzed either by Student's t test or by One-Way and Two-Way ANOVA depending on the number of groups and variables in each experiment, followed by Bonferroni post-hoc test. P-values are indicated in the figures or figure legends.

5.4 Genomic experiments

5.4.1 CUT&Tag

CUT&Tag was performed following the detailed protocol available at nature protocol, previously described by (Kaya-Okur et al., 2019). Briefly, after obtaining a single-cell suspension for each experimental condition, cells were counted, and three biological experimental replicates of 100,000 cells were used (per condition). Afterwards, nuclei are extracted with nuclear extraction buffer (Glycerol, Spermidin, Protease Inhibitor, Hepes 7.9 ph, KCl), light-fixed with 0.1%

formaldehyde, bound to pre-activated concavalin beads, and then incubated over-night with a primary antibody (V5, Abcam, ab15828) or control anti-body (rabbit, immunoglobulin G). The following day, nuclei suspensions are incubated with secondary antibody and washed with washing buffer. Fragmentation of DNA is performed using protein A-Tn5 conjugates (Diagenode, C01070001). Next, DNA is then released from the nuclei, and sequencing libraries are amplified using a single-indexed barcode according to a previously published protocol. Lastly, each individual library has been paired end and sequenced on an Illumina NovaSeq platform by Genewix.

5.4.2 SAMMY-Seq

All experiments were performed in collaboration with the research group of Doctor Chiara Lanzuolo at the IEO Genomic Unit in Milan, performing protocols found in (Sebestyén *et al*, 2020).

Chromatin fractionation was carried out as previously described in (Marasca *et al*, 2016; Sebestyén et al, 2020) with minor adaptions. Briefly, 200.000 postnatal and mature astrocytes purified from the mice brain were washed in PBS (1×), centrifuged at 300g for 5 minutes. To obtain the different chromatin fractions:

First, the supernatant was discarded, and cellular pellet was resuspended in cytoskeleton buffer (CSK: 10 mM PIPES pH 6.8; 100 mM NaCl; 1 mM EGTA; 300 mM Sucrose; 3 mM $MgCl_2$; 1× protease Inhibitors by Roche Diagnostics; 1 mM PMSF) supplemented with 1 mM DTT and 0.5% Triton X-100. After 10 min at 4 °C on a wheel rotator, the cytoskeletal structure was separated from soluble proteins by centrifugation at 900×*g* for 3 min at 4ºC, the supernatant was then stored in a new Eppendorf corresponding to the S1 fraction.

Then pellets were washed with an additional volume of cytoskeleton buffer. Chromatin was solubilized by DNA digestion with 10U of RNase–free DNase (Turbo DNAse; Invitrogen AM2238) in CSK buffer for 60 min at 37 °C. To stop

digestion, ammonium sulfate $(NH_4)_2\ SO_4$ was added in CSK buffer to a final concentration of 250 mM. After 5 min at RT, samples were pelleted at 2350×*g* for 3 min at 4 °C. Here we obtained the S2 fraction.

To further obtain the S3 fraction, pellets were again washed in CSK buffer. Next, we added 2 M NaCl in CSK buffer for 5 min at 4 °C, centrifuged at 2400×*g* 3 min at 4 °C. This treatment enabled us to remove most histones from the chromatin.

To finally obtain the S4 fraction, which corresponds with highly compacted chromatin, the pellets were solubilized in 8 M urea buffer to remove any remaining protein component by applying highly denaturing conditions.

In parallel, for the scaled-down experiment, samples of 100,000 or 10,000 cells were treated analogously, except for a reduction of buffers volumes to half of those used for 10 million cells and a decrease of DNase to 7.5U. Afterwards, samples were stored at -80ºC or -20ºC depending on the time before DNA extraction and library preparation.

5.5 Genomics data analysis

5.5.1 Single ATAC Data processing

Single cell ATAC preprocessed dataset for postnatal (Mattia *et al*, 2022) and adult mice cortex (10xGenomics, https://support.10xgenomics.com/single-cell-atac/datasets/1.2.0/atac_v1_adult_brain_fresh_5k). Data were analyzed using ArchR package (Granja et al., 2021). Latent Semantic Indexing (LSI) (Cusanovich et al., 2015) to perform dimensionality reduction and clustering. Subsequently UMAP algorithm was used to obtain dimensionality reduction coordinates to visualize the result. Clusters where manually inspected to associate each one to a specific cell type based on markers peaks. Feature plot of expressed markers were obtained using ArchR a command plotEmbedding.

5.5.2 ATAC-seq and CUT&Tag data pre-processing

All data processing was performed as described (Mattia *et al*, 2022). Publicly available ATAC-seq data of postnatal and mature astrocytes were obtained from (Lattke *et al*, 2021) GSE152219. A Custom-made pipeline available at GitHub - edobelini/Sessa-Lab, was to perform all the initial steps of the data analysis.

Briefly, FastQC (Andrews, S. FastQC A Quality Control tool for High Throughput Sequence Data) was used to perform an initial quality check on raw sequencing data. Reads adaptor trimming was performed using Trimmomatic (v0.39) (Bolger *et al*, 2014). Trimmed reads were aligned to the mouse reference genome (mm10) using Bowtie2 (Langmead & Salzberg, 2012) with the -very-sensitive optional command. PCR optical duplicates were removed with Picard tools ("Picard Toolkit." 2019. Broad Institute, GitHub Repository. https://broadinstitute.github.io/picard/). Before moving on with further data processing, reads aligned to the non-canonical, the X and M chromosomes were all removed from the files containing the aligned reads with Samtools (v1.9) (Danecek *et al*, 2021). Normalized genomics tracks for visualization and for subsequent analysis were generated using deepTools (v3.5.1) command (Ramírez *et al*, 2016) 'bamCoverage with the following parameters –normalizeUsing RPKM --binSize 10 --smoothLength 300 – effectiveGenomeSize --ignoreDuplicates --skipNAs – exactScaling'. Normalized tracks of each experimental replicate were then merged to create a single file for each experimental condition using UCSC bigWigMerge. Significantly enriched regions a.k.a peaks for Cut & Tag were calculated using GoPeaks (Yashar *et al*, 2022) with the following parameters ' -p 0.01 –broad' using IgG as control for each condition. For ATAC-seq, peak calling was performed on the Tn5 corrected single base using Macs2 (Zhang *et al*, 2008) insertions using the following parameters ' shift 75 extsize 150 --nomodel --call-summits –keep-dup all –nolamba -q 0.01'. After evaluating the correlation level between the different replicates, we move on to obtain a unique consensus region set for sample and mark. This was performed using BedTools (Quinlan & Hall, 2010) sort and merge

function. We did not exclude any significant peak associated with each replicate to avoid any signal loss.

5.5.3 Differential histone marks/Open Chromatin enrichment during astrocytes maturation

To determine regions with increase/decrease in heterochromatinic marks or chromatin accessibility presence comparing the postnatal and mature astrocytes, the H3K27me3/K9me3 or Ascl1 peaks, were divided into three different clusters using deeptools (v3.5.1) computeMatrix and plotHeatmap functions by k-means clustering (n=3) based on H3K27me3/K9me3 or ATAC normalized signal of the postnatal and mature astrocytes condition. The median of the signal for each region was then plotted in the heatmap. To annotate the genomic position of each region associated with each cluster we used ChipSeeker R package (Yu *et al*, 2015), setting the promoter region between -3kb /+3kb from TSS. Functional enrichment was performed using gprofiler2 R package for all genes associated to a specific peak.

5.5.4 Motif enrichment in ATAC analysis.

Motif enrichment inside genomic regions of interest was performed using HOMER package scanning around 200bp from each peak center using the command findMotifsGenome.pl. The following options were used '-mask -nomotif' to perform just the scanning for known motif.

5.5.5 RNA-seq data analysis

Astrocytes RNA-seq data and analysis were obtained from publicly available data-set (Lattke et al, 2021) (GSE152223). Data were processed using the publicly available pipeline Pypette built by the Centre of Omics San Raffaele (COSR).

Differential gene expression was calculated with DESeq2, using a p-adjusted value cut-off of 0.05 (Love *et al*, 2014).

6 Bibliography

Aboelnour E & Bonev B (2021) Decoding the organization, dynamics, and function of the 4D genome. *Dev Cell* 56: 1562–1573

Aboelnour E & Bonev B (2022) Evolutionary conservation and cell type specificity of nuclear compartments in the brain. *Trends Neurosci* 45: 3–5

Adcock IM & Caramori G (2009) Transcription factors. In *Asthma and COPD*

Addis RC, Hsu F-C, Wright RL, Dichter MA, Coulter DA & Gearhart JD (2011) Efficient conversion of astrocytes to functional midbrain dopaminergic neurons using a single polycistronic vector. *PLoS One* 6: e28719

Ali FR, Cheng K, Kirwan P, Metcalfe S, Livesey FJ, Barker RA & Philpott A (2014) The phosphorylation status of Ascl1 is a key determinant of neuronal differentiation and maturation in vivo and in vitro. *Development* 141: 2216–2224

Amendola M & van Steensel B (2015) Nuclear lamins are not required for lamina-associated domain organization in mouse embryonic stem cells. *EMBO Rep* 16: 610–617

Annunziato AT (2012) Assembling chromatin: The long and winding road. *Biochim Biophys Acta - Gene Regul Mech* 1819: 196–210

Aravantinou-Fatorou K & Thomaidou D (2020) In vitro direct reprogramming of mouse and human astrocytes to induced neurons. In *Methods in Molecular Biology*

Arendt T, Stieler JT & Holzer M (2016) Tau and tauopathies. *Brain Res Bull* doi:10.1016/j.brainresbull.2016.08.018 [PREPRINT]

Armingol E, Baghdassarian HM, Martino C, Perez-Lopez A, Aamodt C, Knight R & Lewis NE (2022) Context-aware deconvolution of cell–cell

communication with Tensor-cell2cell. *Nat Commun* 13: 3665

Arvidsson A, Collin T, Kirik D, Kokaia Z & Lindvall O (2002) Neuronal replacement from endogenous precursors in the adult brain after stroke. *Nat Med* 8: 963–970

Asmar F, Søgaard A & Grønbæk K (2015) Chapter 2 - DNA Methylation and Hydroxymethylation in Cancer. In, Gray SGBT-ECT (ed) pp 9–30. Boston: Academic Press

Aydin B, Kakumanu A, Rossillo M, Moreno-Estellés M, Garipler G, Ringstad N, Flames N, Mahony S & Mazzoni EO (2019) Proneural factors Ascl1 and Neurog2 contribute to neuronal subtype identities by establishing distinct chromatin landscapes. *Nat Neurosci* 22: 897–908

Azzarelli R, McNally A, Dell'Amico C, Onorati M, Simons B & Philpott A (2022) ASCL1 phosphorylation and ID2 upregulation are roadblocks to glioblastoma stem cell differentiation. *Sci Rep* 12: 2341

Baker M (2011) The next step for the synthetic genome. *Nature* 473: 403–408

Bannister AJ & Kouzarides T (2011) Regulation of chromatin by histone modifications. *Cell Res* 21: 381–395

Bardehle S, Krüger M, Buggenthin F, Schwausch J, Ninkovic J, Clevers H, Snippert HJ, Theis FJ, Meyer-Luehmann M, Bechmann I, *et al* (2013) Live imaging of astrocyte responses to acute injury reveals selective juxtavascular proliferation. *Nat Neurosci* 16: 580–586

Barker RA, Götz M & Parmar M (2018) New approaches for brain repair—from rescue to reprogramming. *Nature* 557: 329–334

Basu A & Tiwari VK (2021) Epigenetic reprogramming of cell identity: lessons from development for regenerative medicine. *Clin Epigenetics* 13: 144

Batiuk MY, Martirosyan A, Wahis J, de Vin F, Marneffe C, Kusserow C, Koeppen J, Viana JF, Oliveira JF, Voet T, *et al* (2020) Identification of region-specific astrocyte subtypes at single cell resolution. *Nat Commun* 11: 1220

Baumann V, Wiesbeck M, Breunig CT, Braun JM, Köferle A, Ninkovic J, Götz M & Stricker SH (2019) Targeted removal of epigenetic barriers during transcriptional reprogramming. *Nat Commun*

Becker JS, McCarthy RL, Sidoli S, Donahue G, Kaeding KE, He Z, Lin S, Garcia BA & Zaret KS (2017) Genomic and Proteomic Resolution of Heterochromatin and Its Restriction of Alternate Fate Genes. *Mol Cell*

Becker JS, Nicetto D & Zaret KS (2016) H3K9me3-Dependent Heterochromatin: Barrier to Cell Fate Changes. *Trends Genet* doi:10.1016/j.tig.2015.11.001 [PREPRINT]

Bendandi A, Dante S, Zia SR, Diaspro A & Rocchia W (2020) Chromatin Compaction Multiscale Modeling: A Complex Synergy Between Theory, Simulation, and Experiment. *Front Mol Biosci* 7: 15

Berdasco M & Esteller M (2019) Clinical epigenetics: seizing opportunities for translation. *Nat Rev Genet* 20: 109–127

Berninger B, Costa MR, Koch U, Schroeder T, Sutor B, Grothe B & Götz M (2007) Functional Properties of Neurons Derived from In Vitro Reprogrammed Postnatal Astroglia. *J Neurosci* 27: 8654 LP – 8664

Bernstein BE, Meissner A & Lander ES (2007) The Mammalian Epigenome. *Cell* doi:10.1016/j.cell.2007.01.033 [PREPRINT]

Bertrand N, Castro DS & Guillemot F (2002) Proneural genes and the specification of neural cell types. *Nat Rev Neurosci* 3: 517–530

Betzig E, Patterson GH, Sougrat R, Lindwasser OW, Olenych S, Bonifacino JS, Davidson MW, Lippincott-Schwartz J & Hess HF (2006) Imaging Intracellular Fluorescent Proteins at Nanometer Resolution. *Science (80-)* 313: 1642–1645

Bhattacharya S, Zhang Q & Andersen ME (2011) A deterministic map of Waddington's epigenetic landscape for cell fate specification. *BMC Syst Biol*

Blanchard JW, Eade KT, Szűcs A, Lo Sardo V, Tsunemoto RK, Williams D, Sanna PP & Baldwin KK (2015) Selective conversion of fibroblasts into peripheral sensory neurons. *Nat Neurosci*

Bocchi R, Masserdotti G & Götz M (2022) Direct neuronal reprogramming: Fast forward from new concepts toward therapeutic approaches. *Neuron* 110: 366–393

Boettiger AN, Bintu B, Moffitt JR, Wang S, Beliveau BJ, Fudenberg G, Imakaev M, Mirny LA, Wu C & Zhuang X (2016) Super-resolution imaging reveals distinct chromatin folding for different epigenetic states. *Nature* 529: 418–422

Bolger AM, Lohse M & Usadel B (2014) Trimmomatic: a flexible trimmer for Illumina sequence data. *Bioinformatics* 30: 2114–2120

Bonev B & Cavalli G (2016) Organization and function of the 3D genome. *Nat Rev Genet* 17: 661–678

Bonev B, Mendelson Cohen N, Szabo Q, Fritsch L, Papadopoulos GL, Lubling Y, Xu X, Lv X, Hugnot J-P, Tanay A, *et al* (2017) Multiscale 3D Genome Rewiring during Mouse Neural Development. *Cell* 171: 557-572.e24

Bradbury EM (1989) K. E. Van Holde. Chromatin. Series in molecular biology. Springer-Verlag, New York. 1988. 530 pp. $98.00. *J Mol Recognit* 2: i–i

Breiling A, Turner BM, Bianchi ME & Orlando V (2001) General transcription

factors bind promoters repressed by Polycomb group proteins. *Nature* 412: 651–655

Brumbaugh J, Di Stefano B & Hochedlinger K (2019) Reprogramming: identifying the mechanisms that safeguard cell identity. *Development* 146: dev182170

Buffo A, Rite I, Tripathi P, Lepier A, Colak D, Horn AP, Mori T & Götz M (2008) Origin and progeny of reactive gliosis: A source of multipotent cells in the injured brain. *Proc Natl Acad Sci U S A*

Buffo A, Vosko MR, Ertürk D, Hamann GF, Jucker M, Rowitch D & Götz M (2005) Expression pattern of the transcription factor Olig2 in response to brain injuries: implications for neuronal repair. *Proc Natl Acad Sci U S A* 102: 18183–18188

Caiazzo M, Dell'Anno MT, Dvoretskova E, Lazarevic D, Taverna S, Leo D, Sotnikova TD, Menegon A, Roncaglia P, Colciago G, *et al* (2011) Direct generation of functional dopaminergic neurons from mouse and human fibroblasts. *Nature* doi:10.1038/nature10284 [PREPRINT]

Caiazzo M, Giannelli S, Valente P, Lignani G, Carissimo A, Sessa A, Colasante G, Bartolomeo R, Massimino L, Ferroni S, *et al* (2015) Direct conversion of fibroblasts into functional astrocytes by defined transcription factors. *Stem cell reports* 4: 25–36

Casamassimi A & Ciccodicola A (2019) Transcriptional Regulation: Molecules, Involved Mechanisms, and Misregulation. *Int J Mol Sci* 20 doi:10.3390/ijms20061281 [PREPRINT]

Castro DS, Martynoga B, Parras C, Ramesh V, Pacary E, Johnston C, Drechsel D, Lebel-Potter M, Garcia LG, Hunt C, *et al* (2011) A novel function of the proneural factor Ascl1 in progenitor proliferation identified by genome-wide characterization of its targets. *Genes Dev* 25: 930–945

Cesarini E, Mozzetta C, Marullo F, Gregoretti F, Gargiulo A, Columbaro M, Cortesi A, Antonelli L, Di Pelino S, Squarzoni S, *et al* (2015) Lamin A/C sustains PcG protein architecture, maintaining transcriptional repression at target genes. *J Cell Biol* 211: 533–551

Chanda S, Ang CE, Davila J, Pak C, Mall M, Lee QY, Ahlenius H, Jung SW, Südhof TC & Wernig M (2014) Generation of induced neuronal cells by the single reprogramming factor ASCL1. *Stem cell reports* 3: 282–296

Cheloufi S, Elling U, Hopfgartner B, Jung YL, Murn J, Ninova M, Hubmann M, Badeaux AI, Euong Ang C, Tenen D, *et al* (2015) The histone chaperone CAF-1 safeguards somatic cell identity. *Nature* 528: 218–224

Chen G (2021) In vivo confusion over in vivo conversion. *Mol Ther* 29: 3097–3098

Chen W, Zheng Q, Huang Q, Ma S & Li M (2022) Repressing PTBP1 fails to convert reactive astrocytes to dopaminergic neurons in a 6-hydroxydopamine mouse model of Parkinson's disease. *Elife* 11: e75636

Chen Y-C, Ma N-X, Pei Z-F, Wu Z, Do-Monte FH, Keefe S, Yellin E, Chen MS, Yin J-C, Lee G, *et al* (2020) A NeuroD1 AAV-Based Gene Therapy for Functional Brain Repair after Ischemic Injury through In Vivo Astrocyte-to-Neuron Conversion. *Mol Ther* 28: 217–234

Chouchane M & Costa MR (2019) Instructing neuronal identity during CNS development and astroglial-lineage reprogramming: Roles of NEUROG2 and ASCL1. *Brain Res* 1705: 66–74

Chouchane M, Melo de Farias AR, Moura DM de S, Hilscher MM, Schroeder T, Leão RN & Costa MR (2017) Lineage Reprogramming of Astroglial Cells from Different Origins into Distinct Neuronal Subtypes. *Stem cell reports* 9: 162–176

Cieślar-Pobuda A, Knoflach V, Ringh M V., Stark J, Likus W, Siemianowicz K, Ghavami S, Hudecki A, Green JL & Łos MJ (2017) Transdifferentiation and reprogramming: Overview of the processes, their similarities and differences. *Biochim Biophys Acta - Mol Cell Res* doi:10.1016/j.bbamcr.2017.04.017 [PREPRINT]

Colasante G, Rubio A, Massimino L & Broccoli V (2019) Direct Neuronal Reprogramming Reveals Unknown Functions for Known Transcription Factors. *Front Neurosci* 13: 283

Cosenza M & Pozzi S (2018) The Therapeutic Strategy of HDAC6 Inhibitors in Lymphoproliferative Disease. *Int J Mol Sci* 19

Danecek P, Bonfield JK, Liddle J, Marshall J, Ohan V, Pollard MO, Whitwham A, Keane T, McCarthy SA, Davies RM, *et al* (2021) Twelve years of SAMtools and BCFtools. *Gigascience* 10: giab008

Davis RL, Weintraub H & Lassar AB (1987) Expression of a single transfected cDNA converts fibroblasts to myoblasts. *Cell*

Dennis DJ, Han S & Schuurmans C (2019) bHLH transcription factors in neural development, disease, and reprogramming. *Brain Res* 1705: 48–65

Dey S, Fan C, Gothelf K V, Li J, Lin C, Liu L, Liu N, Nijenhuis MAD, Saccà B, Simmel FC, *et al* (2021) DNA origami. *Nat Rev Methods Prim* 1: 13

Dixon JR, Selvaraj S, Yue F, Kim A, Li Y, Shen Y, Hu M, Liu JS & Ren B (2012) Topological domains in mammalian genomes identified by analysis of chromatin interactions. *Nature* 485: 376–380

Escartin C, Galea E, Lakatos A, O'Callaghan JP, Petzold GC, Serrano-Pozo A, Steinhäuser C, Volterra A, Carmignoto G, Agarwal A, *et al* (2021) Reactive astrocyte nomenclature, definitions, and future directions. *Nat Neurosci* 24: 312–325

Fan Y, Winanto & Ng SY (2020) Replacing what's lost: A new era of stem cell therapy for Parkinson's disease. *Transl Neurodegener* doi:10.1186/s40035-019-0180-x [PREPRINT]

Fang L, El Wazan L, Tan C, Nguyen T, Hung SSC, Hewitt AW & Wong RCB (2018) Potentials of cellular reprogramming as a novel strategy for neuroregeneration. *Front Cell Neurosci* doi:10.3389/fncel.2018.00460 [PREPRINT]

Fasching L, Jang Y, Tomasi S, Schreiner J, Tomasini L, Brady M V., Bae T, Sarangi V, Vasmatzis N, Wang Y, *et al* (2021) Early developmental asymmetries in cell lineage trees in living individuals. *Science (80-)*

Federation AJ, Bradner JE & Meissner A (2014) The use of small molecules in somatic-cell reprogramming. *Trends Cell Biol* doi:10.1016/j.tcb.2013.09.011 [PREPRINT]

Flynn RA & Chang HY (2014) Long noncoding RNAs in cell-fate programming and reprogramming. *Cell Stem Cell* 14: 752–761

Fujita J, Tohyama S, Kishino Y, Okada M & Morita Y (2019) Concise Review: Genetic and Epigenetic Regulation of Cardiac Differentiation from Human Pluripotent Stem Cells. *Stem Cells* 37: 992–1002

Galante C, Marichal N, Schuurmans C, Berninger B & Péron S (2022) Low-efficiency conversion of proliferative glia into induced neurons by Ascl1 in the postnatal mouse cerebral cortex <i>in vivo</i> doi:10.1101/2022.04.13.488173 [PREPRINT]

Gascón S, Masserdotti G, Russo GL & Götz M (2017) Direct Neuronal Reprogramming: Achievements, Hurdles, and New Roads to Success. *Cell Stem Cell* doi:10.1016/j.stem.2017.06.011 [PREPRINT]

Gascón S, Murenu E, Masserdotti G, Ortega F, Russo GL, Petrik D, Deshpande A, Heinrich C, Karow M, Robertson SP, *et al* (2016) Identification and

Successful Negotiation of a Metabolic Checkpoint in Direct Neuronal Reprogramming. *Cell Stem Cell* 18: 396–409

Ghazale H, Park E, Vasan L, Mester J, Saleh F, Trevisiol A, Zinyk D, Chinchalongporn V, Liu M, Fleming T, *et al* (2022) Ascl1 phospho-site mutations enhance neuronal conversion of adult cortical astrocytes in vivo. *Front Neurosci* 16: 917071

Glozak MA & Seto E (2007) Histone deacetylases and cancer. *Oncogene* 26: 5420–5432

Grande A, Sumiyoshi K, López-Juárez A, Howard J, Sakthivel B, Aronow B, Campbell K & Nakafuku M (2013) Environmental impact on direct neuronal reprogramming in vivo in the adult brain. *Nat Commun* 4: 2373

Greenberg MVC & Bourc'his D (2019) The diverse roles of DNA methylation in mammalian development and disease. *Nat Rev Mol Cell Biol* 20: 590–607

Greer EL & Shi Y (2012) Histone methylation: a dynamic mark in health, disease and inheritance. *Nat Rev Genet* 13: 343–357

Guo Z, Zhang L, Wu Z, Chen Y, Wang F & Chen G (2014) In vivo direct reprogramming of reactive glial cells into functional neurons after brain injury and in an Alzheimer's disease model. *Cell Stem Cell*

GURDON JB, ELSDALE TR & FISCHBERG M (1958) Sexually Mature Individuals of Xenopus laevis from the Transplantation of Single Somatic Nuclei. *Nature* 182: 64–65

Hafner A & Boettiger A (2022) The spatial organization of transcriptional control. *Nat Rev Genet*

Hansen JL, Loell KJ & Cohen BA (2022) A test of the pioneer factor hypothesis using ectopic liver gene activation. *Elife* 11: e73358

Héberlé É & Bardet AF (2019) Sensitivity of transcription factors to DNA methylation. *Essays Biochem* 63: 727–741

Heinrich C, Bergami M, Gascón S, Lepier A, Viganò F, Dimou L, Sutor B, Berninger B & Götz M (2014) Sox2-mediated conversion of NG2 glia into induced neurons in the injured adult cerebral cortex. *Stem cell reports* 3: 1000–1014

Heinrich C, Blum R, Gascón S, Masserdotti G, Tripathi P, Sánchez R, Tiedt S, Schroeder T, Götz M & Berninger B (2010) Directing astroglia from the cerebral cortex into subtype specific functional neurons. *PLoS Biol*

Heins N, Malatesta P, Cecconi F, Nakafuku M, Tucker KL, Hack MA, Chapouton P, Barde Y-A & Götz M (2002) Glial cells generate neurons: the role of the transcription factor Pax6. *Nat Neurosci* 5: 308–315

Herrero-Navarro Á, Puche-Aroca L, Moreno-Juan V, Sempere-Ferràndez A, Espinosa A, Susín R, Torres-Masjoan L, Leyva-Díaz E, Karow M, Figueres-Oñate M, *et al* (2021) Astrocytes and neurons share region-specific transcriptional signatures that confer regional identity to neuronal reprogramming. *Sci Adv* 7

Hersbach BA, Fischer DS, Masserdotti G, Deeksha, Mojžišová K, Waltzhöni T, Rodriguez-Terrones D, Heinig M, Theis FJ, Götz M, *et al* (2022) Probing cell identity hierarchies by fate titration and collision during direct reprogramming. *Mol Syst Biol* 18: e11129

Hoang T, Kim DW, Appel H, Pannullo NA, Ozawa M, Zheng S, Yu M, Peachey NS, Kim J & Blackshaw S (2021) Ptbp1 deletion does not induce glia-to-neuron conversion in adult mouse retina and brain. *bioRxiv*: 2021.10.04.462784

Hogan BLM (1996) Bone morphogenetic proteins in development. *Curr Opin Genet Dev* 6: 432–438

Hörmanseder E (2021) Epigenetic memory in reprogramming. *Curr Opin Genet Dev* 70: 24–31

Huangfu D, Osafune K, Maehr R, Guo W, Eijkelenboom A, Chen S, Muhlestein W & Melton DA (2008) Induction of pluripotent stem cells from primary human fibroblasts with only Oct4 and Sox2. *Nat Biotechnol*

Huisinga KL, Brower-Toland B & Elgin SCR (2006) The contradictory definitions of heterochromatin: transcription and silencing. *Chromosoma* 115: 110–122

Hyland EM, Cosgrove MS, Molina H, Wang D, Pandey A, Cottee RJ & Boeke JD (2005) Insights into the role of histone H3 and histone H4 core modifiable residues in Saccharomyces cerevisiae. *Mol Cell Biol* 25: 10060–10070

Imayoshi I & Kageyama R (2014) Oscillatory control of bHLH factors in neural progenitors. *Trends Neurosci* 37: 531–538

Inukai S, Kock KH & Bulyk ML (2017) Transcription factor-DNA binding: beyond binding site motifs. *Curr Opin Genet Dev* 43: 110–119

Isbel L, Grand RS & Schübeler D (2022) Generating specificity in genome regulation through transcription factor sensitivity to chromatin. *Nat Rev Genet*

Jacob J, Kong J, Moore S, Milton C, Sasai N, Gonzalez-Quevedo R, Terriente J, Imayoshi I, Kageyama R, Wilkinson DG, *et al* (2013) Retinoid acid specifies neuronal identity through graded expression of Ascl1. *Curr Biol* 23: 412–418

Janowska J, Gargas J, Ziemka-Nalecz M, Zalewska T, Buzanska L & Sypecka J (2019) Directed glial differentiation and transdifferentiation for neural tissue regeneration. *Exp Neurol* doi:10.1016/j.expneurol.2018.08.010 [PREPRINT]

Jeltsch A, Broche J & Bashtrykov P (2018) Molecular Processes Connecting DNA Methylation Patterns with DNA Methyltransferases and Histone

Modifications in Mammalian Genomes. *Genes (Basel)* 9 doi:10.3390/genes9110566 [PREPRINT]

Jones PA (2012) Functions of DNA methylation: islands, start sites, gene bodies and beyond. *Nat Rev Genet* 13: 484–492

Jönsson ME, Nelander Wahlestedt J, Åkerblom M, Kirkeby A, Malmevik J, Brattaas PL, Jakobsson J & Parmar M (2015) Comprehensive analysis of microRNA expression in regionalized human neural progenitor cells reveals microRNA-10 as a caudalizing factor. *Development* 142: 3166–3177

Jorstad NL, Wilken MS, Grimes WN, Wohl SG, VandenBosch LS, Yoshimatsu T, Wong RO, Rieke F & Reh TA (2017) Stimulation of functional neuronal regeneration from Müller glia in adult mice. *Nature* 548: 103–107

Jorstad NL, Wilken MS, Todd L, Finkbeiner C, Nakamura P, Radulovich N, Hooper MJ, Chitsazan A, Wilkerson BA, Rieke F, *et al* (2020) STAT Signaling Modifies Ascl1 Chromatin Binding and Limits Neural Regeneration from Muller Glia in Adult Mouse Retina. *Cell Rep* 30: 2195-2208.e5

Jr ELP & Waddington CH (1943) Organisers and Genes. *Am Midl Nat*

Kaya-Okur HS, Wu SJ, Codomo CA, Pledger ES, Bryson TD, Henikoff JG, Ahmad K & Henikoff S (2019) CUT&Tag for efficient epigenomic profiling of small samples and single cells. *Nat Commun* 10: 1930

Kelaini S, Cochrane A & Margariti A (2014) Direct reprogramming of adult cells: Avoiding the pluripotent state. *Stem Cells Cloning Adv Appl* doi:10.2147/SCCAA.S38006 [PREPRINT]

Kempfer R & Pombo A (2020) Methods for mapping 3D chromosome architecture. *Nat Rev Genet* 21: 207–226

Kempuraj D, Thangavel R, Natteru PA, Selvakumar GP, Saeed D, Zahoor H,

Zaheer S, Iyer SS & Zaheer A (2016) Neuroinflammation Induces Neurodegeneration. *J Neurol Neurosurg spine*

Khurana I, Al-Hasani K, Maxwell S, K.N. H, Okabe J, Cooper ME, Collombat P & El-Osta A (2021) DNA methylation status correlates with adult β-cell regeneration capacity. *npj Regen Med* 6: 7

Kim JB, Zaehres H, Wu G, Gentile L, Ko K, Sebastiano V, Araúzo-Bravo MJ, Ruau D, Han DW, Zenke M, *et al* (2008) Pluripotent stem cells induced from adult neural stem cells by reprogramming with two factors. *Nature* 454: 646–650

Kim K-P, Li C, Bunina D, Jeong H-W, Ghelman J, Yoon J, Shin B, Park H, Han DW, Zaugg JB, *et al* (2021) Donor cell memory confers a metastable state of directly converted cells. *Cell Stem Cell* 28: 1291-1306.e10

Kim K, Doi A, Wen B, Ng K, Zhao R, Cahan P, Kim J, Aryee MJ, Ji H, Ehrlich LIR, *et al* (2010) Epigenetic memory in induced pluripotent stem cells. *Nature* 467: 285–290

Kind J, Pagie L, Ortabozkoyun H, Boyle S, de Vries SS, Janssen H, Amendola M, Nolen LD, Bickmore WA & van Steensel B (2013) Single-Cell Dynamics of Genome-Nuclear Lamina Interactions. *Cell* 153: 178–192

Kind J & van Steensel B (2010) Genome–nuclear lamina interactions and gene regulation. *Curr Opin Cell Biol* 22: 320–325

Klum S, Zaouter C, Alekseenko Z, Björklund ÅK, Hagey DW, Ericson J, Muhr J & Bergsland M (2018) Sequentially acting SOX proteins orchestrate astrocyte- and oligodendrocyte-specific gene expression. *EMBO Rep* 19: e46635

Langmead B & Salzberg SL (2012) Fast gapped-read alignment with Bowtie 2. *Nat Methods* 9: 357–359

Lardenoije R, Iatrou A, Kenis G, Kompotis K, Steinbusch HWM, Mastroeni D, Coleman P, Lemere CA, Hof PR, van den Hove DLA, *et al* (2015) The epigenetics of aging and neurodegeneration. *Prog Neurobiol* doi:10.1016/j.pneurobio.2015.05.002 [PREPRINT]

Larson ED, Komori H, Gibson TJ, Ostgaard CM, Hamm DC, Schnell JM, Lee C-Y & Harrison MM (2021) Cell-type-specific chromatin occupancy by the pioneer factor Zelda drives key developmental transitions in Drosophila. *Nat Commun* 12: 7153

Lattke M, Goldstone R, Ellis JK, Boeing S, Jurado-Arjona J, Marichal N, MacRae JI, Berninger B & Guillemot F (2021) Extensive transcriptional and chromatin changes underlie astrocyte maturation in vivo and in culture. *Nat Commun* 12: 4335

Leaman S, Marichal N & Berninger B (2022) Reprogramming cellular identity in vivo. *Development* 149: dev200433

Lee QY, Mall M, Chanda S, Zhou B, Sharma KS, Schaukowitch K, Adrian-Segarra JM, Grieder SD, Kareta MS, Wapinski OL, *et al* (2020) Pro-neuronal activity of Myod1 due to promiscuous binding to neuronal genes. *Nat Cell Biol* 22: 401–411

Leemans C, van der Zwalm MCH, Brueckner L, Comoglio F, van Schaik T, Pagie L, van Arensbergen J & van Steensel B (2019) Promoter-Intrinsic and Local Chromatin Features Determine Gene Repression in LADs. *Cell* 177: 852-864.e14

Leib D, Chen YH, Monteys AM & Davidson BL (2022) Limited astrocyte-to-neuron conversion in the mouse brain using NeuroD1 overexpression. *Mol Ther* 30: 982–986 doi:10.1016/j.ymthe.2022.01.028 [PREPRINT]

Li H & Chen G (2016) In Vivo Reprogramming for CNS Repair: Regenerating Neurons from Endogenous Glial Cells. *Neuron* 91: 728–738

Li S, Mattar P, Dixit R, Lawn SO, Wilkinson G, Kinch C, Eisenstat D, Kurrasch DM, Chan JA & Schuurmans C (2014) RAS/ERK signaling controls proneural genetic programs in cortical development and gliomagenesis. *J Neurosci Off J Soc Neurosci* 34: 2169–2190

Li S, Shi Y, Yao X, Wang X, Shen L, Rao Z, Yuan J, Liu Y, Zhou Z, Zhang Z, *et al* (2019) Conversion of Astrocytes and Fibroblasts into Functional Noradrenergic Neurons. *Cell Rep*

Lieberman-Aiden E, van Berkum NL, Williams L, Imakaev M, Ragoczy T, Telling A, Amit I, Lajoie BR, Sabo PJ, Dorschner MO, *et al* (2009) Comprehensive Mapping of Long-Range Interactions Reveals Folding Principles of the Human Genome. *Science (80-)* 326: 289–293

Liu ML, Zang T, Zou Y, Chang JC, Gibson JR, Huber KM & Zhang CL (2013) Small molecules enable neurogenin 2 to efficiently convert human fibroblasts into cholinergic neurons. *Nat Commun*

Liu Z, Cai Y, Wang Y, Nie Y, Zhang C, Xu Y, Zhang X, Lu Y, Wang Z, Poo M, *et al* (2018) Cloning of Macaque Monkeys by Somatic Cell Nuclear Transfer. *Cell* 172: 881-887.e7

Llorens-Bobadilla E, Chell JM, Le Merre P, Wu Y, Zamboni M, Bergenstråhle J, Stenudd M, Sopova E, Lundeberg J, Shupliakov O, *et al* (2020) A latent lineage potential in resident neural stem cells enables spinal cord repair. *Science (80-)* 370: eabb8795

Love MI, Huber W & Anders S (2014) Moderated estimation of fold change and dispersion for RNA-seq data with DESeq2. *Genome Biol* 15

Luo C, Lee QY, Wapinski O, Castanon R, Nery JR, Mall M, Kareta MS, Cullen SM, Goodell MA, Chang HY, *et al* (2019) Global DNA methylation remodeling during direct reprogramming of fibroblasts to neurons. *Elife* 8

Luo H, Xi Y, Li W, Li J, Li Y, Dong S, Peng L, Liu Y & Yu W (2017) Cell

identity bookmarking through heterogeneous chromatin landscape maintenance during the cell cycle. *Hum Mol Genet* 26: 4231–4243

Ma NX, Yin JC & Chen G (2019) Transcriptome analysis of small molecule–mediated astrocyte-to-neuron reprogramming. *Front Cell Dev Biol*

Mall M, Kareta MS, Chanda S, Ahlenius H, Perotti N, Zhou B, Grieder SD, Ge X, Drake S, Euong Ang C, *et al* (2017) Myt1l safeguards neuronal identity by actively repressing many non-neuronal fates. *Nature* 544: 245–249

Marasca F, Marullo F & Lanzuolo C (2016) Determination of Polycomb Group of Protein Compartmentalization Through Chromatin Fractionation Procedure. *Methods Mol Biol* 1480: 167–180

de Martin X, Sodaei R & Santpere G (2021) Mechanisms of Binding Specificity among bHLH Transcription Factors. *Int J Mol Sci* 22 doi:10.3390/ijms22179150 [PREPRINT]

Marullo F, Cesarini E, Antonelli L, Gregoretti F, Oliva G & Lanzuolo C (2016) Nucleoplasmic Lamin A/C and Polycomb group of proteins: An evolutionarily conserved interplay. *Nucleus* 7: 103–111

Masserdotti G, Gascón S & Götz M (2016) Direct neuronal reprogramming: Learning from and for development. *Dev* doi:10.1242/dev.092163 [PREPRINT]

Masserdotti G, Gillotin S, Sutor B, Drechsel D, Irmler M, Jørgensen HF, Sass S, Theis FJ, Beckers J, Berninger B, *et al* (2015) Transcriptional Mechanisms of Proneural Factors and REST in Regulating Neuronal Reprogramming of Astrocytes. *Cell Stem Cell*

Matoba S, Liu Y, Lu F, Iwabuchi KA, Shen L, Inoue A & Zhang Y (2014) Embryonic development following somatic cell nuclear transfer impeded by persisting histone methylation. *Cell* 159: 884–895

Mattia Z, Banfi F, Massimino L, Volpin M, Bellini E, Brusco S, Merelli I, Barone C, Bruni M, Bossini L, *et al* (2022) Balanced SET levels favor the correct enhancer repertoire during cell fate acquisition. *bioRxiv*: 2022.09.12.507599

Mayran A & Drouin J (2018) Pioneer transcription factors shape the epigenetic landscape. *J Biol Chem* 293: 13795–13804

Mayran A, Khetchoumian K, Hariri F, Pastinen T, Gauthier Y, Balsalobre A & Drouin J (2018) Pioneer factor Pax7 deploys a stable enhancer repertoire for specification of cell fate. *Nat Genet* 50: 259–269

Mellor J (2006) It Takes a PHD to Read the Histone Code. *Cell* doi:10.1016/j.cell.2006.06.028 [PREPRINT]

Mertens J, Paquola ACM, Ku M, Hatch E, Böhnke L, Ladjevardi S, McGrath S, Campbell B, Lee H, Herdy JR, *et al* (2015) Directly Reprogrammed Human Neurons Retain Aging-Associated Transcriptomic Signatures and Reveal Age-Related Nucleocytoplasmic Defects. *Cell Stem Cell* 17: 705–718

Methot SP, Padeken J, Brancati G, Zeller P, Delaney CE, Gaidatzis D, Kohler H, van Oudenaarden A, Großhans H & Gasser SM (2021) H3K9me selectively blocks transcription factor activity and ensures differentiated tissue integrity. *Nat Cell Biol* 23: 1163–1175

Ming G-L & Song H (2011) Adult neurogenesis in the mammalian brain: significant answers and significant questions. *Neuron* 70: 687–702

Mohn F & Schübeler D (2009) Genetics and epigenetics: stability and plasticity during cellular differentiation. *Trends Genet* doi:10.1016/j.tig.2008.12.005 [PREPRINT]

Moore LD, Le T & Fan G (2013) DNA methylation and its basic function. *Neuropsychopharmacol Off Publ Am Coll Neuropsychopharmacol* 38: 23–38

Morris SA (2016) Direct lineage reprogramming via pioneer factors; a detour through developmental gene regulatory networks. *Development* 143: 2696–2705

Murry CE & Keller G (2008) Differentiation of Embryonic Stem Cells to Clinically Relevant Populations: Lessons from Embryonic Development. *Cell* 132: 661–680

Neyrinck K, Van Den Daele J, Vervliet T, De Smedt J, Wierda K, Nijs M, Vanbokhoven T, D'hondt A, Planque M, Fendt S-M, *et al* (2021) SOX9-induced Generation of Functional Astrocytes Supporting Neuronal Maturation in an All-human System. *Stem Cell Rev Reports* 17: 1855–1873

Nicetto D, Donahue G, Jain T, Peng T, Sidoli S, Sheng L, Montavon T, Becker JS, Grindheim JM, Blahnik K, *et al* (2019) H3K9me3-heterochromatin loss at protein-coding genes enables developmental lineage specification. *Science (80-)* 363: 294–297

Nicetto D & Zaret KS (2019) Role of H3K9me3 heterochromatin in cell identity establishment and maintenance. *Curr Opin Genet Dev* 55: 1–10

Noack F, Vangelisti S, Raffl G, Carido M, Diwakar J, Chong F & Bonev B (2022) Multimodal profiling of the transcriptional regulatory landscape of the developing mouse cortex identifies Neurog2 as a key epigenome remodeler. *Nat Neurosci* 25: 154–167

O'Sullivan JM, Tan-Wong SM, Morillon A, Lee B, Coles J, Mellor J & Proudfoot NJ (2004) Gene loops juxtapose promoters and terminators in yeast. *Nat Genet* 36: 1014–1018

Padeken J, Methot SP & Gasser SM (2022) Establishment of H3K9-methylated heterochromatin and its functions in tissue differentiation and maintenance. *Nat Rev Mol Cell Biol* 23: 623–640

Paksa A & Rajagopal J (2017) The epigenetic basis of cellular plasticity. *Curr*

Opin Cell Biol doi:10.1016/j.ceb.2018.01.003 [PREPRINT]

Palmer TD, Markakis EA, Willhoite AR, Safar F & Gage FH (1999) Fibroblast growth factor-2 activates a latent neurogenic program in neural stem cells from diverse regions of the adult CNS. *J Neurosci Off J Soc Neurosci* 19: 8487–8497

Pang ZP, Yang N, Vierbuchen T, Ostermeier A, Fuentes DR, Yang TQ, Citri A, Sebastiano V, Marro S, Südhof TC, *et al* (2011) Induction of human neuronal cells by defined transcription factors. *Nature* 476: 220–223

Park I-H, Arora N, Huo H, Maherali N, Ahfeldt T, Shimamura A, Lensch MW, Cowan C, Hochedlinger K & Daley GQ (2008) Disease-specific induced pluripotent stem cells. *Cell* 134: 877–886

Park NI, Guilhamon P, Desai K, McAdam RF, Langille E, O'Connor M, Lan X, Whetstone H, Coutinho FJ, Vanner RJ, *et al* (2017) ASCL1 Reorganizes Chromatin to Direct Neuronal Fate and Suppress Tumorigenicity of Glioblastoma Stem Cells. *Cell Stem Cell* 21: 209-224.e7

Parkinson LM, Gillen SL, Woods LM, Chaytor L, Marcos D, Ali FR, Carroll JS & Philpott A (2022) The proneural transcription factor ASCL1 regulates cell proliferation and primes for differentiation in neuroblastoma . *Front Cell Dev Biol* 10 (https://www.frontiersin.org/articles/10.3389/fcell.2022.942579) [PREPRINT]

Parras CM, Schuurmans C, Scardigli R, Kim J, Anderson DJ & Guillemot F (2002) Divergent functions of the proneural genes Mash1 and Ngn2 in the specification of neuronal subtype identity. *Genes Dev* 16: 324–338

Păun O, Tan YX, Patel H, Strohbuecker S, Ghanate A, Cobolli-Gigli C, Sopena ML, Gerontogianni L, Goldstone R, Ang S-L, *et al* (2022) ASCL1 interacts with the mSWI/SNF at distal regulatory elements to regulate neural

differentiation. *bioRxiv*: 2022.10.09.510609

Pelham-Webb B, Murphy D & Apostolou E (2020) Dynamic 3D Chromatin Reorganization during Establishment and Maintenance of Pluripotency. *Stem Cell Reports* 15: 1176–1195

Pereira M, Birtele M, Shrigley S, Benitez JA, Hedlund E, Parmar M & Ottosson DR (2017) Direct Reprogramming of Resident NG2 Glia into Neurons with Properties of Fast-Spiking Parvalbumin-Containing Interneurons. *Stem Cell Reports*

Peric-Hupkes D, Meuleman W, Pagie L, Bruggeman SWM, Solovei I, Brugman W, Gräf S, Flicek P, Kerkhoven RM, van Lohuizen M, *et al* (2010) Molecular Maps of the Reorganization of Genome-Nuclear Lamina Interactions during Differentiation. *Mol Cell*

Perrimon N, Pitsouli C & Shilo BZ (2012) Signaling mechanisms controlling cell fate and embryonic patterning. *Cold Spring Harb Perspect Biol*

Podobinska M, Szablowska-Gadomska I, Augustyniak J, Sandvig I, Sandvig A & Buzanska L (2017) Epigenetic Modulation of Stem Cells in Neurodevelopment: The Role of Methylation and Acetylation. *Front Cell Neurosci* 11: 23

Pollak J, Wilken MS, Ueki Y, Cox KE, Sullivan JM, Taylor RJ, Levine EM & Reh TA (2013) ASCL1 reprograms mouse Muller glia into neurogenic retinal progenitors. *Development* 140: 2619–2631

Puls B, Ding Y, Zhang F, Pan M, Lei Z, Pei Z, Jiang M, Bai Y, Forsyth C, Metzger M, *et al* (2020) Regeneration of Functional Neurons After Spinal Cord Injury via in situ NeuroD1-Mediated Astrocyte-to-Neuron Conversion. *Front cell Dev Biol* 8: 591883

Qian H, Kang X, Hu J, Zhang D, Liang Z, Meng F, Zhang X, Xue Y, Maimon R, Dowdy SF, *et al* (2020) Reversing a model of Parkinson's disease with in

situ converted nigral neurons. *Nature* 582: 550–556

Qian L, Huang Y, Spencer CI, Foley A, Vedantham V, Liu L, Conway SJ, Fu J & Srivastava D (2012) In vivo reprogramming of murine cardiac fibroblasts into induced cardiomyocytes. *Nature* 485: 593–598

Qin H, Zhao A & Fu X (2017) Small molecules for reprogramming and transdifferentiation. *Cell Mol Life Sci* 74: 3553–3575

Quinlan AR & Hall IM (2010) BEDTools: a flexible suite of utilities for comparing genomic features. *Bioinformatics* 26: 841–842

Rajagopal J & Stanger BZ (2016) Plasticity in the Adult: How Should the Waddington Diagram Be Applied to Regenerating Tissues? *Dev Cell* doi:10.1016/j.devcel.2015.12.021 [PREPRINT]

Ramírez F, Ryan DP, Grüning B, Bhardwaj V, Kilpert F, Richter AS, Heyne S, Dündar F & Manke T (2016) deepTools2: a next generation web server for deep-sequencing data analysis. *Nucleic Acids Res* 44: W160–W165

Rao SSP, Huntley MH, Durand NC, Stamenova EK, Bochkov ID, Robinson JT, Sanborn AL, Machol I, Omer AD, Lander ES, *et al* (2014) A 3D Map of the Human Genome at Kilobase Resolution Reveals Principles of Chromatin Looping. *Cell* 159: 1665–1680

Rao Z, Wang R, Li S, Shi Y, Mo L, Han S, Yuan J, Jing N & Cheng L (2021) Molecular Mechanisms Underlying Ascl1-Mediated Astrocyte-to-Neuron Conversion. *Stem cell reports* 16: 534–547

Raposo AASF, Vasconcelos FF, Drechsel D, Marie C, Johnston C, Dolle D, Bithell A, Gillotin S, van den Berg DLC, Ettwiller L, *et al* (2015) Ascl1 Coordinately Regulates Gene Expression and the Chromatin Landscape during Neurogenesis. *Cell Rep* 10: 1544–1556

Raven A, Lu W-Y, Man TY, Ferreira-Gonzalez S, O'Duibhir E, Dwyer BJ,

Thomson JP, Meehan RR, Bogorad R, Koteliansky V, *et al* (2017) Cholangiocytes act as facultative liver stem cells during impaired hepatocyte regeneration. *Nature* 547: 350–354

Ring KL, Tong LM, Balestra ME, Javier R, Andrews-Zwilling Y, Li G, Walker D, Zhang WR, Kreitzer AC & Huang Y (2012) Direct reprogramming of mouse and human fibroblasts into multipotent neural stem cells with a single factor. *Cell Stem Cell*

Rivetti Di Val Cervo P, Romanov RA, Spigolon G, Masini D, Martín-Montañez E, Toledo EM, La Manno G, Feyder M, Pifl C, Ng YH, *et al* (2017) Induction of functional dopamine neurons from human astrocytes in vitro and mouse astrocytes in a Parkinson's disease model. *Nat Biotechnol*

Rodríguez-Paredes M & Esteller M (2011) Cancer epigenetics reaches mainstream oncology. *Nat Med* 17: 330–339

Rowitch DH & Kriegstein AR (2010) Developmental genetics of vertebrate glial-cell specification. *Nature* 468: 214–222

Rowley MJ & Corces VG (2018) Organizational principles of 3D genome architecture. *Nat Rev Genet* 19: 789–800

Russo GL, Sonsalla G, Natarajan P, Breunig CT, Bulli G, Merl-Pham J, Schmitt S, Giehrl-Schwab J, Giesert F, Jastroch M, *et al* (2021) CRISPR-Mediated Induction of Neuron-Enriched Mitochondrial Proteins Boosts Direct Glia-to-Neuron Conversion. *Cell Stem Cell* 28: 524-534.e7

Rust MJ, Bates M & Zhuang X (2006) Sub-diffraction-limit imaging by stochastic optical reconstruction microscopy (STORM). *Nat Methods* 3: 793–796

Salvarani N, Crasto S, Miragoli M, Bertero A, Paulis M, Kunderfranco P, Serio S, Forni A, Lucarelli C, Dal Ferro M, *et al* (2019) The K219T-Lamin mutation induces conduction defects through epigenetic inhibition of SCN5A in human cardiac laminopathy. *Nat Commun* 10: 2267

van Schaik T, Liu NQ, Manzo SG, Peric-Hupkes D, de Wit E & van Steensel B (2022) CTCF and cohesin promote focal detachment of DNA from the nuclear lamina. *Genome Biol* 23: 185

van Schaik T, Vos M, Peric-Hupkes D, HN Celie P & van Steensel B (2020) Cell cycle dynamics of lamina-associated DNA. *EMBO Rep* 21: e50636

Schaub JR, Huppert KA, Kurial SNT, Hsu BY, Cast AE, Donnelly B, Karns RA, Chen F, Rezvani M, Luu HY, *et al* (2018) De novo formation of the biliary system by TGFβ-mediated hepatocyte transdifferentiation. *Nature* 557: 247–251

Schier AF (2003) Nodal Signaling in Vertebrate Development. *Annu Rev Cell Dev Biol* 19: 589–621

Sebestyén E, Marullo F, Lucini F, Petrini C, Bianchi A, Valsoni S, Olivieri I, Antonelli L, Gregoretti F, Oliva G, *et al* (2020) SAMMY-seq reveals early alteration of heterochromatin and deregulation of bivalent genes in Hutchinson-Gilford Progeria Syndrome. *Nat Commun* 11: 6274

Seeley WW, Crawford RK, Zhou J, Miller BL & Greicius MD (2009) Neurodegenerative Diseases Target Large-Scale Human Brain Networks. *Neuron*

Siletti K, Hodge R, Mossi Albiach A, Hu L, Lee KW, Lönnerberg P, Bakken T, Ding S-L, Clark M, Casper T, *et al* (2022) Transcriptomic diversity of cell types across the adult human brain. *bioRxiv*: 2022.10.12.511898

Sirko S, Behrendt G, Johansson PA, Tripathi P, Costa M, Bek S, Heinrich C, Tiedt S, Colak D, Dichgans M, *et al* (2013) Reactive glia in the injured brain acquire stem cell properties in response to sonic hedgehog. [corrected]. *Cell Stem Cell* 12: 426–439

Smith DK, He M, Zhang C-L & Zheng JC (2017) The therapeutic potential of cell identity reprogramming for the treatment of aging-related neurodegenerative

disorders. *Prog Neurobiol* 157: 212–229

Smith ZD, Sindhu C & Meissner A (2016) Molecular features of cellular reprogramming and development. *Nat Rev Mol Cell Biol* doi:10.1038/nrm.2016.6 [PREPRINT]

Soares DS, Homem CCF & Castro DS (2022) Function of Proneural Genes Ascl1 and Asense in Neurogenesis: How Similar Are They? *Front cell Dev Biol* 10: 838431

Soldner F, Laganière J, Cheng AW, Hockemeyer D, Gao Q, Alagappan R, Khurana V, Golbe LI, Myers RH, Lindquist S, *et al* (2011) Generation of isogenic pluripotent stem cells differing exclusively at two early onset Parkinson point mutations. *Cell* 146: 318–331

Soufi A, Donahue G & Zaret KS (2012) Facilitators and impediments of the pluripotency reprogramming factors' initial engagement with the genome. *Cell* 151: 994–1004

Steiner JA, Quansah E & Brundin P (2018) The concept of alpha-synuclein as a prion-like protein: ten years after. *Cell Tissue Res* doi:10.1007/s00441-018-2814-1 [PREPRINT]

Sun S, Li S, Luo Z, Ren M, He S, Wang G & Liu Z (2021) Dual expression of Atoh1 and Ikzf2 promotes transformation of adult cochlear supporting cells into outer hair cells. *Elife* 10

Sun W, Cornwell A, Li J, Peng S, Osorio MJ, Aalling N, Wang S, Benraiss A, Lou N, Goldman SA, *et al* (2017) SOX9 Is an Astrocyte-Specific Nuclear Marker in the Adult Brain Outside the Neurogenic Regions. *J Neurosci Off J Soc Neurosci* 37: 4493–4507

Tabata H (2015) Diverse subtypes of astrocytes and their development during corticogenesis. *Front Neurosci* 9: 114

Takahashi K & Yamanaka S (2006) Induction of Pluripotent Stem Cells from Mouse Embryonic and Adult Fibroblast Cultures by Defined Factors. *Cell*

Takahashi K & Yamanaka S (2015) A developmental framework for induced pluripotency. *Development* 142: 3274–3285

Tam RY, Fuehrmann T, Mitrousis N & Shoichet MS (2014) Regenerative Therapies for Central Nervous System Diseases: a Biomaterials Approach. *Neuropsychopharmacology* 39: 169–188

Tanabe K, Ang CE, Chanda S, Olmos VH, Haag D, Levinson DF, Südhof TC & Wernig M (2018) Transdifferentiation of human adult peripheral blood T cells into neurons. *Proc Natl Acad Sci U S A*

Tian C, Wang Y, Sun L, Ma K & Zheng JC (2011) Reprogrammed mouse astrocytes retain a 'memory' of tissue origin and possess more tendencies for neuronal differentiation than reprogrammed mouse embryonic fibroblasts. *Protein Cell* 2: 128–140

Tiwari N, Pataskar A, Péron S, Thakurela S, Sahu SK, Figueres-Oñate M, Marichal N, López-Mascaraque L, Tiwari VK & Berninger B (2018) Stage-Specific Transcription Factors Drive Astrogliogenesis by Remodeling Gene Regulatory Landscapes. *Cell Stem Cell* 23: 557-571.e8

Tobin SC & Kim K (2012) Generating pluripotent stem cells: Differential epigenetic changes during cellular reprogramming. *FEBS Lett* 586: 2874–2881

Torper O, Ottosson DR, Pereira M, Lau S, Cardoso T, Grealish S & Parmar M (2015) InVivo Reprogramming of Striatal NG2 Glia into Functional Neurons that Integrate into Local Host Circuitry. *Cell Rep*

Torper O, Pfisterer U, Wolf DA, Pereira M, Lau S, Jakobsson J, Björklund A, Grealish S & Parmar M (2013) Generation of induced neurons via direct conversion in vivo. *Proc Natl Acad Sci U S A* 110: 7038–7043

Treutlein B, Lee QY, Camp JG, Mall M, Koh W, Shariati SAM, Sim S, Neff NF, Skotheim JM, Wernig M, *et al* (2016) Dissecting direct reprogramming from fibroblast to neuron using single-cell RNA-seq. *Nature* 534: 391–395

Turgay Y, Eibauer M, Goldman AE, Shimi T, Khayat M, Ben-Harush K, Dubrovsky-Gaupp A, Sapra KT, Goldman RD & Medalia O (2017) The molecular architecture of lamins in somatic cells. *Nature* 543: 261–264

Ullrich NJ & Gordon LB (2015) Chapter 18 - Hutchinson–Gilford progeria syndrome. In *Neurocutaneous Syndromes*, Islam MP & Roach ESBT-H of CN (eds) pp 249–264. Elsevier

Vierbuchen T, Ostermeier A, Pang ZP, Kokubu Y, Südhof TC & Wernig M (2010) Direct conversion of fibroblasts to functional neurons by defined factors. *Nature* 463: 1035–1041

Waddington CH (2012) The epigenotype. 1942. *Int J Epidemiol* 41: 10–13

Wang C, Liu X, Gao Y, Yang L, Li C, Liu W, Chen C, Kou X, Zhao Y, Chen J, *et al* (2018) Reprogramming of H3K9me3-dependent heterochromatin during mammalian embryo development. *Nat Cell Biol* 20: 620–631

Wang H, Yang Y, Liu J & Qian L (2021a) Direct cell reprogramming: approaches, mechanisms and progress. *Nat Rev Mol Cell Biol* 22: 410–424

Wang L-L, Serrano C, Zhong X, Ma S, Zou Y & Zhang C-L (2021b) Revisiting astrocyte to neuron conversion with lineage tracing in vivo. *Cell* 184: 5465-5481.e16

Wang Z, Chivu AG, Choate LA, Rice EJ, Miller DC, Chu T, Chou S-P, Kingsley NB, Petersen JL, Finno CJ, *et al* (2022) Prediction of histone post-translational modification patterns based on nascent transcription data. *Nat Genet* 54: 295–305

Wilmut I, Beaujean N, de Sousa PA, Dinnyes A, King TJ, Paterson LA, Wells

DN & Young LE (2002) Somatic cell nuclear transfer. *Nature* 419: 583–587

Wonders CP & Anderson SA (2006) The origin and specification of cortical interneurons. *Nat Rev Neurosci* 7: 687–696

Wong LL & Rapaport DH (2009) Defining retinal progenitor cell competence in Xenopus laevis by clonal analysis. *Development* 136: 1707–1715

Woods LM, Ali FR, Gomez R, Chernukhin I, Marcos D, Parkinson LM, Tayoun ANA, Carroll JS & Philpott A (2022) Elevated ASCL1 activity creates de novo regulatory elements associated with neuronal differentiation. *BMC Genomics* 23: 255

Wu Z, Parry M, Hou X-Y, Liu M-H, Wang H, Cain R, Pei Z-F, Chen Y-C, Guo Z-Y, Abhijeet S, *et al* (2020) Gene therapy conversion of striatal astrocytes into GABAergic neurons in mouse models of Huntington's disease. *Nat Commun* 11: 1105

Xiang Z, Xu L, Liu M, Wang Q, Li W, Lei W & Chen G (2021) Lineage tracing of direct astrocyte-to-neuron conversion in the mouse cortex. *Neural Regen Res* 16

Yagi M, Ji F, Charlton J, Cristea S, Messemer K, Horwitz N, Di Stefano B, Tsopoulidis N, Hoetker M, Huebner A, *et al* (2021) Dissecting dual roles of MyoD during lineage conversion to mature myocytes and myogenic stem cells. *Genes Dev* 35

Yamaguchi TP (2001) Heads or tails: Wnts and anterior–posterior patterning. *Curr Biol* 11: R713–R724

Yamanaka S (2009) Elite and stochastic models for induced pluripotent stem cell generation. *Nature* doi:10.1038/nature08180 [PREPRINT]

Yang X-J & Seto E (2007) HATs and HDACs: from structure, function and regulation to novel strategies for therapy and prevention. *Oncogene* 26:

5310–5318

Yang Y, Chen R, Wu X, Zhao Y, Fan Y, Xiao Z, Han J, Sun L, Wang X & Dai J (2019) Rapid and Efficient Conversion of Human Fibroblasts into Functional Neurons by Small Molecules. *Stem Cell Reports*

Yang Y, Higashimori H & Morel L (2013) Developmental maturation of astrocytes and pathogenesis of neurodevelopmental disorders. *J Neurodev Disord* 5: 22

Yashar WM, Kong G, VanCampen J, Curtiss BM, Coleman DJ, Carbone L, Yardimci GG, Maxson JE & Braun TP (2022) GoPeaks: histone modification peak calling for CUT&Tag. *Genome Biol* 23: 144

Ye Z & Sarkar CA (2018) Towards a Quantitative Understanding of Cell Identity. *Trends Cell Biol* 28: 1030–1048

Yu G, Wang L-G & He Q-Y (2015) ChIPseeker: an R/Bioconductor package for ChIP peak annotation, comparison and visualization. *Bioinformatics* 31: 2382–2383

Zamboni M, Llorens-Bobadilla E, Magnusson JP & Frisén J (2020) A Widespread Neurogenic Potential of Neocortical Astrocytes Is Induced by Injury. *Cell Stem Cell* 27: 605-617.e5

Zhang Y, Liu T, Meyer CA, Eeckhoute J, Johnson DS, Bernstein BE, Nusbaum C, Myers RM, Brown M, Li W, *et al* (2008) Model-based Analysis of ChIP-Seq (MACS). *Genome Biol* 9: R137

Zheng H & Xie W (2019) The role of 3D genome organization in development and cell differentiation. *Nat Rev Mol Cell Biol* 20: 535–550

Zhou J & Sun J (2019) A Revolution in Reprogramming: Small Molecules. *Curr Mol Med* 19: 77–90

Zhou Q & Melton DA (2018) Pancreas regeneration. *Nature* 557: 351–358

Ziller MJ, Gu H, Müller F, Donaghey J, Tsai LT-Y, Kohlbacher O, De Jager PL, Rosen ED, Bennett DA, Bernstein BE, *et al* (2013) Charting a dynamic DNA methylation landscape of the human genome. *Nature* 500: 477–481

Zocher S, Overall RW, Berdugo-Vega G, Rund N, Karasinsky A, Adusumilli VS, Steinhauer C, Scheibenstock S, Händler K, Schultze JL, *et al* (2021) De novo DNA methylation controls neuronal maturation during adult hippocampal neurogenesis. *EMBO J* 40: e107100

7 Supplementary results.

S1. Ectopic expression of *Rorβ* and *Fezf2* Induces maturation in postnatal cortical astrocytes *in vitro*.

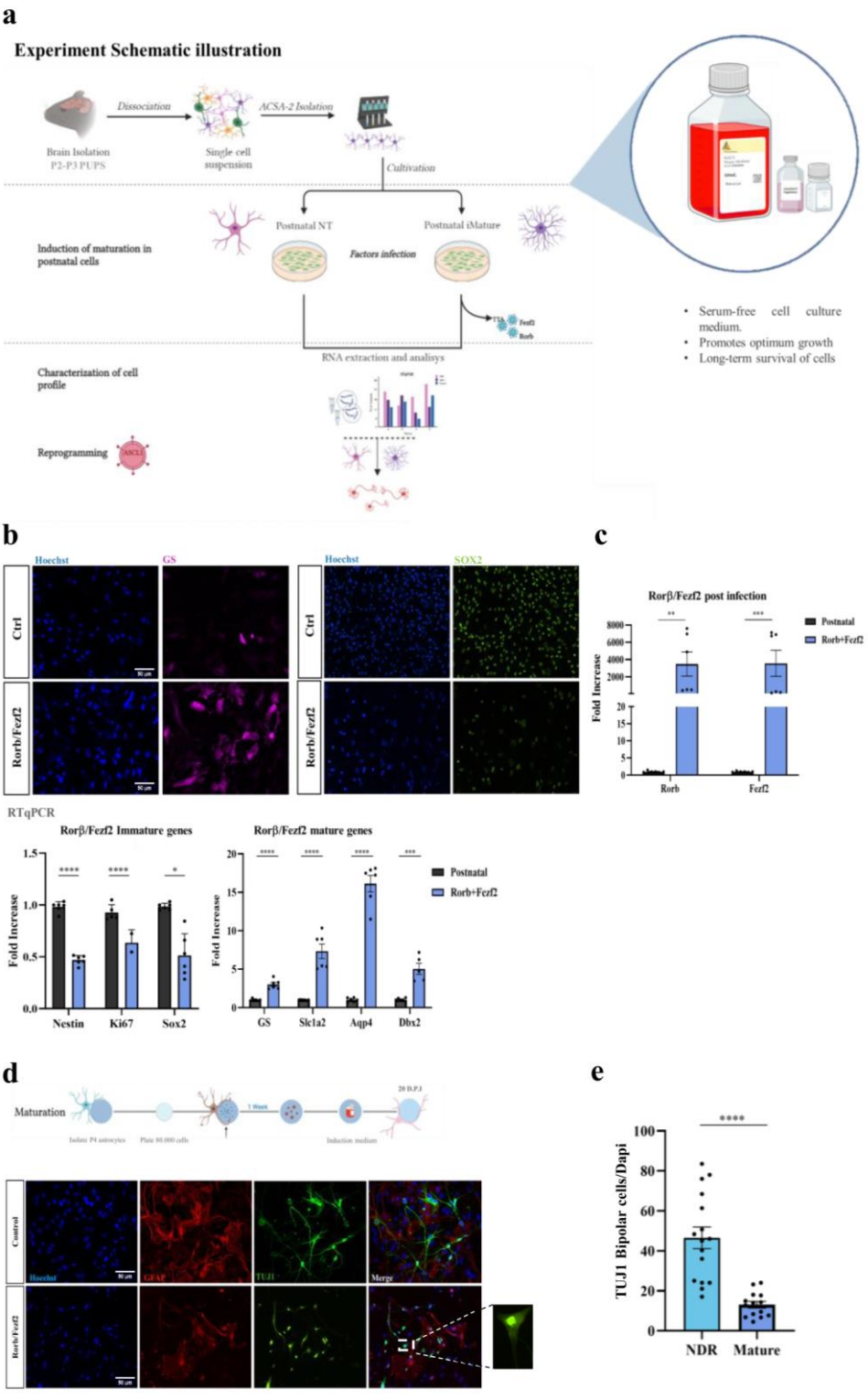

Supplementary Figure S.1. In vitro direct reprogramming of young astrocytes-induced maturation. ***a****. Diagram illustrating the experimental workflow to isolate, infect and reprogram with Ascl1 postnatal (P4) astrocytes.* ***b****. Immunostaining and RNA levels for the characterization of postnatal (P3-P4) cortical astrocytes at 7 d.p.i of Rorβ and Fezf2. Immunostaining markers shown are Glutamine synthetase (GS.) and SOX2; cells in control (top) and treated conditions (below). Mature and immature genes mRNA expression through RTqPCR. Normalization of all conditions was done based on S18 mRNA expression.* ***c****. Panel showing the fold expression of the transcriptional factors used to induce maturation in postnatal astrocytes by RTqPCR 7d.p.i.* ***d.*** *Scheme of the reprogramming conditions. (NDR: Normal direct reprogramming, MDR: Mature direct reprogramming). Immunostaining panel of in vitro induced mature astrocytes during reprogramming with Ascl1 alone. Timepoint shown 20 d.p.i****.*** *Next to the panel is the graph with the efficiency of the conversion calculated based on percentage of bipolar TUJ! positive cells (NDR: 46,64 ±5,4%; MDR: 13,05 ±2%). n=6 independent experiments. Error bars represent ± SEM. *p<0.05, **p<0.01, ***p<0.001, ****p<0.0001. Statistical test: Unpaired Student t-test.*

In vitro, differentiated astrocytes are thought to maintain an immature profile (Lattke *et al*, 2021). Therefore, possibly the mechanisms identified so far are still unclear, as cells in culture seem to lack the complete maturation profile shown in vivo. This immature profile can bias reprogramming results as it may add to the enhanced ease to undergo differentiation. Initially, to tackle this maturation aspect, we first followed previous work (Lattke *et al*, 2021), where the forced expression of the factors, *Rorβ* and *Fezf2* induced maturation in the primary culture of postnatal cortical astrocytes. In parallel to our optimized conversion experiment (*Fig.3.1*), we performed conversion to measure the reprogramming outcome in both conditions.

When assessing maturation in vitro, we treated cells obtained from the cortex of postnatal (P3-P4) C57BL6-J mice with two Tet-On inducible lentiviruses expressing *Rorβ* and *Fezf2 (Fig. S1a)*. To ensure proper expression of the factors in culture, we treated cells for a week with doxycycline. Then, cells were

characterized in parallel, for a mature profile by looking at Glutamine Synthetase (GS) and SOX2 in the immunostaining *(Fig. S1 b)*. Moreover, we tested the fold expression of the factors employed *(Fig S1 c*). We confirmed how the former (GS) increased whereas the latter, an immature marker, got downregulated. For immature genes, we choose genes that were seen to be upregulated in culture astrocytes (Lattke *et al*, 2021); (*Sox2, Nestin*, and *Ki67*) and the same criteria for mature genes (*GS, Slc1a2, Aqp4, and Dbx2*). We observed how the first set of genes got downregulated and in contrast, the latter group showed an increased in their expression *(Fig. S1 b).* Overall, these results confirm previous results where upon expression of *Rorβ* and *Fezf2*, postnatal cortical astrocytes mature in vitro (Lattke *et al,* 2021).

To test if these new in vitro cells could efficiently convert into neurons, we repeated the experiment together with normal postnatal astrocytes (*Fig. S1 d*). 21 d.p.i., cells were fixed and tested immune-positive for TUJ1 *(Fig. S1 d).* The analysis showed that around 20% of cells transfected were $TUJ1^{+}$ bipolar cells *(Fig.s1 e).* Interestingly, in this experiment many converted cells presented a complete astrocyte morphology, despite being positive for a neuronal marker (*Fig. S1 d*). Overall, these results show that in vitro, with a change in gene expression in the direction of a more mature state, cells are less prone as immature astrocytes to be converted into a neuronal fate.

S2. ACSA2 purification of in vivo postnatal and adult astrocytes.

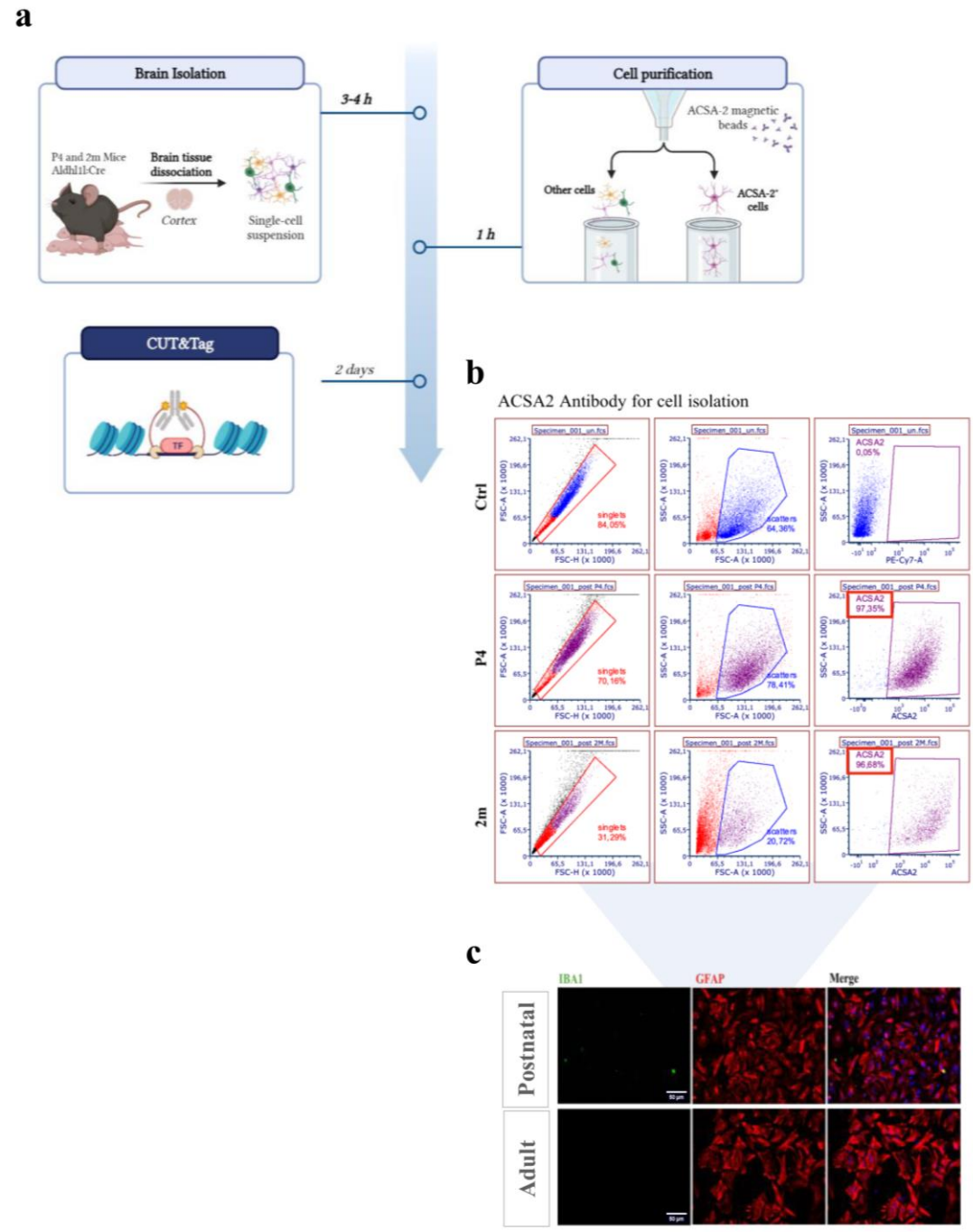

Supplementary Figure S.2. ACSA2 purification of in vivo postnatal and adult astrocytes. ***a.*** *Diagram illustrating the experimental work flow to isolate post-natal and adult astrocytes.* ***b****. Analysis for the quantification of the yield ACSA2 cells per developmental stage (P4: 97,37%; 2M: 96,68%).* ***c****. Immunostaining of the characterization of ACSA2 purified astrocytes from postnatal and adults mice looking at the astrocytic marker GFAP and the microglial mark IBA1. (n=4 adult and n=7 postnatal mice).*

S3. In vivo characterization of *Ascl1* induced chromatin rearrangement.

a

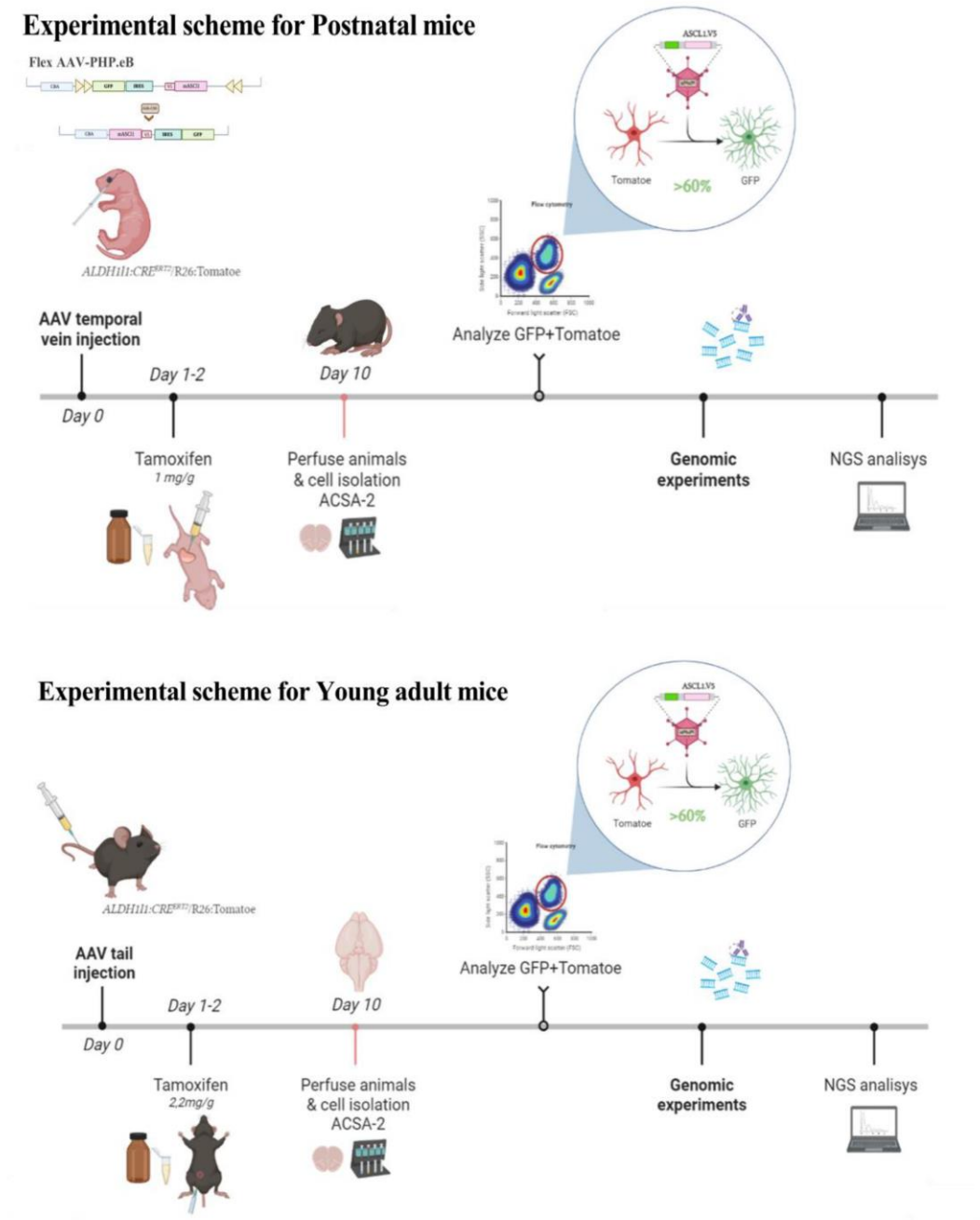

Supplementary Figure S3. In vivo characterization of Ascl1 induced chromatin rearrangement.

a. *Schematic illustration of the In vivo workflow for characterizing the chromatin landscape in postnatal and young adult mice.* ***Aldh1l1:Cre/R26:Tomatoe*** *mice are infected with an AAV expressing Ascl1 tagged with V5 and GFP.*